UC Irvine

UC Irvine Electronic Theses and Dissertations

Title

Mechanisms of Epilepsy Development

Permalink

https://escholarship.org/uc/item/60t3m268

Author

Patterson, Katelin Patrice

Publication Date

2016

Peer reviewed|Thesis/dissertation

eScholarship.org Powered by the California Digital Library
University of California

UNIVERSITY OF CALIFORNIA,
IRVINE

Mechanisms of Epilepsy Development

DISSERTATION

Submitted in partial satisfaction of the requirements
for the degree of

DOCTOR OF PHILOSOPHY

in Biomedical Sciences

by

Katelin Patrice Patterson

Dissertation Committee:
Professor Tallie Z. Baram, MD, PhD, Chair
Professor Christine Marie Gall, PhD
Professor Diane O'Dowd, PhD

2016

Chapter 1 © 2014 Springer
Portions of Chapter 2 © 2014 Springer
Chapter 3 © 2014 Society for Neuroscience
Chapter 4 © 2015 Society for Neuroscience
All other materials © 2016 Katelin Patrice Patterson

DEDICATION

To

My Grandmother

Helen Mary Riedele
(1912-2005)

Who believed that a woman should,

above all other things,

be well educated

TABLE OF CONTENTS

	Page
LIST OF FIGURES	iii
LIST OF TABLES	v
ACKNOWLEDGMENTS	vi
CURRICULUM VITAE	vii
ABSTRACT OF THE DISSERTATION	xi
CHAPTER 1: Temporal lobe epilepsy is a disruption of the limbic circuit and its provocation by febrile status epilepticus (FSE)	1
CHAPTER 2: Challenges in preventing FSE-induced TLE: models, mechanisms and predictive biomarkers	14
CHAPTER 3: Novel and non-invasive magnetic resonance imaging predicts which individual with eFSE will develop epilepsy	18
CHAPTER 4: MRI changes predictive of epilepsy and acute activation of inflammatory cascades take place in the same febrile status epilepticus –experiencing individuals	64
CHAPTER 5: Blocking inflammation after eFSE prevents hippocampal hyper-excitability	101
CHAPTER 6: Enduring cognitive deficits following eFSE are mediated by functional and structural effects of the neuronal repressive silencing factor (NRSF)	122
CHAPTER 7: Summary and Conclusion	174
REFERENCES	176

LIST OF FIGURES

		Page
Figure 3.1	Brain T2 is reduced 2 h after FSE	26
Figure 3.2	The severity and duration of the inciting FSE and the resulting epileptogenesis	37
Figure 3.3	Amygdala T_2 values 2 hours after FSE distinguish rats that progressed on to epilepsy	46
Figure 3.4	Reduced T_2 values after FSE correlate with increased deoxyhemoglobin levels	50
Figure 3.5	Translocation of high-mobility box 1 (HMGB1) from the nucleus to the cytoplasm in amygdala neurons correlates with lowered T_2 signal on MRI	54
Figure 3.6	Lower-field, more clinically relevant MRI scanners identify the same epilepsy-predictive changes as high-field MRI	57
Figure 4.1	eFSE parameters	76
Figure 4.2	Activated microglia after eFSE	79
Figure 4.3	Activated astrocytes after eFSE	82
Figure 4.4	HMGB1 translocation in hippocampal neurons after eFSE	85
Figure 4.5	Transient cytokine upregulation after eFSE	89
Figure 4.6	Inter-animal variation of inflammatory mediator expression after eFSE	92
Figure 4.7	Inflammation profiles of individual animals correlates with predictive measure of post eFSE epilepsy	96
Figure 5.1	The relationship between spike series and seizures after eFSE	109
Figure 5.2	Schematic of experimental design	112

Figure 5.3	Dexamethasone reduces spike series after eFSE	115
Figure 5.4	Dexamethasone prevents inflammation after eFSE	119
Figure 6.1	Binding of augmented NRSF to chromatin after eFSE is prevented using a decoy system	139
Figure 6.2	Blocking NRSF binding to chromatin after eFSE has long term influences in learning and memory	145
Figure 6.3	eFSE modulates hippocampal rhythms	153
Figure 6.4	Blocking NRSF activity post eFSE reduces augmented dendritic arborization	159
Figure 6.5	Dendritic hindrance in CA1 pyramidal cells generated by eFSE is NRSF independent	163
Figure 6.6	An *in vitro* system of the development of GC after seizure-like activity	167

List of Tables

		Page
Table 3.1	Characteristics of spontaneous limbic Behavioral / electrographical seizures in adult epileptic rats after eFSE	35
Table 3.2	Exploratory factor analysis on T_2 values revealed distinct patterns that predicted epilepsy	41
Table 3.3	Exploratory factor analysis on T_2 values that were normalized to brain T2 revealed distinct patterns that were similar to raw T2 values	42
Table 4.1	Primer sequences used for rt-PCR	73

.

ACKNOWLEDGMENTS

To my committee chair and mentor, Dr. Tallie Z. Baram. Thank you for always demanding my best and seeing potential in me that at times I could not see in myself. The way I think has been fundamentally altered by your mentorship and I am not the person today as I was when I first walked into your lab 5 years ago. You set a high bar for me in every facet of my life here and I am a better scientist and person for it. Your unwavering commitment to your lab and research has always and will continue to inspire me. I am forever proud and grateful that I had the opportunity to work with and learn from you. Thank you.

To my dissertation committee members: Dr. Christine Gall, who is an exemplar of what academic research should be and to Dr. Diane O'Dowd whose commitment to higher education is inspiring and laudable.

To the financial support from the American Epilepsy Society, Pre-Doctoral Fellowship and the NIH NINDS T32 Training Award in Epilepsy, without which this work would not be possible.

To my father, Robert Patterson, whose passion for science and the natural world inspired me as a child to pursue research. Who taught me to question everything and to find beauty and purpose in nature.

To my mother, Patrice Patterson, who taught me that I could be whatever I wanted to be as long as I looked presentable doing it. Your unwavering love and belief in me is the reason I get through every day.

To my younger brother Philip Patterson. For teaching me to follow my dreams and pursue my passions at all costs.

To my friends, my chosen family. Your support has gotten me through this experience and I am nothing but grateful to have you all in my life.

To my fellow INP Graduate Students and lab members. We have all grown so much together over these years and I am nothing but humbled to call you colleagues.

To my dogs, Penny and Darwin. The joy you bring to my life is worth all the trouble you cause.

Finally, to my fiancé, Eric Gold. It is poetic that we met as we began our doctorates 5 years ago and as I write this we are 3 weeks away from our wedding. Walking this path with you has been my greatest honor and you are the reason I have made it through these years. Thank you for always believing in me and championing my dreams. I love you.
P.S. We made a bet 5 years ago that whoever defended first would have a nice dinner provided for them by the other person. I wait with baited breath.

CURRICULUM VITAE

Katelin Patrice Patterson
Department of Anatomy and Neurobiology
University of California, Irvine School of Medicine
Medical Sciences 1, Room B150
Irvine, California 92697

EDUCATION

2009 B.A. Psychology, University of San Francisco

2016 Ph.D. Biomedical Sciences, Anatomy and Neurobiology, University of California-Irvine

HONORS AND AWARDS

2016 Department of Anatomy & Neurobiology Grad Day: 3rd Place Oral Presentation

2015 Department of Anatomy & Neurobiology Grad Day: 2nd Place Poster Presentation

2014 NIH NINDS T32 Training Award

2014 Department of Anatomy & Neurobiology Grad Day: 1st Place Oral Presentation

2014 Gordon Research Conference, Epilepsy & Synchronization: Travel Award

2013 Department of Anatomy & Neurobiology Grad Day: 1st Place Poster Presentation

2013 Individual Fellowship Bonus: UC-Irvine School of Medicine

2012 American Epilepsy Society: Pre-Doctoral Research Training Fellowship

2012 Graduate Fellow Award: HHMI-UC-Irvine Teaching Fellows Program

2012 Gordon Research Conference, Epilepsy and Synchronization: Travel Award

PUBLICATIONS

Manuscripts:

Patterson KP, Barry JM, Curran MM, Singh-Taylor A, Matias P, Noam Y, Holmes GL & Baram TZ (2016) Enduring cognitive deficits following developmental seizures are mediated by functional and structural effects of the neuronal repressive silencing factor (NRSF/REST1). *Under Review*.

Patterson KP, Brennan GP, Curran M, Kinney- Lang E, Dube CM, Rashid F, Ly C, Obenaus A & Baram TZ (2015) Rapid, coordinate inflammatory responses after experimental febrile status epilepticus: Implications for epileptogenesis. *eNeuro*, DOI: 10.1523/ENERUO.0034-15.2015.

Choy M[*], Patterson KP[*], Dubé CM[*], Barnes SR, Maras P, Blood AB, Hasso AN, Obenaus A, Baram TZ. (2014) A novel, non-invasive, predictive epilepsy biomarker with clinical potential. *Journal of Neuroscience*. 34:8672-84.
[*]Authors contributed equally

Patterson KP, Baram TZ, Shinnar S (2014) Origins of temporal lobe epilepsy: febrile seizures and febrile status epilepticus. *Neurotherapeutics*. 11:242-50.

Chen Y, Molet J, Lauterborn JC, Trieu BH, Bolton JL**, Patterson KP**, Gall CM, Lynch G & Baram TZ (2016) Novel convergent actions of multiple stress hormones mediate enduring memory impairments after acute simultaneous stresses. *Under Review*

Brennan GP, Dey D, Chen Y, **Patterson KP**, Magnetta EJ, Hall AM, Dubé CM, Mei TY & Baram TZ (2016) Dual and opposing roles of microRNA-124 in epilepsy are mediated through Inflammatory and NRSF-dependent gene networks. *Cell reports*. 14:2402-2412.

Barry JM, Sakkaki S, Barriere SJ, **Patterson KP**, Lenck-Santini PP, Scott RS, Baram TZ & Holmes GL (2016) Temporal coordination of hippocampal neurons reflects cognitive outcome post- febrile status epilepticus. *EBioMedicine*. 7:175-190.

Siegenthaler JA, Choe Y, **Patterson KP**, Hsieh I, Li D, Jaminet SC, Daneman R, Kume T, Huang EJ, Pleasure SJ. (2013) Foxc1 is required by pericytes during fetal brain angiogenesis. *Biology Open*. 7:647-59.

Hecht JH, Siegenthaler JA, **Patterson KP**, Pleasure SJ. (2010) Primary cellular meningeal defects cause neocortical dysplasia and dyslamination. *Annals of Neurology*. 4:454-64.

Siegenthaler JA, Ashique AM, Zarbalis K, **Patterson KP**, Hecht JH, Kane MA, Folias AE, Choe Y, May SR, Kume T, Napoli JL, Pererson AS, Pleasure SJ. (2009) Retinoic

acid from the meninges regulates cortical neuron generation. *Cell*. 3:597-609.

Publications in final preparation

Patterson KP, Curran MM & Baram TZ (2016) Dexamethasone reduces hippocampal hyperexcitability after experimental febrile status epilepticus. *In Preparation.*

Abstracts/ Presentations

Patterson KP. Enduring cognitive deficits following developmental seizures are mediated by functional and structural effects of the neuronal repressive silencing factor (NRSF/REST1). Anatomy & Neurobiology annual grad day; June 9, 2016: Irvine, CA.

Patterson KP. Rapid, coordinate inflammatory responses after experimental febrile status epilepticus: implications for epileptogenesis. UC-Irvine Immunology Fair; December 3, 2015: Irvine, CA.

Patterson KP. Rapid, coordinate inflammatory responses after experimental febrile status epilepticus: implications for epileptogenesis. UC-Irvine EpiCenter Symposium; March 15, 2015: Irvine, CA.

Patterson KP. Developmental plasticity of dentate gyrus granule cells following epileptiform activity in vitro: Anatomy & Neurobiology annual grad day; June 20, 2014: Newport Beach, CA.

Patterson, KP, Noam, Y, Chen, Y, Brennan, GP, Ly, C & Baram TZ. Mechanisms of aberrant dentate gyrus granule cell development following status epilepticus. Poster Session: Gordon Research Conference- Mechanisms of Epilepsy and Neuronal Synchronization; August 20, 2014: Mount Snow, VT.

Patterson KP. The role of the transcription factor NRSF in developmental structural plasticity of dentate gyrus granule cells: UC-Irvine, department of Anatomy & Neurobiology, Progress in Neuroscience Seminar; April 25, 2014: Irvine, CA.

Patterson KP, Dubé CM, Choy M, Baram TZ. Rapid Inflammatory Process Following Febrile Status Epilepticus: a Biomarker of Epileptogenesis? Poster Session: American Epilepsy Society Annual Meeting; December 7th & 8th, 2013.

Patterson KP, Dubé CM, Choy M, Baram TZ. Rapid Inflammatory Process Following Febrile Status Epilepticus: a Biomarker of Epileptogenesis? Poster Session: Society for Neuroscience; November 10, 2013: San Diego, CA.

Patterson KP, Dubé CM, Choy M, Baram TZ. Rapid Inflammatory Process Following Febrile Status Epilepticus: a Biomarker of Epileptogenesis? Poster Session: UC-Irvine Department of Anatomy & Neurobiology Grad Day;June 10, 2013: Irvine, CA.

Patterson KP, Dubé CM & Baram, TZ. Blood brain barrier disruption following experimental febrile status epilepticus. Poster session: UC-Irvine EpiCenter; March 12, 2013: Irvine, CA.

ABSTRACT OF THE DISSERTATION

Mechanisms of Epilepsy Development

By

Katelin Patrice Patterson

Doctor of Philosophy in Biomedical Science

University of California, Irvine, 2016

Professor Tallie Z. Baram MD, PhD, Chair

Temporal lobe epilepsy (TLE) commonly arises following long seizures early in life, especially long fever-associated seizures (febrile status epilepticus; FSE). TLE, in addition to spontaneous seizures, is also commonly characterized by cognitive deficits. However, there are major gaps in our knowledge regarding the causal relationships of FSE and TLE, including its cognitive disturbances, and the mechanisms of how FSE can lead to TLE. To answer these questions a rodent model of experimental (e)FSE has been established, and, as in the human, a proportion of rats with eFSE develop TLE. This enables addressing fundamental questions that are required for diagnosis and intervention in humans: Which individuals with FSE will fall among the 40% that develop TLE? Are there predictive markers for those at risk? How does FSE provoke TLE and what are the mechanisms? Can we prevent FSE-provoked TLE and FSE-induced cognitive deficits? Addressing these questions is the goal and core of this thesis project.

Chapter 1

Introduction: Temporal lobe epilepsy: a disruption of the limbic circuit and its provocation by febrile status epilepticus (FSE)

Temporal lobe epilepsy (TLE) commonly arises following early-life long seizures, and especially febrile status epilepticus (FSE). However, our knowledge is incomplete regarding the causal relationships of FSE, TLE and cognitive disturbances. These gaps hamper the diagnosis, biomarker development and prevention of epilepsy and the associated cognitive impairments. A fundamental question is the causal relationship between FSE and TLE. There is a broad spectrum of views regarding this question. For example, some believe that FSE arises primarily in individuals with a predisposed or compromised brain. This predisposition might derive from genetic factors, a developmental dysplasia, or a pre- or postnatal 'acquired' problem such as stroke or trauma. In this scenario, FSE might simply be a marker of individuals who are destined to develop TLE. Alternatively, FSE might occur in children with a 'normal' or uncompromised brain, but lead to TLE only in a compromised, predisposed child. Finally, some authorities consider that FSE in and of itself might lead to TLE in individuals, compromised or not, who otherwise might not develop epilepsy. Uncovering the contribution of FSE to TLE is important for FSE management and potential preventive interventions. If FSE does not contribute to TLE, then its management should be conservative. Alternatively, if FSE contributes to TLE (either in the setting of a predisposed brain or in all individuals) two types of interventions should be considered: (a) aggressive management of the FSE itself or (b) an opportunity to intervene subsequent to the FSE and prevent TLE. This possibility requires understanding of the mechanisms by which FSE promotes TLE. Also needed are suitable biomarkers that will

distinguish children who will develop TLE from those who will not. A similar set of questions pertain to cognitive impairments found in individuals with epilepsy that follows FSE as well as in animal studies. Do the same mechanisms that govern post FSE epileptogenesis also mediate memory and other cognitive deficits? Are the cognitive problems a result of the original insult or of the ensuing epilepsy? This introduction addresses these major questions in the field and presents our current knowledge of these issues.

Epidemiology of Febrile Seizures (FS) FS are defined as seizures associated with a febrile illness without a CNS infection or electrolyte imbalance in children 1 month and older without prior afebrile seizures (Commission on Epidemiology and Prognosis of the International League Against Epilepsy, 1993; Febrile seizures, 1980). While most FS are brief and benign, a proportion are prolonged and 5% to 9% last >30 minutes (Nelson & Ellenberg, 1987; Berg & Shinnar, 1996a; Hesdorffer et al., 2011) meeting criteria for status epilepticus (SE) (Dodson et al., 1993; Maytal et al., 1989). FS are common, occurring in 2–5 % of all children (Nelson & Ellenberg, 1987; Stafstrom, 2012; Verity et al., 1985; Subcommittee on Febrile Seizures, 2011). FS are so frequent that although FSE represents a minority of FS cases, they account for 25 % of childhood SE (Dodson et al., 1993; Maytal et al., 1989; Shinnar et al., 1997; DeLorenzo et al., 1996) and over 70% of SE that takes place in the second year of life (Shinnar et al., 1997). It is estimated that there are 25,000 to 35,000 cases of FSE annually in the US.

Genetics The occurrence of FS is both sporadic and familial, suggesting a contribution of both environmental and genetic components to their onset (Bethune et al., 1993). Increased susceptibility to the development of FS is now known to result from mutations of several genes, including sodium channels (Wallace et al., 1998; Escayg et al., 2000; Catterall, 2000), GABAA receptors (Mulley et al., 2003; Hill et al., 2011; Petrou et al., 2012; Kang et al., 2006), and hyperpolarization-activated cyclic nucleotidegated (HCN) channels (Dibbens et al., 2010; Nakamura et al., 2013; Noam et al., 2011). Other single gene mutations, such as in the interleukin (IL-1) gene promoter, have also been implicated in a vulnerability to FS or TLE (Kauffman et al., 2008; Kira et al., 2010) and interaction among several genes might increase the probability of developing FS in a given individual (van Gassen et al., 2008; Escayg et al., 2010). In immature rodents, fever is very difficult to generate (Dubé et al., 2012). FS-like seizures can be induced by hyperthermia (Holtzman et al., 1981; Hjeresen et al., 1983; Morimoto et al., 1993; Baram et al., 1997; Toth et al., 1998; Dubé et al., 2006; Dubé et al., 2010; Chang et al., 2005; Kamal et al., 2006; Notenboom et al., 2010) or hyperthermia coupled with lipopolysaccharide (LPS) and kainic acid (KA) (Heida et al., 2004; Reid et al., 2012). Seizures typically arise in all hyperthermia-sustaining animals (Lemmens et al., 2009) suggesting that genetic susceptibility is not necessarily required for their generation. However, seizure-temperature thresholds (a measure of excitability) vary among mouse strains with differing genetic make-up (van Gassen et al., 2008; Martin et al., 2010). In addition, single gene mutations, including those found to be associated with FS and FS related epilepsy syndromes, modulate the threshold to the onset of FS-like hyperthermia-induced seizures (Catterall et al., 2000; Nakamura et al., 2013; Martin et

al., 2010; Hill et al., 2011). These findings support the involvement of genetic factors in these seizures. Thus, in rodents, the contribution of genetic factors to FS and to their consequences is complex. The contribution of genetic factors to FS in children is vastly more complex than in rodent models, where many variables can be controlled. FS in general and FSE in particular can clearly occur without any predisposing factors. In fact, more than half the cases of FS in a population occur in children with no risk factors and no family history of FS or epilepsy (Bethune et al., 1993). However, FS are one of the classic examples of interplay between underlying susceptibility and an environmental insult. Thus, the children that do have a predisposition based on either genetic or structural reasons are more likely to experience a FS when a febrile illness occurs during the susceptible age window. For example, approximately 20% of children with childhood onset epilepsy of all types, including those thought to be genetic in origin such as childhood absence and Rolandic Epilepsy, will experience an episode of FS during early childhood (Berg et al., 1999; Camfield et al., 1994). These are clearly not causally related. In addition, if one looks at children with FSE, there is an over-representation of children with pre-existing neurological abnormalities (Maytal et al., 1989,1990; Shinnar et al., 1997). These complexities make it more difficult to tease out the role of pre-existing genetic factors versus the actual FS/FSE in causing subsequent TLE.

How are FS Generated? Fever involves an elevation of brain temperature, and temperature influences both pyramidal cells (Wu et al., 2001) and interneurons (Kim et al., 2012) through several mechanisms. These include modulation of the function of

specific ions channels. For example, the transient-receptor-potential vanilloid (TRPV) 1 and 4 channels are regulated by brain temperature in the physiological and fever ranges, and have been implicated in FS in animal models (Hunt et al., 2012) where elevated brain temperature leads to augmented neuronal firing, facilitating seizures. Similarly, HCN channels (Nakamura et al., 2013; Santoro et al., 2010) and Cav1.2 calcium channels (Randzicki et al., 2013) seem to contribute to the hyperexcitability that results in febrile seizures. In children, increased temperature *per se*, resulting from hot baths or anticholinergics overdose, may lead to seizures (Dubé et al., 2007), but the mechanisms are likely multifactorial (Klyueva et al., 2001) and remain obscure. In addition to raising brain temperature, fever involves inflammatory mediators including cytokines such as TNF-α and interleukin-1β (IL-1β) that promote neuronal hyperexcitability. IL-1β augments calcium permeability of glutamate receptors (Viviani et al., 2003) and the function of kinases (ceramide-induced Src-family of tyrosine kinases) enhancing seizures of many kinds (Vezzani et al., 2007). Endogenous IL-1β contributes to the generation of experimental FS, and a mutation in the IL-1β gene promoter that results in higher levels of this cytokine has been reported in some individuals with FS and TLE (Kauffman et al., 2008; Kira et al., 2010). Whereas some infections (especially human herpes virus 6) seem to be a strong provoker of FS (Theodore et al., 2008), it is unknown if this augments levels of cytokines in a child's brain. Clearly, a number of additional factors, including dehydration or alkalosis (Morimoto et al., 1996; Schuchmann et al., 2006), might interact with the genetic background of a given child to contribute to the mechanisms by which a febrile seizure arises (Dubé et al., 2007).

TLE and FSE: Clinical Data There is little evidence for an enduring adverse impact of short FS on the developing brain in either animal models or epidemiological data (Dubé et al., 2007; Shinnar et al., 2012; Abou-Khalil et al., 1993). However, prolonged FS and especially FSE have been associated with a higher risk of epilepsy in general and TLE in particular but until recently it has been difficult to distinguish association from causal relationship. Retrospective studies from tertiary epilepsy centers report that many adults with intractable TLE give a history of prior prolonged FS in childhood (Abou-Khalil et al., 1993; Cendes et al., 1993; French et al., 1993; Mathern et al., 1995a,b). Children with prolonged FS are at increased risk for developing epilepsy and those with FSE are at highest risk (Nelson et al., 1978; Annegers et al., 1987; Verity et al., 1993; Maher et al., 1995; Berg et al., 1996b). Despite this, cohort studies of FS have minimized the role of prolonged FS in causing TLE, attributing both the FS and ensuing epilepsy to pre-existing pathology (Nelson et al., 1978; Annegers et al., 1987). Consistent with this hypothesis, recent studies of FSE have reported low morbidity and a high proportion of pre-existing neurological abnormalities (Hesdorffer et al., 2011). However, because MRIs were not performed in these studies, and the latency to the development of TLE is 8–11 years (French et al., 1993; Mathern et al., 1995a,b), which is longer than the follow-up period in many of these prospective studies, acute hippocampal injury and subsequent TLE may have been missed. More recently, imaging studies utilizing MRI show that hippocampal injury can occur after FSE but the small numbers, inability to exclude pre-existing hippocampal abnormalities, and lack of long-term follow-up make definitive conclusions difficult (Vanlandingham et al., 1998; Fernandez et al., 1998; Chan et al., 1996; Lewis et al., 2002; Scott et al., 2003; Scott et al., 2006). FEBSTAT, a

prospective study of children with FSE was specifically designed to address the occurrence of hippocampal injury and atrophy following FSE, the evolution of epilepsy syndromes (including TLE), and the relationship between FSE and subsequent epilepsy (Hesdorffer et al., 2012). Early findings are now available. They demonstrate that there are subtle pre-existing hippocampal abnormalities in a subgroup of children with FSE. However, the majority appears to have normal hippocampi, with neuroradiological evidence of hippocampal injury in approximately 12% (Shinnar et al., 2012; Lewis et al., 2014). While the neurobiological basis for the relationship between FSE and subsequent TLE are not fully understood, the preponderance of data is now in favor of a causal relationship between FSE and TLE though not with other forms of epilepsy. One should note that a predisposition and causality are not mutually exclusive. For example, in a series of children with familial hippocampal malformation and febrile seizures, Fernandez et al. (1998) demonstrated that those with prolonged FS go on to have TLE whereas those with brief FS do not, though they do have abnormal hippocampi. These data suggest that FSE is required for TLE even in the presence of predisposing factors. Because it is practically impossible to eliminate the predisposition, understanding how FSE contributes to TLE is crucial to prevent the epileptogenic effects of this insult on the brain. This question is discussed below.

The Mechanistic Relationship of TLE and FSE The examination of questions surrounding the mechanism or mechanisms linking FSE to TLE has been greatly facilitated by the employment of animal models. These models allow for causal and mechanistic studies to be carried out and for the time frame of prospective studies

investigating the evolution of FSE to TLE to be shortened (Dubé et al., 2007; Dedeurwaaerdere et al., 2012). However, creating such a model is hampered by the fact that immature rodents do not readily develop fever (Dubé et a., 2012;2007). There have been several animal models used to approximate FSE (Holtzman et al., 1981; Hjeresen et al., 1983; Morimoto et al., 1993; Baram et al., 1997; Toth et al., 1998; Dubé et al., 2006,2010; Chang et al., 2005; Kamal et al., 2006; Notenboom et al., 2010; Heida et al., 2004; Reid et al., 2012). Some strive to generate febrile convulsions (FC) in rats by injecting the bacterial endotoxin LPS accompanied by a usually subconvulsive dose of the pro-convulsant drug kainic acid while maintaining animals in a warm room (30 °C) (Heida et al., 2005). LPS raises the rat's temperature by 1–1.5 °C which mimics fever and enhances the convulsant actions of kainic acid. This method creates FC in approximately 50 % of experimental animals (Heida et al., 2004,2005). While this model imitates important features of FSE (an inflammatory response and fever), a drawback is that these animals do not have seizures with LPS alone and need KA, which draws concerns about which mechanisms are specific to the febrile (LPS and/or the warm room) or convulsive (KA) events. While these animals have a prolonged reduction in seizure threshold (as shown with amygdala kindling 8 to 10 weeks after LPS/KA injections), they do not develop spontaneous seizures later in life (Heida et al., 2004). Several groups have employed a hyperthermic model of FSE in immature rodents at ages where the development of the hippocampus is analogous to that of human infants (P10-11 in rats) (Avishai-Eliner et al., 2002). This model relies on a stream of warm air, which raises core and brain temperature and leads to seizures. Endogenous inflammatory mediators including IL-1β are involved in the generation of these

experimental febrile seizures, because mice deficient in the IL-1β receptor were resistant to hyperthermic seizures (Dubé et a., 2005). The durations of hyperthermia and the seizures are regulated to generate “experimental FSE” (Dubé et al., 2006,2009,2010). Whereas control rats never become epileptic, hyperthermic seizures generate a susceptibility to KA (Dubé et al., 2000), and a subset of experimental FSE rats (~40%) becomes epileptic later in life (Dubé et al., 2010). This demonstrates that experimental FSE alone can create epilepsy in a brain that would have been normal without this insult, suggesting that epileptogenic processes are initiated by the FSE itself (Dubé et al., 2007,2010). To date these models have led to the discovery of many of the consequences of FSE, in terms of both epilepsy and cognitive problems. These include HCN channelopathies, deficits in synaptic plasticity and decreased inhibition by the endocannabinoid system amongst others (Richichi et al., 2008; Chang et al., 2005; Chen et al., 2007). The hyperthermia model also allows for the study of epileptogenic mechanisms that could ultimately lead to post FSE interventions to prevent TLE (McClelland et al., 2011; Dubé et al., 2012). What are these mechanisms and how might they be addressed? Inflammatory mediators and mechanisms are an attractive possibility for two reasons. First, a large body of work (see Vezzani, et al. 2011 for review), has demonstrated that many insults that provoke epileptogenesis also lead to activation of inflammatory mechanisms. Second, evidence for inflammation is found in human epileptic hippocampi (Ravizza et al., 2008). In the instance of FSE-related epilepsy, the case for inflammation is even stronger, and derives from the interplay between inflammation and fever. Generation of fever requires the action of inflammatory mediators (prostaglandins and cytokines) (Ostberg et al., 2000). Conversely, our

collaborative group and others, found that increased brain temperature (hyperthermia) *per se* leads to activation of inflammatory pathways, and specifically cytokine release (Dubé et al., 2005; Haveman et al., 1996). Indeed, IL-1β release seems to be required for the generation of FS in the experimental model of hyperthermia induced seizures. In the context of FS related epileptogenesis, inflammation occurs both during and as a result of FSE (Vezzani et al., 2007; Dubé et a., 2005). Therefore, inflammation (cytokine expression, morphological changes of glia, infiltration of pro-inflammatory cells into the CNS) has been a focus of intense study. Refuting or validating a role for inflammation in FSE related epilepsy is important, because it will enable translating the results to the clinic. Dubé et al. (2005) demonstrated the importance of the proinflammatory cytokine IL-1β in a hyperthermic model of FSE. An upregulation of IL-1β occurs 24 hours post FSE in the hippocampus of all FSE rodents. Interestingly, only rats that go on to experience TLE have maintained IL-1β upregulation in hippocampus. Whether or not this upregulation is a cause or consequence of spontaneous seizures is unknown. In the HC model using LPS and KA, a similar role of IL-1β has been found, in that there was an increase in hippocampal IL- 1β 2 and 4 hours post seizures (Heida et al., 2005, 2009). These studies suggest that because inflammation is induced by seizures, and has been shown to be involved in epilepsy in other contexts, inflammation may aid in the development of post-FSE epilepsy. How might inflammation influence brain excitability? IL-1β has been shown to increase excitability by increasing the amount of glutamate in synapses and by enhancing NMDA receptor- mediated intracellular calcium (Mascarucci et al., 1998; Maroso et al., 2010). While compelling, blocking IL-1β production and signaling in other models of epileptogenesis (electrical SE and

pilocarpine) did not change spontaneous seizure onset, intensity or duration (Noe et al ., 2013). While these results would need to be replicated in the more naturalistic eFSE model to enable inferences about translation to FSE related TLE, they suggest that pan-inflammatory interventions rather than targeting individual cytokines might be tried (Dedeurwaurdere et al., 2012). Any intervention given post FSE would preferably be administered as soon as possible post insult. Looking upstream of IL-1β production and release to find a "master regulator" of FSE induced inflammation might be beneficial in preventing complex and intricate inflammatory cascades that potentially lead to TLE (Noe et al., 2013; Patterson et al., 2013). Additionally, preventing global or specific inflammatory cascades post FSE and monitoring the development of TLE will shed light onto the therapeutic potential of anti-inflammatory agents and either confirm or refute inflammation as a cause (rather than a concurrent event) of epileptogenesis. These studies should take place in animal models (preclinical studies) as a preamble to their potential use in the clinic.

Cognitive Consequences of FSE In the hyperthermia model of FSE a subset of rats developed spatial memory deficits when tested months later (Dubé et al., 2009). Remarkably, whereas MRIs obtained one month after the seizures identified rats with cognitive problems, the MRI at this late time-point did not predict development of epilepsy, consistent with the idea that cognitive disturbances were separate from and likely independent from epileptogenesis. The spatial memory deficits were accompanied by, and likely a result of, significant disturbances in the function of hippocampal place cells that encode and sustain information about spatial orientation, a fundamental

prerequisite for spatial cognition. Similar reorganization of cognitive networks has also been described in the HC model of FSE (Lemmens et al., 2009). These findings are important because they suggest that impairments in memory are a result of the inciting FSE rather than of ensuing epilepsy. In several large, well-designed studies utilizing either sibling controls or population based controls, the cognitive and behavioral outcomes of children with FS including FSE are similar to those of children without FS (Nelson et al., 1978; Verity et al., 1993; Hirtz et al., 2002; Verity et al., 1998; Chang et al., 2000, 2001; Baram & Shinnar, 2001). However, these studies did not look specifically at FSE, and often included a very small number of cases of FSE. In addition, they did not specifically address the issue of memory. Memory is of particular concern as animal models have demonstrated that FS appear to be of limbic origin (Baram et al., 1997, Dubé et al., 2007) and both clinical studies and experimental models suggest that when injury occurs following FSE, it is observed in the hippocampus (Toth et al., 1998; Vanlandingham et al., 1998; Lewis et al., 2002, 2014; Dubé et al., 2009; Herman et al., 2002). In addition, memory is well known to be impaired in patients with chronic TLE (Bell et al., 1998; Herman et al., 2002). The FEBSTAT study is designed to address whether or not FSE causes memory deficits in those who have evidence of injury but that portion of the study is still in progress. Obviously, these facts and the deficits found in animal models indicate that it is important to examine if prolonged FS/FSE generate cognitive defects in a subgroup of individuals, to uncover the underlying mechanisms, and to define biomarkers that will identify those at risk and enable intervention. The working hypothesis of the FEBSTAT study, in line with the separation of cognitive problems and epileptogenesis in the animal model (Dubé et al., 2009), is that some

children will have memory deficits that will precede the development of TLE and may be present even in children who do not develop TLE (Hesdorffer et al., 2012).

Chapter 2

Challenges in preventing FSE-related epilepsy: model, predictor and mechanisms

Modeling FSE Recent work in humans, including the prospective FEBSTAT study, has demonstrated that FSE (FS lasting longer than 30minutes) is associated with later epilepsy in children, whereas complex febrile seizures (those lasting 10-30 minutes) do not (Lewis et al., 2014 Berg et al., 1996). Previous work in the Baram laboratory investigated complex febrile seizures (FS ~20 minutes) in a rat model of hyperthermia-induced seizures (Gerth et al., 1997; Dubé et al., 2000,2007,2009). In view of the results in humans, the lab has procedded to model FSE. Indeed, experimental work demonstrated that the duration of the inciting FS drives the development of epilepsy. Rats with longer FS have a higher probability of later life epilepsy, and their spontaneous seizures are longer (Dubé et al., 2010). Thus, it was important to build upon the model of complex FS and create a stable, robust model of eFSE. In the newly established rodent model of eFSE, hyperthermia-induced seizures are maintained for an hour, in analogy to the FEBSTAT study finding that TLE arose in children with median of 55 min-long FSE (VanLandingham et al., 1998; Patterson et al., 2015). We established an eFSE model where hyperthermia-induced seizures are maintained for 60 minutes, with minimal side effects are noted. Specifically, rats do not become alkalotic from hyperventilating due to elevated temperatures or die from the insult. Additionally, no cell death is noted in the hippocampus of eFSE rats (Toth et al., 1998 Dubé et al., 2010; Patterson et al., 2015).

The eFSE model retains important features of the human condition. These include a reliance of the cytokine IL-1β for eFSE initiation and an acute post eFSE inflammatory response (Patterson et al., 2015; Dubé et al., 2005). Furthermore, ~40% of eFSE rats have later-life limbic spontaneous seizures in line with what is found in humans (Choy et al., 2014). Thus that the eSFE model is a valid model for studying predictive markers and mechanisms of TLE and of cognitive problems after eFSE.

Identifying Biomarkers The previous paragraphs indicate that FSE is a significant and likely causal risk factor for developing TLE. However, a major barrier to developing preventive therapies to FSE-related TLE stems from the current inability to identify those who develop TLE after FSE until clinical seizures emerge. Because the mean time to TLE onset following FSE is 8–12 years, a predictive marker should facilitate identification of candidates for future targeted interventions. The optimal surrogate or bio-marker should be non-invasive, quantifiable and amenable to repeating to enable monitoring of disease progression. MRI has most of these characteristics. Indeed several small studies have demonstrated that imaging abnormalities, more specifically increased T2 signal in the hippocampus can occur following FSE (Vanlandingham et al., 1998; Chan et al., 1996; Lewis et al., 2002; Scott et al., 2003, 2006; Cox et al., 1995; Farina et al., 2004). The larger prospective FEBSTAT study has shown that this occurs in approximately 12% of cases (Shinnar et al., 2012). The T2 signal was maximal in CA1 and the Apparent Diffusion Coefficient (ADC) indicates that the T2 signal reflects acute injury rather than gliosis (Lewis et al., 2014). When imaged one year later, almost all the children whose acute post-ictal MRI showed evidence of increased T2 now had a

shrunken hippocampus and usually had evidence of persistent T2 signal (Lewis et al., 2014). The ADC was now consistent with gliosis. Very few of these children had developed epilepsy at this time. In summary, FSE can directly lead to a radiologic picture of hippocampal sclerosis in a small subset of children. These children are now being followed to see if they develop TLE and if they have memory deficits. While clinical TLE may take years to develop, the MRI provides radiologic evidence of hippocampal sclerosis providing a potential marker for injury that can serve as a target for therapeutic interventions to prevent the development of TLE following FSE. MRI has also been used in rodent models of FS and FSE (Dubé et al., 2004, 2009, 2010). MRI signal changes in hippocampal CA1, similar to those found in children were noted one month after the seizures. However, the increased T2 at one month following the FS was not predictive of the development of TLE-like limbic epilepsy. More recently, acute MRI studies, within hours of FSE were investigated as a predictive marker for TLE, employing an established rat model of FSE, where 30–40 % of animals develop TLE (Dubé et al., 2010). These have yielded signal changes in limbic structures that were informative in predicting TLE (Choy et al., 2014). These exciting data are discussed in Chapter 3.

Identifying Mechanisms The eFSE model and the availability of non-invasive imaging techniques that predict epileptogenesis, provide important tools for discovering mechanisms of TLE and cognitive dysfunction after eFSE. Here, I present work demonstrating the use of these techniques in studying these mechanisms. The first is probing the role of inflammation after eFSE and its role in epileptogenesis. I used

predictive imaging technique after eFSE to demonstrate the relationship between inflammation, eFSE and TLE (Chapter 4). Further, I globally blocked inflammation after eFSE and found a reduction in hippocampal hyperexcitability (Chapter 5).

I also investigated the role of the transcription factor Neuron Restrictive Silencing Factor (NRSF) in cognitive deficits derived from eFSE. I demonstrated that blocking NRSF activity after eFSE rescues cognitive deficits found months later (Chapter 6). Together, my thesis examines the consequences of eFSE in a broad and comprehensive manner and uncovers vital mechanisms of epileptogenesis and cognitive dysfunction with clinical relevance.

CHAPTER 3

Novel and non-invasive magnetic resonance imaging predicts which individual with eFSE will develop epilepsy

Overview

Temporal lobe epilepsy (TLE) is a common, often treatment-resistant brain disorder (French et al., 1993; Cendes et al., 1993a). Childhood long febrile seizures, especially febrile status epilepticus (FSE; seizures >30 minutes), are significant risk factors for developing TLE: a history of FSE is found in 35-75% of individuals with TLE (Annegers et al., 1987; Cendes et al., 1993b). Despite significant progress in understanding the mechanisms that underlie epileptogenesis, no preventative treatments are available. A major barrier to developing such therapies stems from the current inability to identify those who develop TLE after FSE until seizures emerge (Mathern et al., 1995; Kelley et al., 2009). Because the mean time to TLE onset following FSE is 8-12 years (Mathern et al., 1995), a predictive marker should facilitate identification of candidates for future targeted interventions.

MRI is quantifiable and repeatable, enabling monitoring of disease onset and progression. MRI at low magnetic-field has been used to study children with FSE and revealed generally unilateral increased T_2 values within 2-5 days (VanLandingham et al., 1998; Scott et al., 2002; Lewis et al., 2014). Similar findings have been observed in immature rodent FSE models employing similar time frames and relatively low-magnetic field MRI systems (Dubé et al., 2004; Jansen et al., 2008). However, it remains unknown if these changes predict epilepsy, and the underlying neurobiological

mechanisms are incompletely understood.

Here, we investigated MRI changes occurring within hours after FSE as potential predictive markers for TLE using a high-resolution high-field scanner. We employed an established rat model of FSE induced by hyperthermia which involves endogenous fever mediators (Dubé et al., 2005a, 2010), in rats at ages when limbic system development approximates that in children with FSE (Avishai-Eliner et al., 2002). Similar to children, 30-40% of animals develop TLE, yet progression to epilepsy is relatively short (months), permitting rapid validation of identified markers (Roch et al., 2002; Grohn and Pitkänen, 2007). Additionally, whereas many factors likely contribute to TLE development following childhood FSE, we have established the causal role of rodent FSE in the subsequent epilepsy. We examined the neurobiological basis of the MRI changes, seeking to identify epileptogenic mechanisms.

At early time-points and using a very high-field magnet (11.7T), novel and specific MRI signal changes were observed in limbic regions, and these changes predicted TLE. The MRI signal changes involved local susceptibility effects derived from the paramagnetic nature of oxygen-poor, unsaturated hemoglobin. They appeared as reduced T_2 on a high-field scanner and likely reflected reduced tissue oxygenation. Additionally, a high-energy and oxygen-demanding process correlated to the T_2 changes: The magnitude and timecourse of the nucleus-to-cytoplasm translocation of high-mobility group box 1 (HMGB1), a molecule considered a sensor of cellular injury (Maroso et al., 2010), paralleled the degree and timecourse of MRI signal changes. Potential clinical

applicability of the TLE-predictive MRI signal was tested using MRI sequences that directly detect susceptibility effects (T_2*). This approach enabled visualization of the predictive MRI signal using lower-field scanners.

Materials and Methods

Animals and induction of experimental FSE All experimental procedures were approved by UC-Irvine or Loma Linda University Institutional Animal Care Committees and conformed to NIH guidelines. Sprague-Dawley-derived rats were maintained in quiet facilities under controlled temperatures and light-dark cycle. Cages were monitored every 12 hours for the presence of pups and the date of birth was considered postnatal day (P) 0. On P2, litters were culled to 10 pups, if needed. When weaned (on P21), rats were housed 2–3 per cage. Male rats were used.

Experimental FSE was induced as previously described (Chen et al., 1999; Dubé et al., 2004; 2010; Koyama et al., 2012). Briefly, on P10, pups were placed in a glass container and their core temperature, which is highly correlated with brain temperature (Dubé et al., 2005b), was increased to approximately 40.5°C (simulating high fever) using a regulated stream of warm air. Core temperatures were measured at baseline, at seizure onset, and every 2 minutes during hyperthermia. Hyperthermic seizures manifest as characteristic behaviors: seizure onset is heralded by a sudden loss of motion (freezing), followed by oral automatisms and forelimb clonus. Seizures progress to body flexion with chewing of an extremity and one or more tonic stage 5 seizures (Racine, 1972). Hyperthermia (39.5 – 41°C) was maintained for ~40 minutes (Dubé et

al., 2010), resulting in behavioral seizures lasting 31.0±0.35 minutes.

Hyperthermic controls were littermates of the experimental rats and subjected to the same duration of hyperthermia, but seizures prevented by treatment with pentobarbital (Nembutal 16-25 mg/kg, i.p) 30 min prior to induction of hyperthermia. An additional control group included littermates of the experimental group that were removed from the cage for the same duration (to control for potential stress) and their core temperatures kept within normal range for age (normothermic controls).

MRI procedure and analysis MRIs were performed on a Bruker Avance 11.7T MR scanner (Bruker Biospin, Billerica), and all quantitative T_2 studies were performed on the same single scanner. Rats were anesthetized for the duration of the imaging using 1.5% isoflurane in 100% O_2 and body temperature was maintained at ~36.5°C with a heated water cushion. A field-of-view of 2.3 cm and a slice thickness of 0.75 mm were used for all scans. T_2-weighted images were acquired using a 2D multi-echo-spin-echo sequence with the following parameters: TR = 4697 ms, TE = 10.21- 100.1 ms, inter-TE=10.21 ms, matrix size = 192 × 192 and number of averages (NA)=2. To examine the relationship between early T_2 changes and epilepsy, 'FSE'-sustaining rats were scanned serially at 2, 18 and 48 h following FSE (n=19). Normothermic controls were scanned on P10 once (*n*=8) or serially (n=14). Hyperthermic controls (n=14) were scanned 2 hours following hyperthermia. Additional groups of rats (6 normothermic controls and 12 FSE) were imaged at both 2 and 4 h, to determine the duration of the obtained signal changes. This sequence was also used to determine relationships

between T_2 and deoxyhemoglobin levels as well as T_2 and HMGB1 translocation.

To probe the relationship between high-field T_2 changes and the deoxyhemoglobin-sensitive T_2* effect, and to enable the visualization of predictive changes in clinically-relevant MRI scanners, a separate rat cohort was imaged on a Bruker Avance 4.7T MRI scanner, and then at 11.7T using the T_2 sequence described above. Rats were scanned 2 h following FSE (*n* = 8), and compared with littermate controls (n=7). T_2* weighted images were acquired with a multi echo-gradient-echo sequence with the following parameters: TR = 500 ms, flip angle = 38.8°, TEs = 3.77- 65.33 ms, inter-TE = 6.84 ms, matrix size = 128 x 128 and NA = 16. Absolute T_2 or T_2* relaxation time values (ms) were calculated by log transform followed by a linear least squares fit on a pixel-by-pixel basis, and T_2 or T_2* maps were generated using in-house software (Matlab, Mathworks, RRID:nlx_153890). T_2 measurements were consistent across the imaging sessions. For example, in the normothermic control rats (n=22), whole brain T_2 across 6 imaging cohorts that spanned 18 months were as follows: cohort 1 (n=4) was 58.1±0.57 ms, cohort 2 (n=3) was 59.9± .26 ms, cohort 3 (n=3) was 57.8 ± 1.7 ms, cohort 4 (n=4) was 57.9 ±0.96 ms, cohort 5 (n=3) was 58.3 ± 0.17 ms, and cohort 6 was 58.9 ± 1.23 ms (mean±sd). No signficant differences were found among these groups (F=1.59, p=0.22).

Images were coded and analyzed without knowledge of treatment group or time of imaging to ensure there was no bias when the measurements were performed. Regions were delineated manually separately in the left and right hemisphere: MRI signal changes are most often unilateral and universally asymmetric in children after FSE and

in adults with epilepsy after FSE. We have previously identified unilateral hippocampal changes on MRI (Dubé et al., 2009, 2010) in this model of FSE, similar to those observed in children with FSE. Thus, we performed separate measurements and analyses of left and right amygdala, hippocampus, medial thalamus and other bilateral limbic structures.

T_2 values were measured using ImageJ software (version 1.25l, NIH, Bethesda, RRID:nif-0000-30467) the regions of interest (ROIs) were defined on grey scale maps, and a dynamic range of 0-100 ms was used. For the figures (e.g. Fig 1), we used a color map and reduced the dynamic range (40-80 ms) to highlight the differences among groups. In 4 rats (3 control and 1 FSE) image artifacts prevented T_2* measurements in basolateral amygdala.

Because of the established unilateral or assymetric nature of the epilepsy focus and the MRI changes after FSE-related epilepsy in humans and rodents, the lower side was analyzed for all of the groups and all of the comparisons.

Figure 3.1. Brain T2 is reduced 2 h after FSE. A–C, Representative color-coded quantitative T2 maps 2 h after the end of hyperthermia from a normothermic (A), hyperthermic (B), and FSE (C) rat. Note that the reduced T2 values occur across the entire brain in the FSE rat. D, Regions of interest are highlighted on a rat atlas. E, T2 values time course after FSE and in normothermic 10-d-old control rats. A reduction of T2 values over the experimental period, characteristic of development, were observed in controls. T2 decreased significantly in a time-dependent manner in FSE rats (n=19) compared with controls (n=14, F=4.11, p=0.035). The largest effect was observed 2 h after FSE (p=0.001) and a significant effect was also observed at 18 h (p=0.007). Blue indicates normothermic control (NT-C) rats and red the FSE rats. Statistical significance was determined by repeated-measures ANOVA followed by post hoc analyses with t tests that were adjusted for multiple-comparisons with Bonferroni's correction. (F) Seizures, not hyperthermia, led to the most robust T2 reduction. T2 values for the FSE group were significantly lower than those of either normothermic (n =22, p=0.001) or hyperthermic (n=14, p=0.014) control groups, indicatingthat brainT2 reductions in FSE rats resulted from hyperthermia-induced seizures and not from hyperthermia. Statistical significance was determined by ANOVA followed by post hoc analysis with Tukey's honestly significant differences (HSD) test. (G) A subset of FSE rats had significantly lower brain T2 values compared with the normothermic controls, which raised the possibility that the reduced T2 values might predict epileptogenesis. T2 values in 9 of 19 FSE rats lay more than 2 SDs from the normothermic controls. Dotted line indicates 2SDs from mean of NT-C rats (n=22). Circles indicate individual rats; blue circles are NT-C rats and red circles are FSE rats. Data are presented as mean SEM. HT-C,

Hyperthermic control; BLA, basolateral amygdala; MEA, medial amygdala; MThal, medial thalamus; DH, dorsal hippocampus; VH, ventral hippocampus. *Statistically significant at $p<0.05$.

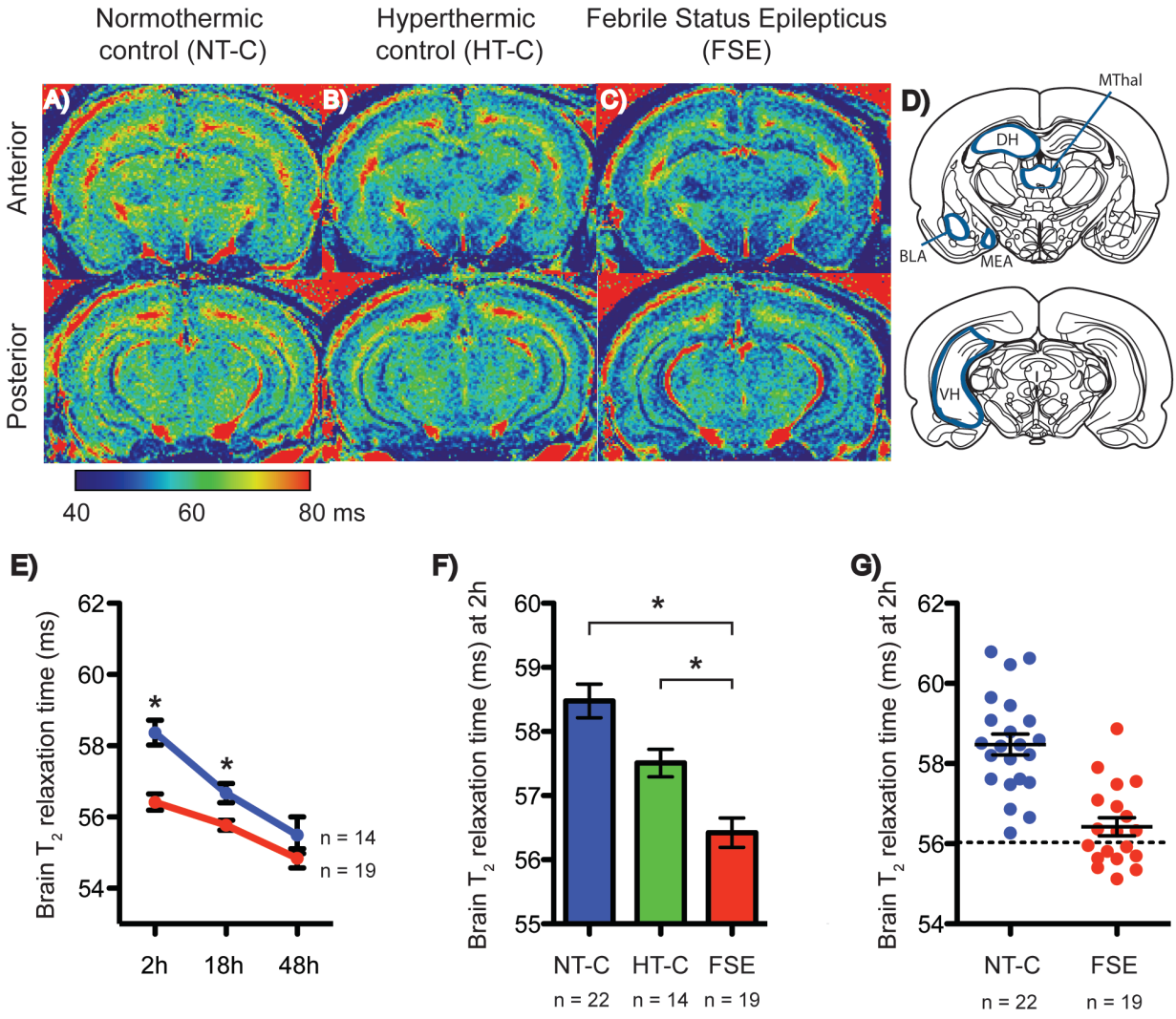
Normothermic control (NT-C)
Hyperthermic control (HT-C)
Febrile Status Epilepticus (FSE)
A)
B)
C)
Anterior
Posterior
40
60
80 ms
D)
MThal
DH
BLA
MEA
VH
E)
Brain T2 relaxation time (ms)
62
60
58
56
54
2h
18h
48h
n = 14
n = 19
F)
Brain T2 relaxation time (ms) at 2h
60
59
58
57
56
55
NT-C
HT-C
FSE
n = 22
n = 14
n = 19
G)
Brain T2 relaxation time (ms) at 2h
62
60
58
56
54
NT-C
FSE
n = 22
n = 19

EEG electrode implantation One month after FSE (*n* = 19 FSE; 16 normothermic controls and 7 hyperthermic controls), bipolar electrodes (Plastics One) were implanted bilaterally in the hippocampus (AP: 3.3; L: 2.3; V: -2.8 mm with reference to bregma), a cortical electrode was placed over the parietal cortex (AP: 2; L: -2 mm), and a ground electrode over the cerebellar cortex. Cortical and hippocampal recordings were conducted in freely moving rats, and electrode placement was verified *post hoc*.

Long-term digital video EEG recordings and analysis Video-EEG monitoring began five days following electrode implantation. EEG recordings were synchronized to video and conducted for a period of up to 10 months. EEG monitoring time was increased progressively, to optimize seizure detection. Prior work in the same model indicated that epilepsy does not commence prior to a month after the inciting FSE, and its incidence increases over the subsequent 2-8 months (Dubé et al., 2006, 2010); this is in accord with a long latent period in humans (e.g., French et al., 1993). Therefore, and in view of limited recording capacity, we sampled progressively over the course of 10 months: In the first month, we monitored for 112 hours (15.6% of a month), 180 hours (25%) in the penultimate month, and 206 hours (28.6%) in the final month. The recordings in the later months consisted of several segments of continuous 24/7 monitoring lasting 3-5 days, enabling sampling of circadian variability and of several consecutive days. Overall, >37,000 hours of video EEG were acquired, including 595±57 hours per normothermic control rat, 430±41 hours per hyperthermic control rat and 1319 ± 89 hours per FSE rat.

EEGs were coded and scanned visually for spike series and seizures by 2 experienced investigators who were blinded to group identity (Dubé et al., 2010), and then re-analyzed using a seizure-detection software (LabChart version 7.3, ADinstruments, CO USA). The concurrent video recordings were analyzed for behavioral manifestations of the apparent seizure. Only events with both EEG and behavioral changes and that lasted over 20 seconds were classified as seizures. We evaluated typical behaviors associated with limbic seizures, including sudden cessation of activity, facial automatisms, head bobbing, prolonged immobility with staring, alternating or bilateral clonus, rearing and falling (Racine, 1972). Rats were considered epileptic if they had at least one documented seizure as defined above. Spike series were defined as clusters of spikes with uniform interspike intervals. A cluster had a minimum of 5 spikes and lasted a minimum of twelve seconds.

Golgi method visualization and analysis of neuronal dendritic structure Golgi impregnation and analysis were performed as described previously (Chen et al., 2004; Ivy et al., 2010). Hemispheres were immersed in Golgi–Cox solution for 10 days followed by a 2-5 day immersion in 30% sucrose, both in the dark. Using a vibratome, 200 μM coronal sections containing dorsal hippocampus were mounted on coated slides and allowed to dry for 1-2 hours. Sections were developed with 14% ammonium hydroxide for 30 minutes followed by 30 minutes in Kodak fixative. Sections were washed and dehydrated in increasing dilutions of ethanol and were finally coverslipped with Permount.

Fully impregnated neurons were sampled for this study without knowledge of treatment group. We were careful to pick neurons from a specific anatomical location within hippocampus to avoid potential confounders derived from location-dependent morphology of CA3 pyramidal cells. Neurons were sampled in dorsal CA3b within 150 microns of the CA3b/CA3c boundary. Neurons were reconstructed in two dimensions using the camera-lucida method without knowledge of treatment group (3-7 neurons per rat, 3-4 rats per treatment group). Dendritic arborization was analyzed using the Sholl method for dendritic complexity and length, and compared among treatment groups.

Visualization and analysis of HMGB1 translocation For this study, normothermic controls (n=9) and FSE littermates (n=24) were used. Rats were deeply anesthitized and transcardally perfused with 4% paraformaldehyde. Brains were removed, post-fixed for 90 minutes and then cryoprotected in 30% sucrose. Free-floating sections were used for HMGB1 ICC using standard methods (Dubé et al., 2010), and rabbit anti-HMGB1 (1:1,000; Abcam, cat #ab18256, RRID: AB_444360; Maroso et al., 2010). The reaction product was visualized using a 3,3'-diaminobezidine (DAB) solution. We evaluated both the number of cells expressing HMGB1 and the proportion of these cells where HMGB1 was translocated from nucleus to cytoplasm, en route to release. HMGB1 translocation was considered absent when the immunoreactive (ir) product was confined to the nucleus. Translocation was considered present when HMGB1-ir filled the soma, and often also the dendrites, delineating the neuronal contour. All analyses were performed without knowledge of treatment group.

Measurements of venous blood deoxyhemoglobin To examine the relationship between T_2 and deoxyhemoglobin, a separate cohort of FSE (n = 12) rats and normothermic controls (n = 7) were imaged. One FSE rat was removed from analysis because of ventricular enlargement indicating a pre-existing abnormality. Because of technical infeasibility of sampling venous cerebral blood, deoxyhemoglobin analysis was performed on cardiac right ventricle blood, also in view of the fact that cerebral metabolism accounts for 25-50% of total body oxygen consumption (Clarke and Sokoloff, 1999). Sampling was performed immediately after MRI under terminal anesthesia, and venous blood samples were placed on ice and analyzed within an hour. Briefly, using a 30-gauge needle connected to a heparinized syringe, a 0.15-0.2 ml venous blood sample from the right cardiac ventricle was withdrawn, placed on ice and analyzed using a hemoximeter (OSM3, Radiometer). Deoxyhemoglobin concentration was calculated using the following formula:

> Deoxyhemoglobin concentration = 100 - (hemoglobin oxygen saturation + carboxyhemoglobin concentration + methemoglobin concentration).

Statistics The following methods were used: (1) To determine if MRI T_2 values time course differed among groups we performed two-way repeated measures analysis of variance (ANOVA) followed by *post hoc* analyses using t-tests with Bonferroni correction for multiple comparisons. (2) Independent t-tests were used to compare the inciting FSE parameters (duration, number of stage 5 seizures, latency to onset from initiation of hyperthermia, seizure threshold temperature, and average core temperature during hyperthermia), of the rats that progressed on to epilepsy and those that did not. (3) One-way ANOVA followed by the Tukey's *post-hoc* test was used to determine the

differences at 2 hours between the FSE, normothermic and hyperthermic controls, for investigating T_2 in the hippocampus and amygdala among controls, non-epileptic and epileptic rats. To determine if the T_2 change was a result of localized regional changes, the same analyses were also performed on the predictive regions following normalization to individual whole brain T_2 values. (4) To investigate the inter-relationships between regional T_2 changes, principal axis factor analysis with varimax rotation was used to derive underlying factors that could describe these regional patterns following FSE. Limbic regions (dorsal and ventral hippocampus, distinct amygdala nuclei, entorhinal cortex, piriform cortex), and limbic-interconnected regions (medial thalamus), as well as non-limbic regions (cerebellum, corpus callosum) and extra-brain tissue (tongue muscle) were included. The Benjamini-Hochberg method was employed to avoid false discovery.

For all bilateral regions in all groups, the lower of the two values were used (see detailed methodology in the MRI analysis section). Scree plots were examined to determine the number of derived factors, and factor scores for individual rats were obtained. In addition, the same analyses were performed for regional T_2 values normalized to whole brain of individual rats. (5) To determine whether MRI performed better than chance at predicting epilepsy following FSE, derived factor scores and regional MRI data from the FSE group under went receiver operating characteristic (ROC) curve analyses. The area under curve (AUC) was then compared to chance (AUC = 0.5). (6) Pearson correlation was used to determine the relationships between the values of T_2 signals and deoxyhemoglobin levels, deoxyhemoglobin levels and

seizure duration, deoxyhemoglobin levels and mean core temperature during the inciting seizure, and between T_2 values at 11.7T and T_2* values at 4.7T. This was also calculated for the relationship between the 2 and 4 hour T_2 signals in the basolateral amygdala and the medial thalamus to determine if the signal persisted. An independent t-test was used to determine if the levels of blood hemoglobin were different between FSE rats and control rats. (7) HMGB1 translocation analyses and dendritic complexity and length comparisons employed one-way ANOVA with Bonferroni *post-hoc* tests to correct for multiple comparisons.

Statistical analyses were performed using IBM SPSS software version 20.0 (IBM SPSS Inc., Chicago). Graphs were generated either on SPSS or Prism 5 software (GraphPad, San Diego). Data are presented as mean ± SEM unless otherwise stated and significance was set at $p<0.05$.

Results

Development of limbic epilepsy after experimental FSE Chronic video-EEG monitoring was conducted for a period of up to 10 months. Prior work in our model indicated that epilepsy did not commence prior to a month following the insult (Dubé et al., 2006, 2010). Therefore, we sampled progressively over the course of 10 months: 15.6% of the time during the first month and 28.6% of time during the final month. The recordings in the later months consisted of several segments of continuous 24/7 monitoring lasting 3-5 days, enabling sampling of circadian variability and potential clustering during consecutive days. Overall, >37,000 hours of video EEG was acquired, including 595±57

hours per normothermic control rat, 430±41 hours per hyperthermic control rat and 1319±89 hours per FSE rat. Spontaneous seizures were detected in 6 of 19 rats following FSE (32%), comparable to previous reports (Table 1 and Fig. 2) (Dubé et al., 2006, 2010), and to estimates in children (Hesdorffer et al., 2007). The epileptic rats had 0.07 seizures/day of recording which, in view of the incomplete recording, is likely to be an underestimate of the true seizure rate. The sparse seizures (Table 1) are in line with many epilepsies generated in immature rodents (e.g., Scantlebury et al., 2005), and the often sparse seizures in community based human studies (Lindsay et al., 1979, Olafsson et al., 2005; Chong et al., 2013; Ablah et al., 2014). The number and duration of the seizures in the epileptic rats is shown in Table 1, and examples are found in Fig. 2. The spontaneous seizures were limbic in semiology, associated with sudden freezing, facial automatisms, head nodding and forelimb clonus (Racine stages 0-3), and averaged 95.1 ± 12.6 seconds in duration. Behavioral seizures coincided with ictal EEG activity that was detected in one or both hippocampal EEGs (Table 1; Fig. 2). Neither seizures nor spike series were detected in the normothermic (n=16) or hyperthermic (n=7) controls, nor in over 10,000 recorded hours in similar previous control cohorts.

The probability of developing epilepsy was not influenced by any parameter of the inciting hyperthermia or FSE (Fig. 2), including length of the hyperthermia (non-epileptic 40.67±0.42 min; epileptic 40.46±0.24 min; p=0.68), length of the experimental FSE (31.2±0.43 min; 30.7±0.67 min; p=0.48), number of stage 5 events (2.0±0.45; 1.8±0.40; p=0.79), latency to onset of FSE from initiation of hyperthermia (260±10.1 sec;

259±16.7 sec; p=0.99), threshold temperature (40.47±0.26°C; 40.17±0.52°C; p=0.62) or average core temperature during hyperthermia (40.5±0.07°C; 40.6±0.1°C; p=0.65). Because seizures in this model of FSE-related TLE are sparse, we examined for other parameters that might distinguish epileptic from non-epileptic rats. We studied epileptic

Rat	Seizure number Duration (sec)	Mean seizure Duration (sec)	Racine scale	Total hours recording / rat	Seizures / recording day	Number spike trains Duration (sec)
6	4 36, 22, 177, 23	64.5	2, 2, 2, 2,	953	0.1007	1 48
7	3 95, 145, 220	153.3	2, 1, 2	2013	0.0358	18 2714
8	8 154, 57, 85, 93, 223, 60, 26, 96	99.2	2, 3, 2, 2, 2, 2, 2, 2	1196	0.1605	3 148
9	1 75	(75)	1	1052	0.0228	2 255
17	4 29, 50, 109, 161	87.2	2, 2, 2, 2	1742	0.0511	0
26	3 52, 76, 124	84	2, 2, 3	1145	0.0629	8 288
Mean ± SEM	3.8 ± 0.9	95.1 ± 12.6	2 ± 0.9	Total: 8101	0.0681	Spike trains: 5.3 Mean duration: 107.9

Table 3.1: Characteristics of spontaneous limbic behavioral/electrographical seizures in adult epileptic rats

Figure 3.2: The severity and duration of the inciting FSE and the resulting epileptogenesis. Within the timeframe of the experimental FSE, neither the duration of hyperthermia nor the duration of the seizures *(*A(i)) or the number of stage 5 seizures during FSE (A(ii)) predicted which rats progressed on to epilepsy. Statistical significance was determined by independent samples t-test; non-epileptic n=13, epileptic n=6. Data presented as mean ± SEM. *(*B) Epilepsy was found in six of 19 rats, and representative EEG traces of spontaneous seizures from each of the six epileptic rats are shown (see Table 1). Areas in the boxes are shown in expanded time-scales. (C) Representative EEG traces from three epileptic rats with interictal spike trains. These were observed in five epileptic rats. (D) Hippocampal pyramidal cells from epileptic rats had reduced dendritic arborization compared with FSE rats not exhibiting spontaneous seizures (NonEpi) and with normothermic controls (NT-C). Shown are (i) representative Golgi-impregnated sections, (ii) traces of reconstructed dorsal hippocampus CA3b neurons, (iii) Sholl analysis of apical dendrites, and (iv) total dendritic length, n=3-4 rats per treatment group. Data presented as mean ± SEM. Abbreviations: NonEpi, non-epileptic; Epi, epileptic, NT-C, normothermic controls.

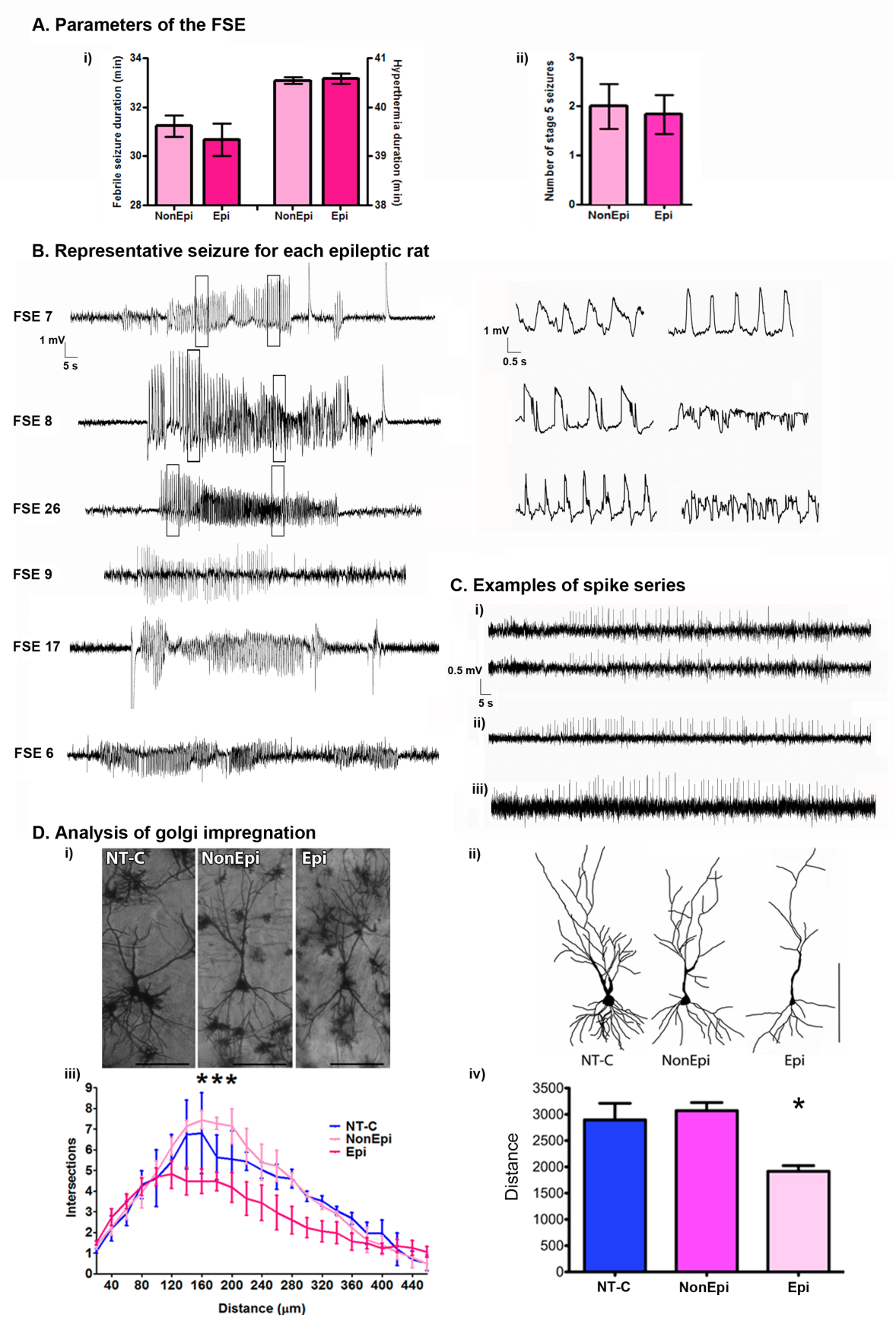
A. Parameters of the FSE
i)
Febrile seizure duration (min)
Hyperthermia duration (min)
NonEpi
Epi
NonEpi
Epi
ii)
Number of stage 5 seizures
NonEpi
Epi
B. Representative seizure for each epileptic rat
FSE 7
1 mV
5 s
FSE 8
FSE 26
FSE 9
FSE 17
FSE 6
1 mV
0.5 s
C. Examples of spike series
i)
0.5 mV
5 s
ii)
iii)
D. Analysis of golgi impregnation
i)
NT-C
NonEpi
Epi
ii)
NT-C
NonEpi
Epi
iii)
***
Intersections
NT-C
NonEpi
Epi
Distance (µm)
iv)
Distance
*
NT-C
NonEpi
Epi

A relationship between T_2 values in specific brain regions, but not in whole brain, and the development of epilepsy The results presented above demonstrated that (1) experimental FSE led to significant decreases in MRI T_2 signal in a subgroup of rats and, (2) in parallel, that limbic epilepsy developed in a subgroup of FSE rats. Therefore, we examined whether the MRI changes 2 h post FSE were predictive of epilepsy in individual subjects. We found that whole brain T_2 values did not distinguish the epileptic rats (mean difference from non-epileptic rats=-0.32±0.56 ms, p=0.84), nor did T_2 values in cranial muscles (0.19±0.43 ms, p=0.90). These findings suggested that global, brain-wide T_2 signal changes that might result from systemic processes do not predict epileptogenesis.

Because TLE involves the limbic circuit and, in children, limbic T_2 changes have been described in the context of FSE and TLE, we measured T_2 values of several limbic structures. We found asymmetry of T_2 values between left and right hippocampus and amygdala in line with findings in children after FSE (VanLandingham et al., 1998; Shinnar et al., 2012; Lewis et al., 2014) and our previous studies in the immature rodent FSE model (Dubé et al., 2009, 2010). Typically, the abnormal MRI delineates the location of the unilateral epilepsy focus in TLE (e.g., Lewis et al., 2014). Based on these facts we focused on comparing, in all groups, the T_2 values in the side with lower values. In individual rats, unilateral T_2 values were reduced in FSE rats that became epileptic compared to those in rats that did not (Fig. 3*A-I*). Specifically, T_2 values in the basolateral amygdala of FSE rats that developed epilepsy were significantly lower than those in controls and in FSE non-epileptic rats (mean difference from controls=-

3.29±0.51 ms, p<0.001; mean difference from non-epileptic rats =-1.52±0.52 ms, p=0.017; Fig. 3G). A similar finding was obtained in medial amygdala (-2.43±0.39 ms, p<0.001; -0.99±0.39 ms, p=0.043; Fig. 3H). Using the Benjamini-Hochberg method to correct for the false discovery rate (potentially resulting from multiple comparisons) for the 6 tests conducted (basolateral amygdala, medial amygdala, medial thalamus, whole brain, dorsal and ventral hippocampus), the adjusted probabilities were as follows: Basolateral amygdala, 0.03; medial amygdala, 0.084; medial thalamus, 0.1; whole brain, 0.648; dorsal hippocampus, 0.375; ventral hippocampus, 0.93. Whereas these changes were moderate in absolute terms, they represent a large effect size: Using Cohen's d, an established measure of effect size where the threshold for a large effect is 0.8, we found for the basolateral amygdala changes a Cohen's d of 1.77, and for the medial amygdala = 1.32. Hippocampal T_2 values were also significantly reduced in epileptic compared with control rats (dorsal: -2.96±0.67 ms, p<0.001, Fig. 3I; ventral: 2.26±0.55 ms, *p*<0.001). However, the values did not distinguish epileptic from non-epileptic rats (-0.54±0.68 ms, p=0.71; 0.6±0.55 ms, *p*=0.99).

These analyses demonstrated that signal changes in specific brain regions but not in the whole brain distinguished epileptic and non-epileptic rats, and suggested that the amygdala T_2 values may be a predictive biomarker of epileptogenesis. Further support for the regional specificity of limbic signal derived from analysis of regional T_2 values normalized to the T_2 of whole brain in each animal (thus controlling for potential systemic or whole brain confounders). Comparing epileptic to the non-epileptic and control rats, we found that the basolateral amygdala T_2 values (p=0.02 and p=0.024,

respectively) of epileptic rats remained significantly different from non-epileptic and control rats (Fig. 3J). In the medial thalamus, differences between the epileptic and control rats were still found (p<0.001), but did not distinguish the epileptic from the non-epileptic rats (p=0.44).

To examine objectively the efficacy of the amygdala T_2 values as a predictive marker of epilepsy following FSE, we employed an independent unbiased measure, i.e. receiving operator characteristic (ROC) curve analysis. ROC curve analyses demonstrated that T_2 values in both basolateral and medial amygdala (area under curve (AUC)=0.91±0.08, p=0.005; AUC=0.82±0.10, p=0.028 respectively; Fig. 3K) predicted epileptogenesis better than chance, as did T_2 values in the medial thalamus (AUC = 0.78 ± 0.11, p = 0.05, Fig. 3*K*). Whole brain (AUC = 0.59±0.15, p=0.54), dorsal hippocampus (AUC=0.67±0.17, p=0.25) or ventral hippocampus values were not predictive (AUC=0.49±0.14, p=0.93, Fig. 3L). Exploratory factor analysis followed by the ROC curve procedure was also performed on raw T_2 values for limbic regions as well as on values normalized to brain T_2 values of each animal (Tables 2 and 3), and the differences remained robust.

	Factor		
Region	1	2	3
Entorhinal cortex	0.89		
Dorsal hippocampus	0.74	0.51	
Piriform cortex	0.65		
Cerebellum	0.63		
Medial amygdala		0.83	
Basolateral amygdala		0.80	
Medial thalamus		0.80	
Muscle			0.76
Ventral hippocampus	0.63		0.71
Corpus callosum		0.52	0.55
Variance (%)	28.15	27.61	18.58
ROC curve AUC	0.5 ± 0.18	0.91 ± 0.07	0.35 ± 0.13
p-value	1.0	0.005	0.29

Table 3.2: Exploratory factor analysis on T_2 values revealed distinct patterns that predicted epilepsy

T_2 values of the lower side in all groups and all bilateral regions were analyzed together using exploratory factor analysis to identify possible patterns of T_2 changes. Three patterns (factors) were identified. Notably, factor 2 was highly represented by the basolateral and medial amygdala and the medial thalamus. For clarity, loadings<0.5 are not shown. Factor scores were then derived and ROC curve analysis was performed, indicating that factor 2 was predictive of epilepsy. Non epileptic group, n=13; epileptic group, n=6.

	Factor		
Region	1	2	3
Medial amygdala	0.84		
Basolateral amygdala	0.75		
Medial thalamus	0.75		
Piriform cortex		0.87	
Ventral hippocampus		0.74	
Entorhinal cortex		0.73	
Dorsal hippocampus			
Muscle			0.74
Cerebellum			−0.59
Corpus callosum			0.52
Variance (%)	21.61	21.09	16.11
ROC curve AUC	0.89 ± 0.08	0.56 ± 0.13	0.39 ± 0.13
p-value	0.009	0.66	0.48

Table 3.3: Exploratory factor analysis on T_2 values that were normalized to brain T2 revealed distinct patterns that were similar to raw T2 values

To remove possible systemic effects that could influence the regional T_2 measurements, each region as normalized to the whole-brain T_2 value for each rat and exploratory factor analysis was performed to identify possible patterns. Three patterns (factors) were found, indicating that certain regions changed together. Notably, factor 1 was highly represented by the basolateral and medial amygdala and the medial thalamus. This was a similar pattern of changes identified without normalization for systemic effects, suggesting that, after FSE, these regions tend to change together. For clarity, loadings<0.5 are not shown. Factor scores were then derived and ROC curve analysis was performed, indicating that factor 1was predictive of epilepsy. Non epileptic group, n=13; epileptic group, n=6.

Together, the region-of-interest approach (focused on limbic structures) and the independent unbiased mathematical approach (exploratory factor- followed by ROC curve analyses) that reduced multiple comparisons (Tables 2 and 3) suggested that T_2 signal reduction (using an 11.7 Tesla magnet) in specific limbic brain regions and at 2 h after FSE are predictive of eventual limbic epilepsy. Therefore, we assessed the persistence of these changes, their origin, and their applicability to clinical settings. Assessing the persistence of the signal, we found that by 18 hours, regional T_2 signals no longer distinguished the epileptic and non-epileptic rats (mean difference of epileptic from non-epileptic rats in basolateral amygdala was -1.03±0.92 ms, p=0.17; medial amygdala was -0.74±0.41, p=0.12; medial thalamus was -0.36±0.47, p=0.45; basolateral amygdala AUC = 0.29 ± 0.14, p = 0.15; medial amygdala AUC=0.73±0.16, p=0.11; medial thalamus AUC = 0.39 ± 0.13, p = 0.43). Experiments using an additional rat cohort showed that the signal persisted at 4 hours following the experimental FSE (correlation between 2 and 4 h T_2 values for basolateral amygdala r=0.69, p=0.002, and medial thalamus r=0.88, p<0.001). These data suggested that the useful time-window for detection of MRI signals that predicted epileptogenesis was ~2-4 hours after the termination of FSE.

Figure 3.3 Amygdala T_2 values 2 hours after FSE distinguish rats that progressed on to epilepsy. Representative color-coded quantitative T_2 maps of a normothermic control, a non-epileptic and an epileptic FSE rat (A-F). Basolateral amygdala is highlighted in the black box. Scale bar indicates 1 mm. T_2 values in the basolateral amygdala (A-G) distinguished the epileptic group from the non-epileptic group, indicating that amygdala T_2 values were predictive of epilepsy: epileptic group compared with normothermic controls $p<0.001$, epileptic group compared with non-epileptic group $p = 0.017$. Similar results were found for medial amygdala (H) ($p<0.001$ and $p=0.043$). *(*I) Hippocampal T_2 did not distinguish epileptic from non-epileptic groups: dorsal hippocampus $p<0.001$, $p=0.71$, ventral hippocampus $p<0.001$, $p=0.99$. (J) To exclude general or systemic effects, amygdala T_2 values were normalized to total brain values. The normalized values, reflecting local changes in the basolateral amygdala, separated the epileptic rats from non-epileptic and control animals; epileptic vs non-epileptic rats $p=0.02$, epileptic vs control $p=0.024$; black line signifies the mean of the controls, and dotted line the SEM of controls). (K) Receiver operating characteristics (ROCs) for limbic structures and brain T_2 values from the FSE rats indicated that amygdala and medial thalamus predicted epilepsy: BLA: area under the cureve (AUC) = 0.91±0.08, p=0.005, MEA 0.82±0.10, $p=0.028$, MThal 0.78±0.11, $p=0.05$. *(*L) Neither hippocampal regions nor brain T_2 predicted epilepsy any better than chance; dorsal hippocampus: 0.67±0.17, p=0.25; ventral hippocampus: 0.49±0.14, p=0.93; brain: 0.59±0.15, p=0.54. Ideally, a predictive marker will have a high sensitivity (near 1.0; Y axis) and specificity ([1-specificity] near zero; X axis). Dotted line indicates AUC of 0.5, a reference to chance. Statistical significance was determined by ANOVA followed by

post hoc analysis with Tukey's HSD. Data presented as mean±SEM. Values were compared among the sides with lower T_2 values in all rats and all groups. Abbreviations: AUC, area under the curve; NT-C, normothermic control; NonEpi, non-epileptic; Epi, epileptic; BLA, basolateral amygdala; MEA, medial amygdala; MThal, medial thalamus; DH, dorsal hippocampus and VH, ventral hippocampus. Normothermic controls n=14, non-epileptic group n=13, epileptic group n=6. * statistically significant $p<0.05$.

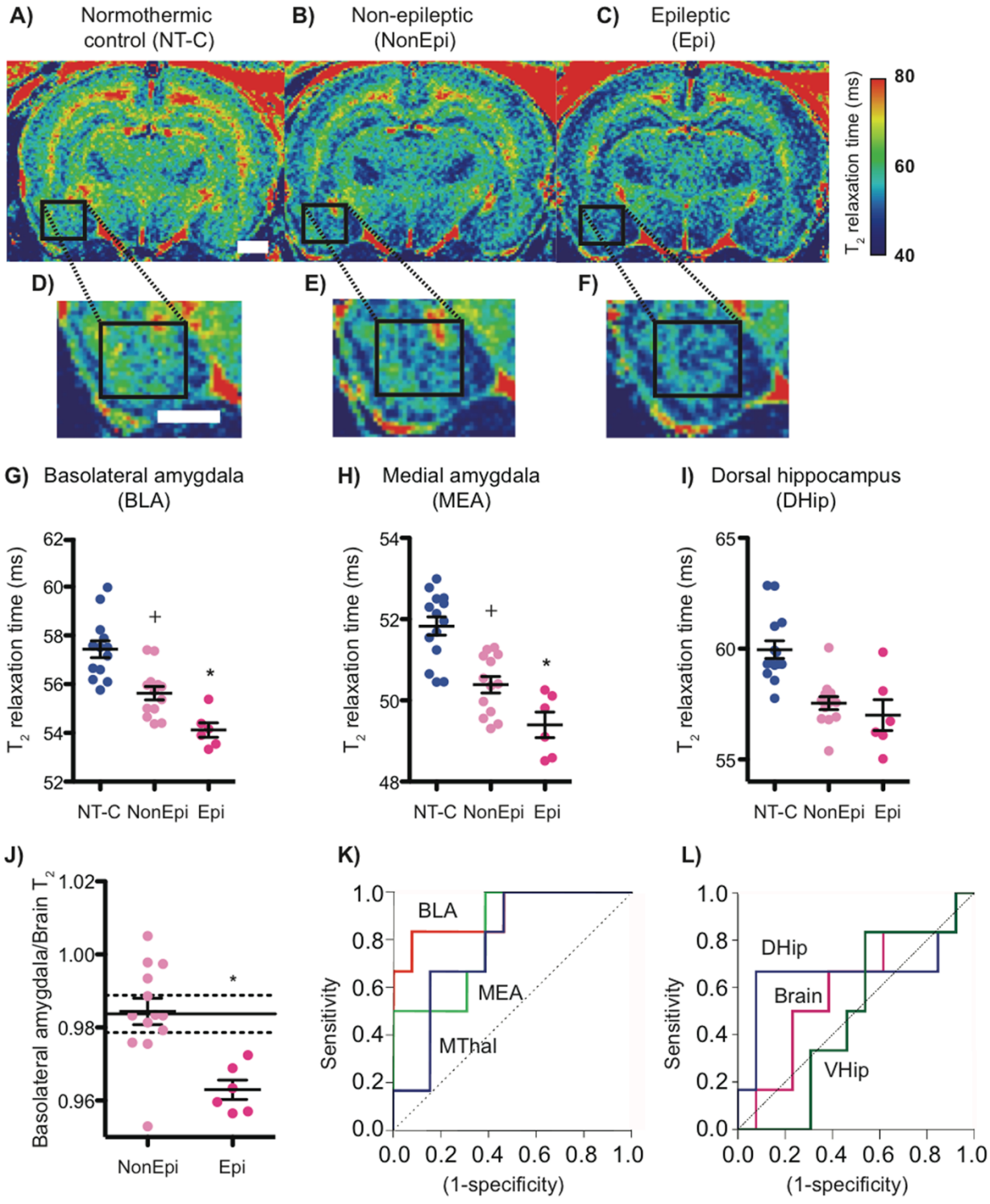
A) Normothermic control (NT-C)
B) Non-epileptic (NonEpi)
C) Epileptic (Epi)
T2 relaxation time (ms)
80
60
40
D)
E)
F)
G) Basolateral amygdala (BLA)
H) Medial amygdala (MEA)
I) Dorsal hippocampus (DHip)
T2 relaxation time (ms)
NT-C NonEpi Epi
J)
Basolateral amygdala/Brain T2
NonEpi Epi
K)
L)
Sensitivity
(1-specificity)
BLA
MEA
MThal
DHip
Brain
VHip

The relationship of the observed reduction in T_2 at very high-field MRI and increased deoxyhemoglobin levels T_2 reduction on MR imaging can be caused by paramagnetic substances including oxygen-poor, unsaturated hemoglobin, which induce local susceptibility effects. These effects, leading to reduced T_2 values, are proportional to magnetic field strength, and our studies employed a high-field, 11.7T magnet (Fig. 4A). Therefore, we queried if the reduced T_2 values might result from enhanced oxygen utilization that endured beyond the FSE itself, and consequent increase in deoxyhemoglobin levels. In a separate cohort we measured venous blood deoxyhemoglobin levels and correlated these with brain and extracranial muscle T_2 values in the same individual rats of both control- and FSE-groups. T_2 measurements in brain correlated strongly with deoxyhemoglobin levels (r=-0.73; p=0.001) suggesting that increased deoxyhemoglobin contributed to the T_2 decrease following FSE (Fig. 4*B*). A weaker correlation was obtained for extracranial muscle T_2 and deoxyhemoglobin (r=0.47; p=0.057). These correlations pertain to systemic venous blood because we failed technically to obtain sufficient quantities of cerebral venous blood to measure reliably hemoglobin levels. However, at developmental ages examined here, 25-50% of oxygen utilization involves cerebral metabolism (Clarke et al., 1999). The robust correlation obtained here between venous blood and T_2 probably underestimated the contribution of cerebral venous deoxyhemoglobin to the reduced T_2 relaxation times.

Neither mean core temperature nor duration of the inciting febrile seizures correlated with deoxyhemoglobin levels, excluding the possibility that the increased

deoxyhemoglobin could be a result of overt differences in the inciting hyperthermia and seizures (r=-0.48, p=0.89; r=-0.11, p=0.76, respectively). Notably, total hemoglobin levels did not differ between the groups (control 10.83±0.24 g/dL and FSE 10.98±0.34 g/dL, p=0.72).

Figure 3.4: Reduced T_2 values after FSE correlate with increased deoxyhemoglobin levels. (A) T_2 values were likely reduced because of a paramagnetic effect of deoxyhemoglobin and increased levels of unsaturated (deoxy)hemoglobin following FSE. This paramagnetic effect increases as a function of magnetic field strength. Significant correlation of reduced (B) brain and (C) muscle T_2 values with increased blood deoxyhemoglobin levels (-0.73, p=0.001; -0.47, p=0.057 respectively). Values were compared among the sides with lower T_2 values in all rats and all groups. Scatter plot of individual rats, with blue circles indicating normothermic control rats (n=7), and red circles the FSE rats (n=11).

A)

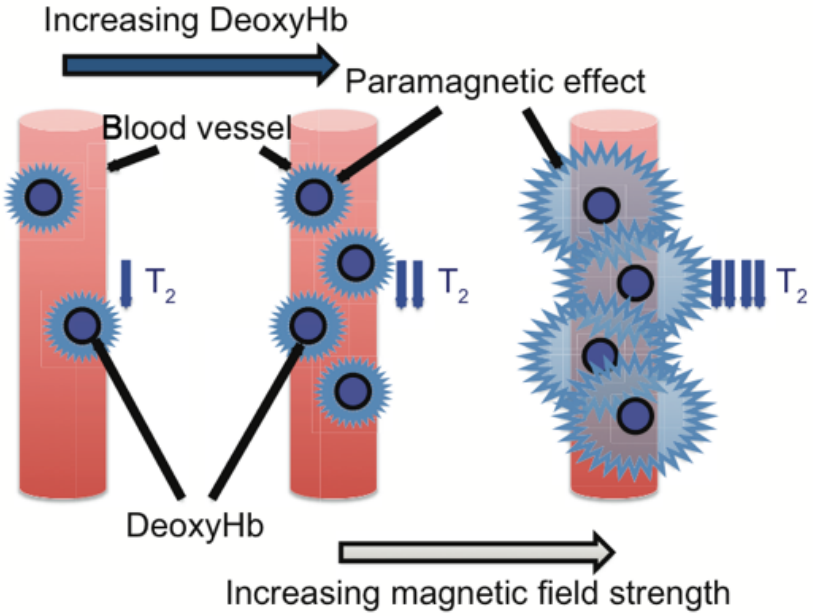
Increasing DeoxyHb
Paramagnetic effect
Blood vessel
T2
T2
T2
DeoxyHb
Increasing magnetic field strength

B)

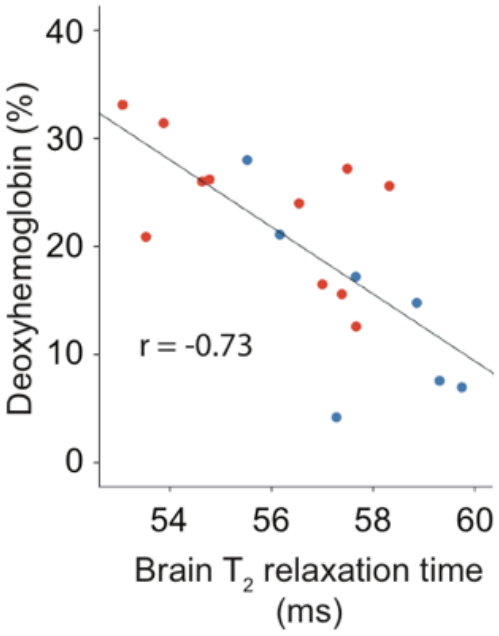
Deoxyhemoglobin (%)
40
30
20
10
0
r = -0.73
54
56
58
60
Brain T2 relaxation time (ms)

C)

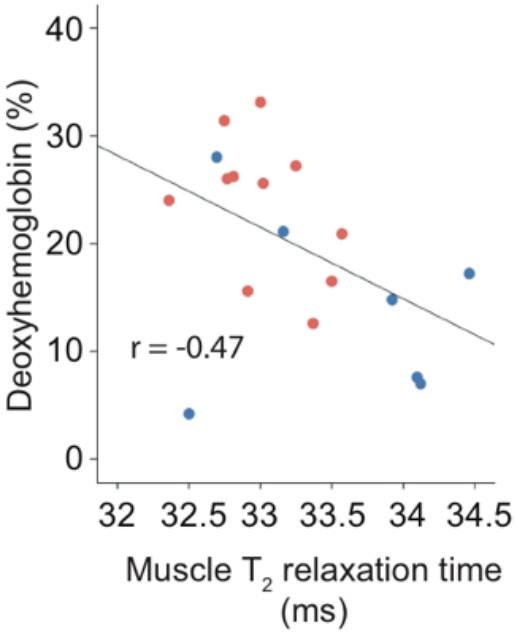
Deoxyhemoglobin (%)
40
30
20
10
0
r = -0.47
32
32.5
33
33.5
34
34.5
Muscle T2 relaxation time (ms)

Early, energy-demanding inflammatory processes correlate with the MRI changes in a subset of FSE subjects Several factors might result in increased deoxygenated hemoglobin levels, and these often involve a mis-match between blood supply and tissue metabolic rates (e.g., Pereira de Vasconcelos et al., 2002; Schridde et al., 2008; DeSalvo et al., 2010). Here we tested the idea that the increased deoxygenated hemoglobin derived from augmented oxygen extraction resulting from energy-demanding cellular processes. These, in turn, may signify the initial steps in the epileptogenic cascade. We focused on inflammatory mechanisms because they have been implicated in the epilepsy that follows experimental FSE (Dubé et al., 2005a; 2010), and in TLE in general (Vezzani et al., 2010). An early step initiating inflammatory processes in the brain is the translocation of the high-mobility group box 1 (HMGB1) molecule from the nucleus into the cytoplasm which is followed by its release out of the cell. This high-energy demanding process takes place in response to cellular injury, and leads to binding of HMGB1 to toll-like receptors and others (Maroso et al., 2010; Vezzani et al., 2010). Therefore, we examined if HMGB1 translocation might account for augmented oxygen extraction and deoxyhemoglobin levels generating the decreased T_2 effect observed in the amygdala of the subset of FSE rats that became epileptic. To this end, a separate cohort of rats was divided into normothermic controls and FSE. They were subjected to MRI at 2 hours, and then euthanized for assessment of HMGB1 expression and translocation (Fig. 5). The number of cells expresing HMGB1 within the nucleus did not differ appreciably among groups (Fig. 5A, B). However, HMGB1 translocation to the cytoplasm, a preamble to its release, was largely confined to the FSE group (Fig. 5B), and correlated with the reduction in T_2 values (Fig. 5D). The

temporal evolution of HMGB1 translocation was also highly congruent with the time-course of the T_2 signal changes (Fig. 5C).

Figure 3.5: Translocation of high-mobility box 1 (HMGB1) from the nucleus to the cytoplasm in amygdala neurons correlates with lowered T_2 signal on MRI. (A) Representative photomicrographs of immunocytochemistry for HMGB1. Top pictures: Identification of basal amygdala. Bottom pictures: differences in HMGB1 localization between normothermic control (NT-C) and experimental febrile status epilepticus (FSE) rats. Arrowheads indicate nuclear HMGB1 whereas arrows indicate cytoplasmic (translocated) HMGB1. (B) Quantitative analysis of HMGB1 expression and localization at 3 hours after the end of FSE showed that while the number of HMGB1 expressing cells was not influenced by the occurrence of FSE, the cytoplasmic localization of HMGB1 was significantly higher in sections from FSE compared with NT-C subjects (left graph; NT-C n=3, FSE n=3). Similar results were obtained when data were represented as a percent of cells with translocated HMGB1 over total HMGB1 positive cells (right graph). (C) Time course of HMGB1 translocation following FSE demonstrates the transient nature of this early inflammatory process: the localization pattern in amygdala sections from FSE rats resembled that of NT-C sections by 8 hours following the end of FSE. Blue=NT-C, n=3; magenta=FSE at the time points indicated, n=3 per time point. (D) Significant correlation of reduced amygdala T_2 values with increased HMGB1 translocation (NT-C, in blue, n=9; FSE, in red, n=9; p=0.02). Values were compared among the sides with lower T_2 values in all rats and all groups. Data presented as mean±SEM. Scale bars, 100 μm. *statistically significant $p<0.05$.

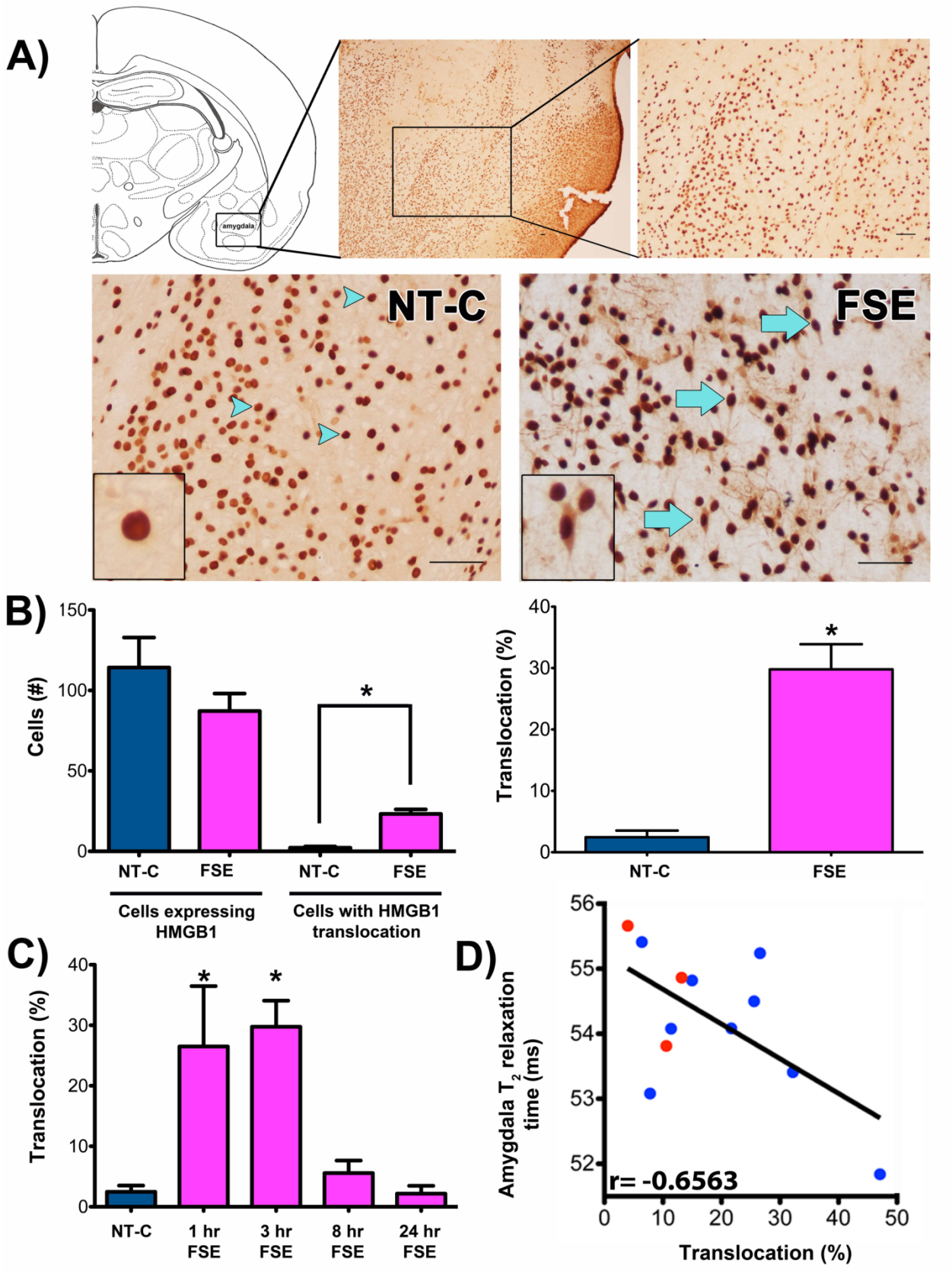
A)
amygdala
NT-C
FSE
B)
Cells (#)
150
100
50
0
NT-C
FSE
NT-C
FSE
*
Cells expressing HMGB1
Cells with HMGB1 translocation
Translocation (%)
40
30
20
10
0
*
NT-C
FSE
C)
Translocation (%)
40
30
20
10
0
*
*
NT-C
1 hr FSE
3 hr FSE
8 hr FSE
24 hr FSE
D)
Amygdala T2 relaxation time (ms)
56
55
54
53
52
r= -0.6563
0
10
20
30
40
50
Translocation (%)

Assessing the MRI signal changes using clinically relevant, lower-field MRI The epilepsy-predicting MRI signal changes described above were obtained using a high-field scanner that was chosen to maximize signal-to-noise ratios. These are crucial for imaging small samples such as immature rat brain, with a volume of ~0.5 cm^3 compared to ~1000 cm^3 for human infants. Once we discovered the predictive value of reduced MRI T_2 values at high magnetic fields and their relationship with increased deoxyhemoglobin levels, we used this information to seek imaging parameters that would enable detection of epilepsy-predictive MRI changes at lower magnetic fields. Specifically, we imaged individual rats using both the T_2 sequence at 11.7T as described above and a deoxyhemoglobin-sensitive T_2* sequence (Fig. 6), using a 4.7T scanner. The latter method, employed in functional MRI studies, is feasible in low-magnetic field MRI scanners used in clinical settings. At 2 h following FSE, low-field T_2* measurements and high-field T_2 measurements identified the same rats, with strong correlations between the 2 methods for the region predictive of epilepsy (basolateral amygdala r = 0.751, p = 0.008 as well as medial thalamus r = 0.846, p<0.001 Fig. 6*G* and *H)*. These findings indicate that predictive signal changes observed using high-field MRI scanners can be detected using more clinically relevant MRI scanners.

Figure 3.6: Lower-field, more clinically relevant MRI scanners identify the same epilepsy-predictive changes as high-field MRI. (A–F) Representative color-coded quantitative T2 map acquired at 11.7 T and T2* map acquired at 4.7 T in a normothermic control and a FSE rat. C–F, Note the decreased T2 at 11.7 T in the basolateral amygdala, with a corresponding reduction in T2* at 4.7 T in the FSE rat compared with the normothermic control rat. Significant relationships between the T2 and T2* were observed in amygdala and thalamus, regions predictive of epileptogenesis. These data indicate that either method suffices to identify rats destined to become epileptic. G, Basolateral amygdala (n=11, r=0.751, p=0.008). (H) Medial thalamus (n=15, r=0.846, p=0.001). Shown is a scatter plot of individual rats. Blue circles indicate normothermic control rats and red circles the FSE rats. Values were compared among the sides with lower T2 values in all rats and all groups. Scale bar, 1 mm.

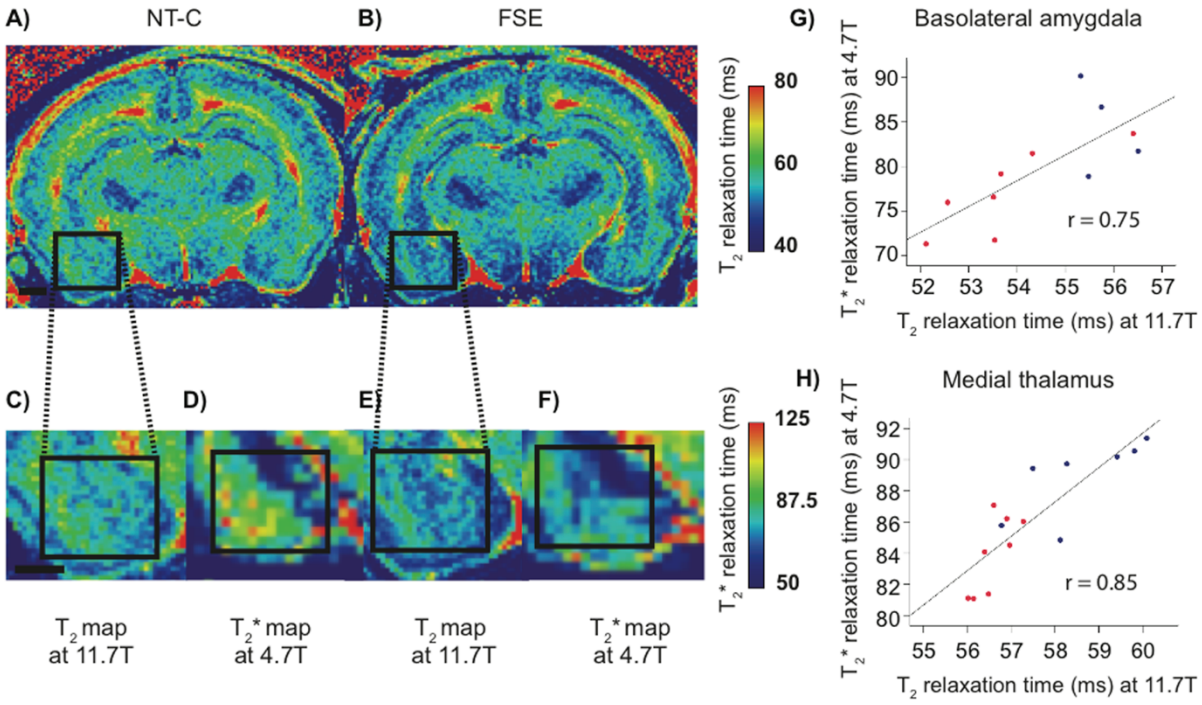
A)
NT-C
B)
FSE
C)
D)
E)
F)
T2 map at 11.7T
T2* map at 4.7T
T2 map at 11.7T
T2* map at 4.7T
T2 relaxation time (ms)
80
60
40
125
87.5
50
G)
Basolateral amygdala
T2* relaxation time (ms) at 4.7T
T2 relaxation time (ms) at 11.7T
r = 0.75
H)
Medial thalamus
T2* relaxation time (ms) at 4.7T
T2 relaxation time (ms) at 11.7T
r = 0.85

Discussion

The principal discovery in these studies is the identification of a novel, noninvasive, and predictive marker of limbic epilepsy after experimental FSE, which suggests salient biological processes and is potentially translatable to the clinical setting. Specifically, on high-magnetic-field scanners, reductions in MRI T_2 relaxation times in amygdala that are detectable hours after FSE predict which rats will develop epilepsy in the ensuing months. The reduced T_2 values may derive from increased deoxyhemoglobin levels—consistent with augmented oxygen utilization in limbic brain regions—that persists for hours after the inciting FSE. The mechanisms requiring oxygen may include the energy-demanding translocation of the pro-inflammatory danger-signal molecule HMGB1 from the nucleus to the cytoplasm, likely followed by its release and an initiation of a cytokine response. Finally, these predictive MRI changes are also observable using T_2* sequences at field strengths applicable to human imaging.

Timing, imaging sequences, and MRI field strength influence signal changes after FSE in immature brain Using high-field, high-resolution MRI, we found that a subset of rats experiencing FSE developed brain changes that were reflected by reduced T_2 values. Whereas these were fairly widespread throughout the brain, localized reduction in amygdala values predicted subsequent epilepsy. Similar to the clinical situation, only a subset of rats had MRI signal abnormalities (Shinnar et al., 2012) and these progressed to epilepsy. Although in humans, preexisting factors might contribute to vulnerability to FSE or its consequences (Shinnar et al., 2012), these factors do not exist in the animal

model. Therefore, the findings suggest that FSE itself can promote MRI signal changes and epileptogenesis.

The most widely reported MRI abnormalities after FSE in children are increases of T_2 in hippocampus within 2–5 d of the event (Cendes et al., 1993a; VanLandingham et al., 1998; Schott et al., 2002; Lewis et al., 2014). Consistent with findings in children, we (Dubé et al., 2004) and other groups (Jansen et al., 2008) found increased MRI signals in rodents 2–7 d after experimental FSE using MRI with field strengths similar to those used clinically. Because these relatively late MRI changes did not predict epilepsy, we were compelled to search for earlier, predictive MRI changes and to use more powerful methods to detect them. The timing of imaging distinguishes the present study from those reported previously and probably enabled detection of epilepsy-predicting signal changes. Previous studies in children and rodents, at the earliest, performed imaging 24 h after FSE compared with 2–4 h here. It is quite likely that the onset of epileptogenic changes is very early after the insult and prior studies were not designed to capture these changes.

A second crucial factor distinguishing the present study involves the use of a very-high-field 11.7 T MRI scanner; previous studies used field strengths ranging from 1.5 to 7 T (Scott et al., 2002; Jansen et al., 2008; Dubé et al., 2008, 2009). Such high fields preclude detection of subtle increases in T_2 values found using lower-field systems because T_2 relaxation times shorten as magnetic field increases. de Graaf et al. (2006) measured T_2 values in adult rat brain at different field strengths and reported

values of 72, 45.4, and 38.9 ms at field strengths of 4, 9.4, and 11.7 T, respectively. After SE in adult rodents, studies at 9.4 T found non significant hippocampal T_2 increases of 1–2 ms, whereas using 2.35 T, the changes were ~5 ms (Greene et al., 2007; Choy et al., 2010; Duffy et al., 2012). In immature rodents, mean hippocampal T_2 values were 120 ms at 4 T, 101.3 ms at 6.3 T, and 59.7 ms at 11.7 T. In other words, compared with T_2 values in a clinical scanner (1.5 T), our 11.7 T scanner yields a 3-fold reduction in relaxation times, which precludes detection of the 3–4 ms increases found in low-field scanners: such changes would comprise 1–2 ms changes at 11.7 T. In contrast, at high field strengths, the susceptibility effects from deoxyhemoglobin, which manifest as T_2 shortening, become stronger and are therefore detectable in the present study (Ogawa et al., 1990; van Zijl et al., 1998; Calamante et al., 1999).

Hippocampal and amygdala signal changes after FSE are asymmetric MRI signal changes are most often unilateral and almost always asymmetric in children after FSE and in adults with TLE and a history of FSE. This provided a strong impetus to examine for similar unilateral changes in rodent models of the human condition. Many adult rodent models of chemoconvulsant-induced epilepsy lead to bilateral MRI changes, yet unilateral hippocampal changes have been reported in adult rodents after kindling and after intrahippocampal or intraamygdala kainic acid (Bouilleret et al., 2000; Jupp et al., 2006; Dunleavy et al., 2010). Here, we found asymmetric T_2 signal changes after experimental FSE. It is helpful to consider two significant differences between the present study and previous studies in chemoconvulsant-induced epilepsy in adult rodents. First, the present study used immature rodents and age has a profound

influence on the nature of brain injury provoked by severe seizures (Nitecka et al., 1984; Holmes & Thompson, 1988; Jensen et al., 1991; Sperger et al., 1991; Stafstrom et al., 1992; Toth et al., 1998; Kubovà et al., 1998; Lee et al., 2001; Raol et al., 2003; Baram et al., 2011). We also aimed to recreate the human insult of FSE, that is, long seizures provoked by combined temperature elevation and inflammatory cytokines induced by fever (Dubé et al., 2005a, 2010; Vezzani et al., 2011). Age and type of insult may underlie the unilateral limbic changes found in the present study and their resemblence to those in children.

Basis of reduced T_2 values using very-high-field MRI Our findings suggested increased levels of deoxygenated hemoglobin as a source of the paramagnetic effects that manifest as reduced T_2 on high-field MRI scanners. Augmented deoxyhemoglobin reflects a mismatch between tissue oxygen demand and supply and is governed by numerous factors, including cerebral blood flow, cerebral blood volume, and oxygen extraction fraction (van Zijl et al., 1998; Schridde et al., 2008; DeSalvo et al., 2010; Goense et al., 2012). We excluded subtle seizures during the MRI as potential bases for ongoing increased oxygen demand uncompensated by blood supply because MRIs were acquired under isoflurane anesthesia, a potent anticonvulsant (Mirsattari et al., 2004). We identified an energetically demanding process, an early “upstream” step in the inflammatory cascade already implicated in FSE (Dubé et al., 2010; Kovac et al., 2012). The correlation of the magnitude and time course of HMGB1 translocation with T_2 changes supported a role for these processes in increased cellular energy and oxygen demand resulting in augmented deoxyhemoglobin levels, although other

potential processes were not excluded (Folbergovà et al., 1985; Young et al., 1987; Lothmam, 1990; Hascoet et al., 1988; Schridde et al., 2008; Varghese et al., 2009; DeSalvo et al., 2010).

Significant and predictive MRI T_2 signal differences between rats that developed epilepsy and those that remained non epileptic were in amygdala and, using factor analysis, in combined medial-thalamus/amygdala. The involvement of these regions is intriguing. First, acute amygdala and thalamic MRI abnormalities have been observed in a subset of children after FSE (Natsume et al., 2007; Shinnar et al., 2012) and their atrophy was more severe in TLE patients with a history of FSE compared with those without (Cendes et al., 1993a; Dreifuss et al., 2001; Bernhardt et al., 2012). Amygdala and limbic thalamus constitute important components of an excitatory circuit involved in TLE in humans and rodents (Gloor et al., 1982; Tremblay & Ben-Ari, 1984; Cassidy & Gale, 1998; Blumenfeld et al., 2004; Englot et al., 2009). Amygdala is one of the most excitable brain regions (Goddard et al., 1969) and is a region of onset of kainate-induced seizures (Tremblay & Ben-Ari, 1984) and of FSE (Baram et al., 1997) in immature rats. Amygdala and medial thalamus may be particularly susceptible to mismatches between oxygen supply and demand, especially in immature brain (Fujikawa et al., 1986; Kubovà et al., 2001; Perira de Vasconcelos et al., 2002; Wasterlain et al., 2010). Indeed, we found amygdala and hippocampal neuronal injury after experimental FSE (Toth et al., 1998).

Potential clinical application of these findings Human MRI studies typically use 1.5–3 T scanners. To explore potential clinical application of our findings, we used a sequence that is more sensitive to deoxyhemoglobin and is readily available in clinical settings—a quantitative T_2* sequence. The predictive effects were reproduced on a 4.7 T scanner, which was not surprising because changes in deoxyhemoglobin levels that are detectable using T_2* imaging are widely exploited as a basis for functional MRI (Ogawa et al., 1990; Dinstein et al., 2012), often using 1.5 T scanners (Dosenbach et al., 2010). Therefore, the predictive signal changes found here should also be readily detectable on standard clinical MRIs.In summary, using an animal model of FSE; high-resolution, high-field MRI; chronic video EEG; neurochemical blood analyses; and molecular and neuroanatomical approaches, we defined an early, noninvasive, predictive marker of epileptogenesis. Because the changes were visible on clinically relevant scanners, we propose that this MRI signature be tested for its efficacy in predicting FSE-related TLE in the clinical setting.

CHAPTER 4

MRI changes predictive of epilepsy and acute activation of inflammatory cascades take place in the same febrile status epilepticus –experiencing individuals

Overview

Epilepsy is a common neurological disorder with many causes. For temporal lobe epilepsy, a disorder associated with cognitive and emotional deficits, antecedent insults are typically found. These risk factors include trauma or history of long fever-associated seizures in childhood (Cendes et al.,1993; French et al., 1993; Dubé et al., 2007).

Febrile status epilepticus (FSE) denotes long seizures (>30 minutes) associated with fever in early childhood (Berg & Shinnar, 1996; Berg et al., 1997). Mounting evidence suggests that FSE leads to temporal lobe epilepsy (TLE) in a subset of individuals (Annegers et al., 1987; Cendes et al.,1993; Dubé et al., 2007; Seinfeld et al., 2014; Lewis et al., 2014). Discerning the epileptogeneic features of FSE have remained elusive, because both in humans (VanLandingham et al., 1998; Seinfeld et al., 2014; Scott et al., 2002) and in rodent models (Toth et al., 1998, Dubé et al., 2004; Jansen et al., 2008) there is evidence for neuronal stress and injury, but not for cell death, so that the epileptogenesis cannot be attributed simply to brain damage. To uncover the potential mechanisms by which FSE promotes epilepsy, several immature rodent models of FSE have been established and characterized (Baram et al., 1997; Heida et al., 2004, 2006; Dubé et al., 2010). In the model used here, ~40% of rats exposed to early life experimental FSE (eFSE) go on to become epileptic. This fact enables a comparison of rats that become epileptic to those who do not, allowing for the dissection

of processes essential for epileptogenesis (that leads to TLE) and those that simply change during or after insult but do not contribute to the resulting epilepsy (Patterson, Baram & Shinnar, 2014).

Inflammation has been implicated in many animal models of acquired epilepsy although its role in epileptogenesis remains unclear (Holtman et al., 2009, 2010, Vezzani et al., 2011). Fever, the initiator of FSE, intrinsically involves inflammation and the cytokine interleukin- 1β (IL-1β) is a crucial component in eFSE generation (Dubé et al., 2005). Further, higher levels of IL-1β are found in the hippocampus of animals that become epileptic (Riazi et al., 2010; Heida et al., 2005, 2009; Luheshi, Stefferl & Turnbull, 1997; Eskilsson et al., 2014; Dubé et al., 2005, 2010).

For these reasons, inflammation has become an attractive target for anti-epileptogenic therapies. (De Simoni et al., 2000; Dedeurwaerdere et al., 2012; Pollut, Dudek & Dingledine, 2013; Ollikainen et al., 2004). The goal of such interventions would be to abort the epileptogenic process before spontaneous seizures begin (Vezzani et al., 2010; Patterson et al., 2014). However, several important pieces of information are lacking, impeding our ability to implicate inflammation in the processes that follow both eFSE and human FSE that may promote epilepsy. First, it is not known which of the many potential inflammatory mediators are activated by eFSE, and the time-courses of their augmented expression have not been delineated. Second, it is unknown if variations in the inflammatory response take place in individual animals which might contribute to the eventual development of epilepsy in a subset of animals.

Answering these important questions has recently been facilitated by the discovery of an early, predictive non-invasive marker of epileptogenesis. On a high-field MRI, reduction of T2 relaxation times throughout the limbic circuit and especially in the basolateral amygdala within hours after eFSE predicted later life epilepsy (Choy et al., 2014). Further, T2 signal changes correlated to an early inflammatory process in the amygdala, the translocation of high mobility group box 1 (HMGB1). HMGB1, classically thought of as a nuclear scaffolding protein, translocates out of the nucleus during cellular stress, and is then released from the cell. It acts as a pro-inflammatory cytokine by binding to toll-like receptor 4 (TLR4), amongst others, to promote an inflammatory response (Bianchi & Manfredi, 2007; Maroso et al., 2010).

Here, we probed important questions about the relationship of inflammatory cascades provoked by eFSE and their implications for epileptogenesis. Specifically, we sought to (1) delineate the temporal course of specific components of the inflammatory response in the hours and days after eFSE. (2) Investigate if and how these inflammatory mediators vary among individual animals after eFSE and (3) correlate the variation found in inflammatory mediators in hippocampus and amygdala to the variation found in MRI signal changes. Together, these studies further our understanding of post eFSE inflammation and how this intricate set of molecules and processes may contribute to epileptogenesis.

Methods and Materials

Experimental Overview To characterize the spectrum of inflammatory changes provoked by eFSE, we induced experimental seizures, then conducted quantitative mRNA analyses at several time points, buttressed by Western blot analyses and immunocytochemistry. We focused on the hippocampal formation, which is involved in both eFSE and the subsequent epileptogenesis, as well as on the amygdala, the location of the epilepsy-predicting MRI signal change. mRNA analyses were performed at multiple time points, including 1, 3, 24 and 96 hours after the end of the eFSE in hippocampus and at 24h in amygdala. Most immunocytochemistry as well as the hematoxylin and eosin stain was performed on tissue collected 24 hours after the end of the eFSE (with additional time points for HMGB1).

Induction of experimental Febrile Status Epilepticus (eFSE) All animal procedures were performed in accordance with the Author University animal care committee's regulations. Postnatal day 10-11 Sprague-Dawley rat pups of both sexes were used for all studies. eFSE was achieved by inducing hyperthermia in pups. Pups were placed, two at a time, inside a 3-liter flask the bottom of which was lined with absorbent paper. Prior to hyperthermia a glycerin-based hydrating ointment was applied to pups' paws, ears and tail, to mitigate potential hyperthermic skin injury. Pups were subjected to a continuous stream of warm air until behaviors indicating seizures began. These behaviors were identified as arrest of hyperthermia-induced hyperkinesis (freezing) followed by chewing automatisms. Core temperatures at the onset of these seizures were then rapidly measured, and seizure-onset time noted. Once seizures commenced, elevated core temperature and seizures were maintained via the warm air stream for 60

minutes. Seizure behaviors typically progressed over the hyperthermia period, including chewing of an extremity, clonic movements and eventual tonic extension. Pups' core temperature was measured every 2 minutes during the eFSE. If the pups' core temperature exceeded 41.5°C they were removed from the chamber and placed on a cool metal surface for the next two minutes. After 60 minutes of hyperthermia (typically 55-58 minutes of seizures) eFSE pups were gently and briefly immersed in cool water (~23.0°C) to aid in return of core temperature to normothermia and promote seizure cessation. Pups were then placed on a euthermic pad maintained at 37°C for 30 minutes then returned to their home cage and dam. In this study, all pups subjected to hyperthermia experienced eFSE and there was no mortality.

qRT-PCR Whole hippocampi or amygdala were rapidly dissected on ice at desired time points after the end of eFSE using RNAse free instruments. Tissue was immediately transferred to pre- chilled centrifuge tubes kept on dry ice. Samples were stored at -80°C until use. Total RNA was extracted from hippocampi using the mirVana miRNA Isolation Kit according to the manufacturer's instructions (Ambion, New York, USA). Double- stranded cDNA was synthesized from total RNA using Roche 1st strand cDNA synthesis kit (Cat # 04379012001; Roche) with random hexamer primers. Analysis of the PCR products was executed using cDNA samples in triplicate on a Roche LIghtcycler 96 system (Roche). Samples were normalized to β-Actin and quantified using the cycle threshold method (2^ΔΔCt). Primers are provided in table 4.

Western blot Whole hippocampus from each hemisphere was dissected from rat brain 24 h post FSE and immediately flash frozen on dry ice and stored at -80°C until use. Tissue was homogenized in a lysis buffer containing 0.01 M Tris-HCl and 1 mM EDTA. Proteins (30 µg) were separated on either gradient gels (8-12%) or 15% polyacrylamide SDS gels (Lonza), transferred to PVDF membranes (GE Healthcare) and blocked with 5% whole milk. Membranes were then incubated with primary antibodies (GFAP 1:1,000 (Millipore), Cox-2 1:1,000 (Abcam), IL-6 1:2,000 (Abcam) and β-Actin 1:20,000 (Abcam) overnight at 4°C. The next day membranes were washed in PBS-T and then incubated with HRP-conjugated secondary antibodies for 1h at room temperature. Excess secondary antibody was removed with repeated washes in PBS-T and then membranes were visualized by repeated ECL (Pierce) exposures of various lengths and non-saturated blots were selected and normalized to β-Actin. Western blots were analyzed using ImageJ and without knowledge of treatment group

Immunocytochemistry Rats were deeply anesthetized with pentobarbital and transcardiacly perfused with 4% paraformaldehyde (PFA) at desired time points post eFSE. Brains were removed and post-fixed in 4% PFA for 90 minutes. Brains were then cryoprotected in 30% sucrose, rapidly frozen and stored at -80°C. 30-micron sections of dorsal hippocampus were obtained on a cryostat and stored in anti- freeze at 4°C until use. Serial sections were blocked in 10% normal goat serum and 0.03% Triton-x in 1x PBS for one hour at 4°C. Primary antibodies were incubated in 4% Normal Goat Serum with 0.03% Triton-x overnight at 4°C. The following antibodies were used: rabbit anti-HMGB11:1,000 (Abcam), mouse anti-GFAP 1:3,000 (Millipore), mouse anti-IBA1

1:4,000 (Wako). Sections were washed with 1x PBS and the reaction product was visualized using a 3,3'-diaminobezidine. Colocalization of cell markers with HMGB1 was achieved by co-incubating rabbit anti-HMGB1 1:1,000 (Abcam) with the following antibodies: mouse anti- NeuN (Chemicon), mouse anti-GFAP 1:3,000 (Millipore) and mouse anti-CD11b (ABD Serotec). After 24-hour incubation, sections were washed in 1x PBS and then incubated in the appropriate secondary antibodies conjugated to Alexa Flour 568 or Alexa Flour 488. Colocalization was visualized using confocal microscopy.

Hematoxylin and Eosin Staining 30 µM coronal sections containing dorsal hippocampus and amygdala were obtained via cryostat and dried onto glass microscope slides. Sections were rinsed 2-3 times in distilled H_2O and then placed in Hematoxylin solution for 5 minutes (Poly Scientific). Slides were placed under running tap water until water was no longer colored with stain and then dunked 2-3 times in acid alcohol (1% HCl in 70% EtOH) until sections turned pink in color. After rinsing 3-5 times in tap water, sections were submerged 5-6 times in ammonia water (1 mL NH_4OH in 1L H_2O) to darken sections. After rinsing sections for 3-5 minutes in tap water, slides were submerged in Eosin Y solutions (Poly Scientific) for 1 minute and then rinsed again in tap water. Slides were dehydrated in ethanol and xylenes, coverslipped in paramount and allowed to dry until analysis.

Quantification of immunocytochemistry Quantification of activated microglia after eFSE in hippocampal CA1, CA3 and hilus was achieved by boxing off 1,000 by 500 µM areas of each studied region. First, all IBA1+ positive cells in the defined region were counted

and compared among groups. Activated microglia were identified as IBA1+ cells that had large, dark soma and few short processes that were thicker in appearance than non-activated microglia (Lenz et al., 2014). Microglia activation is presented as the percent change in activated microglia over the total number of IBA+ cells. Quantification of GFAP+ cells was achieved by using the same hippocampal regions and area delineations. GFAP+ cells were counted and compared among groups. HMGB1 quantification was accomplished by counting all HMGB1+ cells in a 100 by 500 μM region of CA1. Translocation of HMGB1 protein was identified by the presence of immunoreactivity outside the nucleus, i.e., in the somatic cytoplasm and in the processes of cells. Change in HMGB1 translocation is presented as the percent change in translocated cells over the total number of HMGB1+ cells.

MRI procedure and analysis MRIs employed a Bruker Avance 11.7T MR scanner. Rats were anesthetized with 1.5% isoflurane in 100% O_2 and remained anesthetized for the duration of the scan. Their body temperature was maintained at ~36.5°C via a warm-water cushion underneath them. A field-of-view of 2.3 cm and a slice thickness of 0.75 mm were used for scans. T2 weighted images were acquired using a 2D multi-echo-spin-echo sequence with parameters as follows: TR= 4697 ms, TE= 10.21- 100.1 ms, inter-TE= 10.21 ms, matrix size = 192x192, and number of averages (NA)= 2. Animals were imaged 6 hours after the end of eFSE. Control and eFSE animals were intermixed to maximize homogeneity of imaging parameters. Images were coded and analyzed without knowledge of treatment group. Basal amygdalae were delineated manually and separately in the left and right hemispheres. T2 values were measured using ImageJ

software in which the images were defined on gray scale maps and a dynamic range of 1-100 ms was used. MRI signal changes are frequently unilateral in both children with FSE and in rodent models of FSE (Choy et al., 2014 & Dubé et al., 2009). Therefore, each amygdala was analyzed separately and the side with the lower T2 relaxation time was used. The same approach was taken for the control rats, so that the amygdala with the lower T2 value was compared in all groups.

Gene	Forward	Reverse
B-Actin	CAG CCT TCC TTC CTG GGT ATG GA	CAG CAC TGT GTT GGC ATA GAG G
Cd11b	GGG AGC CCC ACA CTG ATA	AGA GGG AGG CCC CAA AAT A
Cox-2	TGG TGC CGG GTC TGA TGA TG	GCA ATG CGG TTC TGA TAC TG
GFAP	TGG CCA CCA GTA ACA TGC AA	CAG TTG GCG GCG ATA GTC AT
HMGB1	AGT TCA AGG ACC CCA ATG C	CAG TGT TGT TCC ACA TCT CTC C
Il1β	TGT GAT GAA AGA CGG CAC AC	CTT CTT CTT TGG GTA TGT TTG G
Il1r1	GCT TGT GAC ATC TTC GGC TA	AAT GAA CCC AAG TAG CAC TTT CA
Il6	CCC TTC AGG AAC AGC TAT GAA	ACA ACA TCA GTC CCA AGA AGG
TLR4	GGA TGA TGC CTC TCT TGC AT	TGA TCC ATG CAT TGG TAG GTA A
TNFα	CCC AGA CCC TCA CAC TCA GAT	TTG TCC CTT GAA GAG AAC CTG

Table 4.1: Primer sequences used for rt-PCR

Results

Description and parameters of the inciting experimental febrile status epilepticus (eFSE)

All animals exposed to hyperthermia developed eFSE. Mean core temperatures did not significantly differ between litters or the experimental groups during 60 minutes of sustained eFSE (Fig. 1A-B). Further, mean core temperatures did not rise above 41.5°C in any animal, nor did they drop below the mean seizure threshold. In general, once seizures commenced (average=3.9 min, Dubé et al., 2007), core temperatures did not significantly change during the course of hyperthermia (Fig. 1C). Twenty-four hours after the end of eFSE, hematoxylin and eosin staining did not suggest overt neuronal staining or drop-out in dorsal hippocampus or amygdala from eFSE experiencing rats (Fig.1D-1F'). These non-quantitative observations are in line with previous exhaustive quantitative analyses in several rat cohorts subjected to the same model and following the same duration of hyperthermia (Toth et al., 1998; Dubé et al., 2010)

Figure 4.1: eFSE parameters: (A) No statistical differences of mean core temperature exists between litters (or day of eFSE induction; n=61 over 14 litters). (B)eFSE data arranged by experimental group shows no difference of mean core temperatures during eFSE (n=61 experimental groups are distinguished with numbers 1-6 on the x-axis). No animal used in this study had a mean core temperature during eFSE that exceeded 41.5°C. (C) Elevated core temperatures after the first two minutes of eFSE were similar for the duration of eFSE (n= 61 time of core temperature reading are delineated in 2 minute epochs across the x-axis). (D-F') No overt differences in structure or cell fallout were apparent 24 hours after the end of eFSE in hippocampus or amygdala using H&E staining.

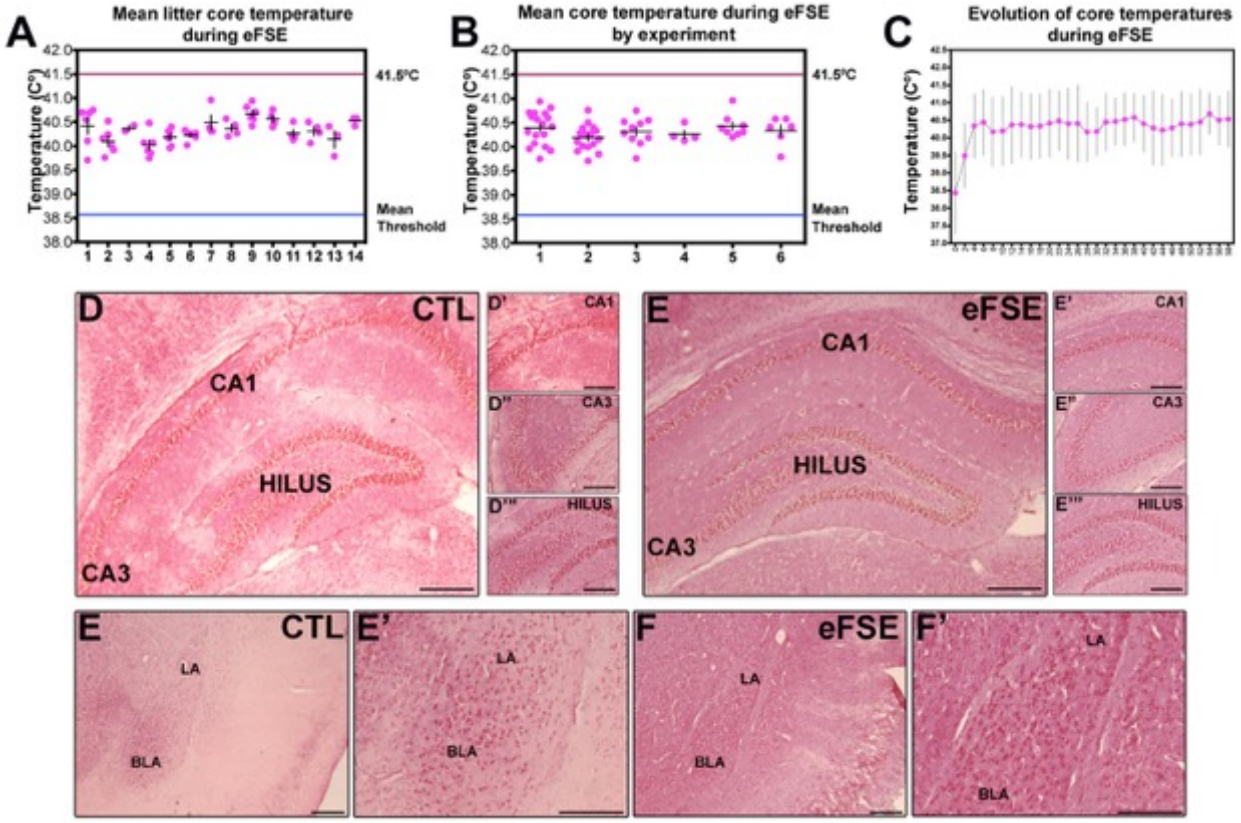
A
Mean litter core temperature during eFSE
Temperature (C°)
41.5°C
Mean Threshold
B
Mean core temperature during eFSE by experiment
Temperature (C°)
41.5°C
Mean Threshold
C
Evolution of core temperatures during eFSE
Temperature (C°)
D
CTL
CA1
HILUS
CA3
D'
CA1
D''
CA3
D'''
HILUS
E
eFSE
CA1
HILUS
CA3
E'
CA1
E''
CA3
E'''
HILUS
E
CTL
LA
BLA
E'
LA
BLA
F
eFSE
LA
BLA
F'
LA
BLA

Activation of astrocytes and microglia in hippocampus after FSE The number of cells expressing the microglia marker, IBA1 (Fig. 2A-C'), was not different between control and eFSE groups 24 hours after the insult. However, there were changes in the shape of IBA1-ir cells between groups (Fig. 2D). In the control group, IBA1-ir cells had long processes, while many cells in the eFSE group had no processes or were more globular in shape (Fig. 2A-C'). IBA1-ir cells with long processes are regarded as ramified microglia (non-activated), indicative of a quiescent state. Globular IBA1-ir cells with short or non-visible processes are indicative of activated or amoeboid microglia (Lenz et al., 2013). Because activated microglia produce CD11b, we measured CD11b mRNA levels. There were no significant changes in the expression of this molecule in the post eFSE hippocampus at any time point (Fig. 2E).

Figure 4.2: Activated microglia after eFSE: (A-C') IBA1- ir cells are visible 24-hours after eFSE in dorsal hippocampus in both eFSE and control rats. (D) While the number of IBA1-ir cells is similar between eFSE (n=4) and control groups (n=4), eFSE rats have a larger percentage of amoeboid microglia. Ramified (or non-activated) microglia have slender, long processes with small soma while ameoboid (or activated) microglia have short thick processes with a distinct, large soma. Solid arrows point to amoeboid microglia while empty arrows point to ramified microglia. (E) There are no differences in mRNA levels for CD11b (1 hr n=5; 3 hr n=6; 24 hr n=6; 96 hr n=4), which can increase as microglia become active. Data are presented as mean ± SEM. Scale bars, 200 μM (insert, 5 μM). *Statistically significant at $p<0.05$.

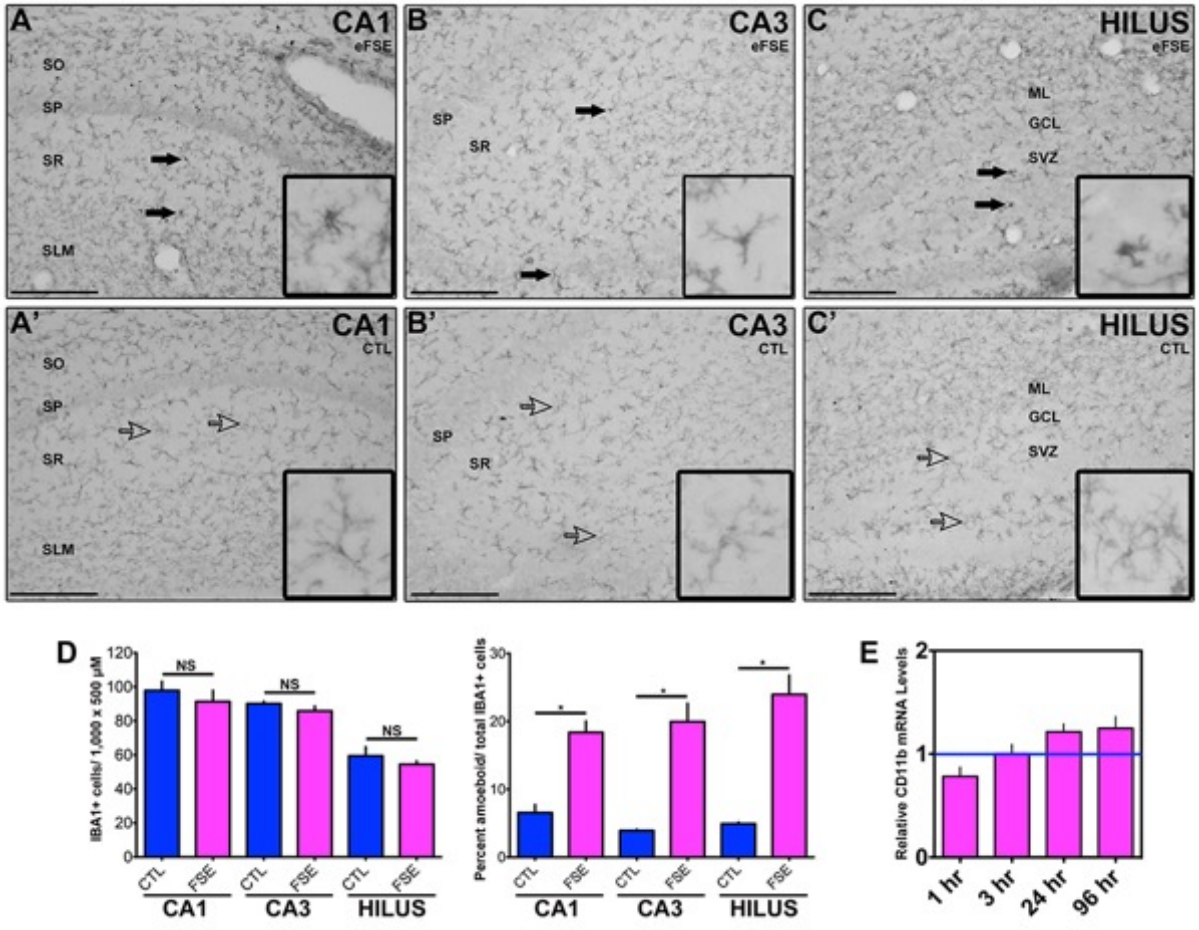
A
CA1
eFSE
SO
SP
SR
SLM
B
CA3
eFSE
SP
SR
C
HILUS
eFSE
ML
GCL
SVZ
A'
CA1
CTL
SO
SP
SR
SLM
B'
CA3
CTL
SP
SR
C'
HILUS
CTL
ML
GCL
SVZ
D
IBA1+ cells/ 1,000 x 500 µM
NS
NS
NS
CTL
FSE
CA1
CA3
HILUS
Percent amoeboid/ total IBA1+ cells
*
*
*
E
Relative CD11b mRNA Levels
1 hr
3 hr
24 hr
96 hr

In hippocampi from rats sacrificed 24 hours following eFSE, the number of GFAP-immunoreactive (ir) cells increased compared to controls in hippocampal CA1, CA3 and the hilus of dentate gyrus (Fig. 3A-D). GFAP mRNA levels were increased at 3 and 24 hours after eFSE and returned to baseline levels at 96 hours as measured with rtPCR (Fig. 3E). Together, these data indicate that GFAP production was increased in astrocytes after eFSE, consistent with activation of this cell population.

Figure 4.3: Activated astrocytes after eFSE: (A-C') GFAP-ir cells are visible in dorsal hippocampus regions CA1, CA3 and the hilus of the dentate gyrus 24-hours after eFSE (n=4) but not in control rats (n=4). Solid arrows depict GFAP+ cells. (D) Quantification reveals a significant increase in the number of GFAP-ir cells compared to controls. (E) mRNA levels of GFAP are significantly increased 3 and 24 hours after eFSE, but not at 1 or 96 hours (1 hr n=5; 3 hr n=6; 24 hr n=6; 96 hr n=4). Data are presented as mean±SEM. Scale bars, 200 μM (insert, 5 μM). *Statistically significant at $p<0.05$.

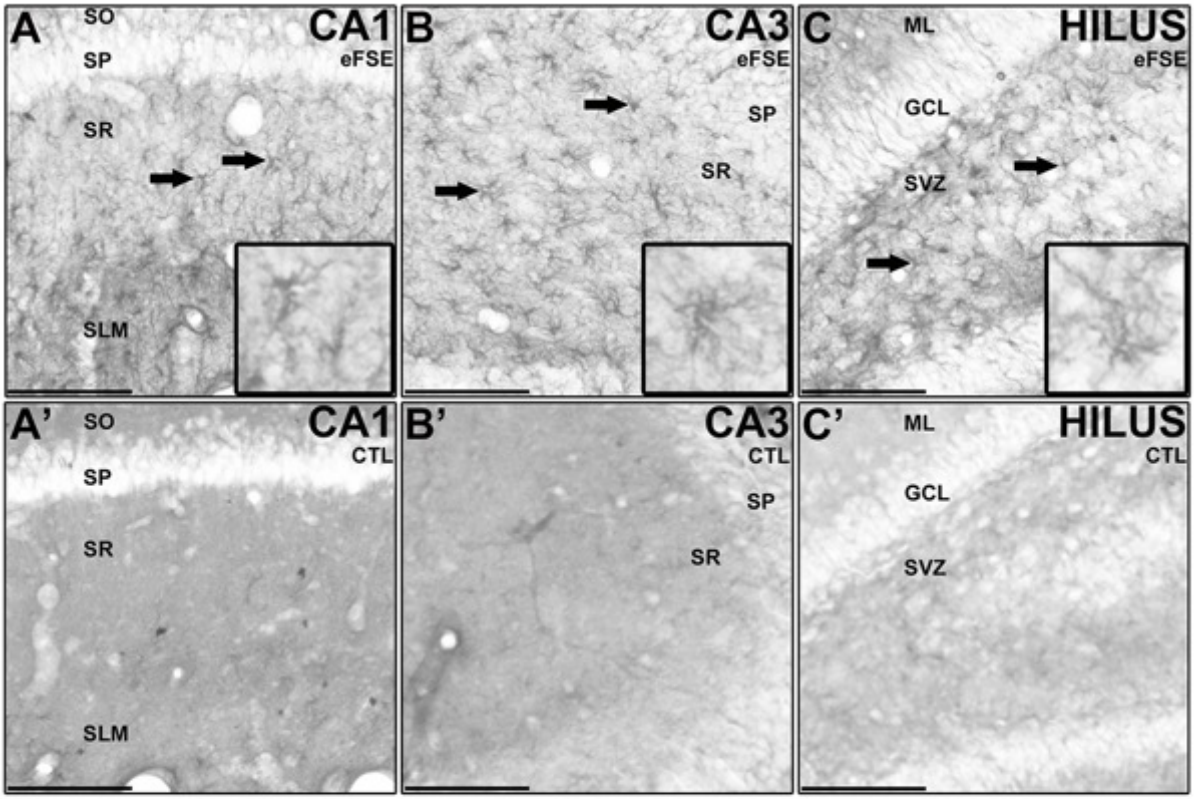
A
SO
SP
SR
SLM
CA1
eFSE
B
CA3
eFSE
SP
SR
C
ML
GCL
SVZ
HILUS
eFSE
A'
SO
SP
SR
SLM
CA1
CTL
B'
CA3
CTL
SP
SR
C'
ML
GCL
SVZ
HILUS
CTL

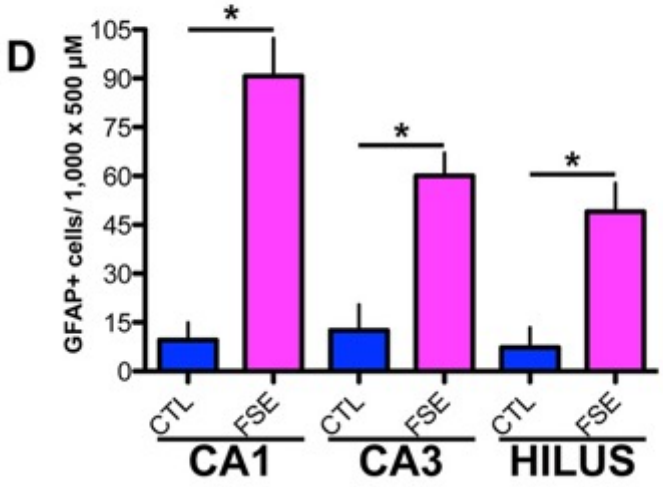
D
GFAP+ cells/ 1,000 x 500 µM
105
90
75
60
45
30
15
0
*
*
*
CTL
FSE
CTL
FSE
CTL
FSE
CA1
CA3
HILUS

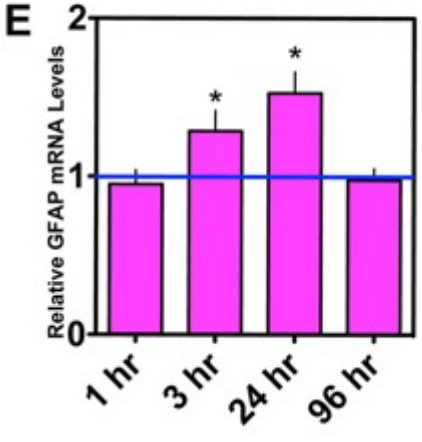
E
Relative GFAP mRNA Levels
2
1
0
*
*
1 hr
3 hr
24 hr
96 hr

HMGB1 translocation in hippocampal neurons after eFSE Our previous studies demonstrated HMGB1 translocation from nuclei to cytoplasm of amygdala neurons in parallel with the appearance of T2 signal changes in the amygdala of the same rats. Here we focused on hippocampus, the origin of spontaneous seizures in rats that become epileptic after eFSE. HMGB1 was localized to the nuclei of cells in control CA1 neurons (Fig. 4A). At 1 and 3 hours after eFSE, HMGB1-ir appeared in the cytoplasm, indicative of translocation of this protein (Fig. 4B-C). Cytoplasmic HMGB1 was no longer present 24 hours after eFSE (Fig. 4E). HMGB1 colocalized with NeuN-ir hippocampal cells, but not with GFAP- or CD11b-ir cells (Fig. 4F-N). No changes in hippocampal HMGB1 mRNA levels were found at any of the examined timepoints (Fig. 4O). mRNA expression of one of the target molecules of HMGB1, toll-like receptor 4 (TLR4), significantly increased at 24 hours after eFSE (Fig. 4P), and was back at baseline levels four days after the eFSE. Together, these data suggest a rapid yet transient translocation of hippocampal HMGB1 from the nucleus to the cytoplasm, likely followed by secretion from the cell and activation of target receptors. This process took place in hippocampal *neurons,* but not in microglia or astrocytes.

Figure 4.4: HMGB1 translocation in hippocampal neurons after eFSE: (A) In control animals (n=3), HMGB1 is confined to the nucleus of cells (open arrows) in area CA1 of dorsal hippocampus. (B) One hour after the end of eFSE, HMGB1-ir is seen in the processes of neurons (closed arrows; n=4) indicating translocation of HMGB1 from the nucleus. (C) Translocation is still evident 3-hours after the end of eFSE (n=4). (D) By 24-hours after eFSE, mostly nuclear HMGB1 is observed (n=4). (E) Quantification of HMGB1 immunocytochemistry as the percent of HMGB1-ir cells with translocation over total HMGB1-ir cells shows a significant increase in the percentage of HMGB1 translocation one- and three-hours after eFSE with a return to control conditions by 24-hours. (F-H) Double labeling of HMGB1 and NeuN (both in soma and processes) demonstrates that HMGB1 translocation occurs from neuron and not from astrocytes, as shown with GFAP (I-K) or microglia, as shown with CD11b (L-M; CTL n=3; 1 hr n=4; 3 hr n=4). (O) There is no increase in the levels of HMGB1 mRNA indicating translocation is achieved using already available protein (1 hr n=5; 3 hr n=6; 24 hr n=6; 96 hr n=4). (P) TLR4, one receptor through which pro- inflammatory HMGB1 acts, mRNA is upregulated 24-hours after eFSE with a return to baseline by 96 hours (1 hr n=5; 3 hr n=6; 24 hr n=6; 96 hr n=4). Data are presented as mean ± SEM. Scale bars, 100 μM. * Statistically significant at $p<0.05$

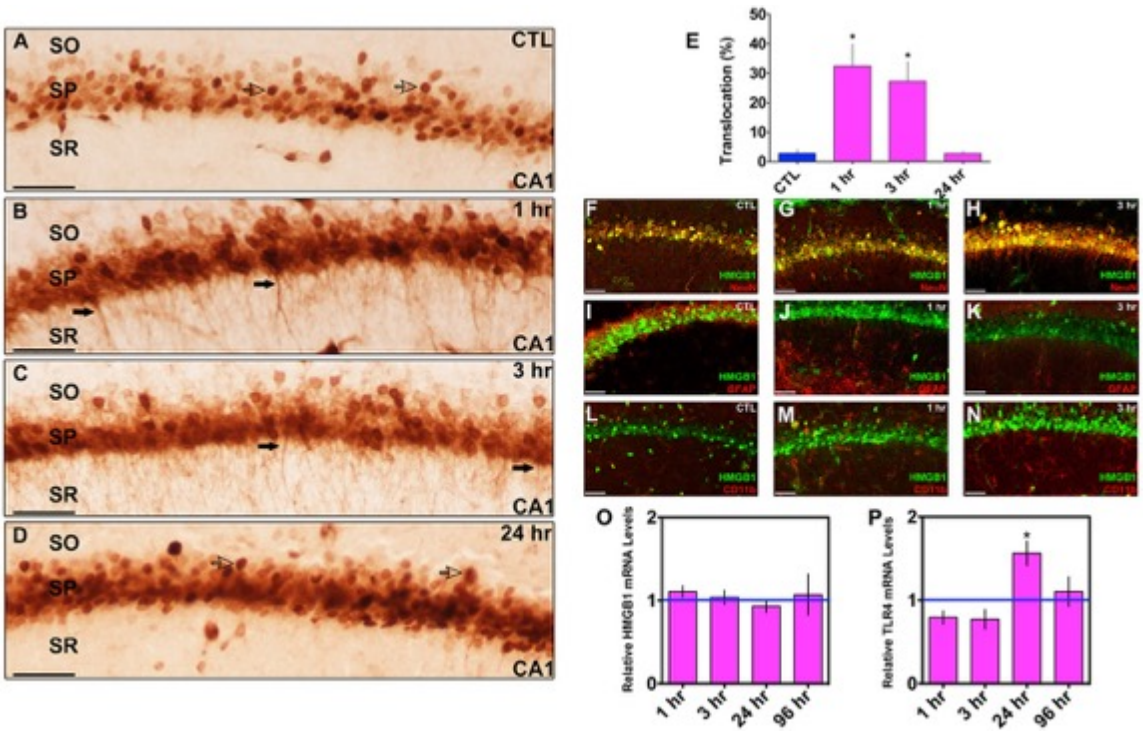
A
SO
SP
SR
CTL
CA1
B
1 hr
C
3 hr
D
24 hr
E
Translocation (%)
CTL
1 hr
3 hr
24 hr
F
G
H
I
J
K
L
M
N
HMGB1
O
Relative HMGB1 mRNA Levels
P
Relative TLR4 mRNA Levels
96 hr

Cytokine expression after eFSE IL-1β mRNA levels increased significantly in hippocampus 1 and 3 hours after eFSE. Levels then declined, so that by 96 hours after eFSE, IL-1β mRNA levels were indistinguishable from those of control rats (Fig. 5A). Notably there was a significant inter-animal variability in the levels and temporal kinetics of IL-1β mRNA expression (Fig. 5B).

Inter-animal variability was prominent upon examination of the time-courses of expression of all other investigated cytokines. Levels of IL-1r1 mRNA (the IL-1β receptor) increased significantly 3 and 24 hours after eFSE and returned to baseline by 96 hours (Fig. 5C). No augmentation of IL-6 mRNA was found at 1 and 3 hours after eFSE, but levels were increased by 24 hours in a subset of rats and returned to baseline in all rats by 96 hours (Fig. 5D). Hippocampal TNFα mRNA was significantly augmented 3 hours after eFSE and returned to baseline by 24 hours (Fig. 5E). COX2 expression was significantly enhanced at all tested time points after eFSE, and remained upregulated at 96 hours, the last time point assessed (Fig. 5F).

To examine if augmented mRNA expression of cytokines translated into increased levels of functional inflammatory mediators, protein levels of GFAP, COX2 and IL-6 were measured in hippocampi 24 hours after eFSE (Fig. 5G-H). These specific proteins were chosen because of upregulation of their mRNA 24 hours after eFSE in some but not all rats. We found a significant increase in protein levels of COX2 and GFAP in hippocampus, with inter-animal variability, similar to the findings at the mRNA level.

Similar to mRNA levels, protein levels of IL-6, measured in hippocampus 24 hours after eFSE were not consistently or significantly increased.

Figure 4.5: Transient cytokine upregulation after eFSE: (A) IL-1β mRNA levels are significantly upregulated one- and three-hours after eFSE (CTL= 23; 1 hr n=10; 3 hr n=10; 24 hr n=12; 96 hr n=4). (B) Variability of IL-1β mRNA expression between rats are apparent when data is presented as individual animals where some rats have high levels of IL-1β expression and others are indistinguishable from controls. (C) IL-1r1 mRNA levels are significantly upregulated 3- and 24-hours after eFSE, with obvious inter-animal variability (CTL n=20, 1 hr n=10; 3 hr n=10; 24 hr n=13; 96 hr n=4). (D) While never statistically significant, IL-6 levels trend upward for some animals at 24 hours with a return to baseline by 96 hours (CTL n=9; 1 hr n=4; 3 hr n=4; 24 hr n=10; 96 hr n=4). (E) TNFα mRNA levels are significantly augmented by 3-hours and return to baseline by 24-hours (CTL n=25; 1hr n=10; 3 hr n=10; 24 hr n=12; 96 hr n=4). (F) COX2 mRNA levels are significantly upregulated at every tested time point (CTL n=11; 1 hr n=6; 3 hr n=6; 24 hr n=6; 96 hr n=4). (G) GFAP, COX2 and IL-6 protein levels are augmented with inter-animal variation 24 hours after eFSE (n=4) as compared to littermate controls (n=4). Densitometric analyses of protein levels normalized and compared to control are provided in H. Data are presented as mean±SEM. *Statistically significant at $p<0.05$.

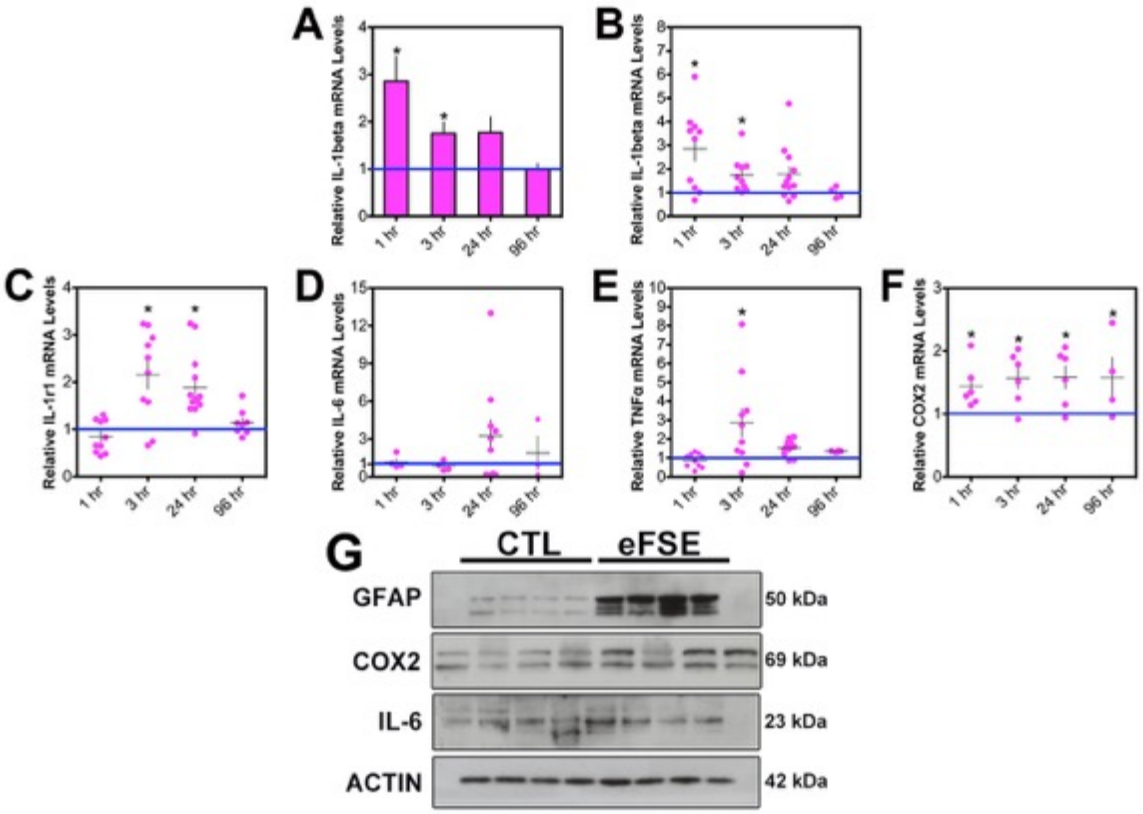
A
Relative IL-1beta mRNA Levels
1 hr
3 hr
24 hr
96 hr
B
Relative IL-1beta mRNA Levels
C
Relative IL-1r1 mRNA Levels
D
Relative IL-6 mRNA Levels
E
Relative TNFα mRNA Levels
F
Relative COX2 mRNA Levels
G
CTL
eFSE
GFAP
50 kDa
COX2
69 kDa
IL-6
23 kDa
ACTIN
42 kDa

Distinct inflammatory cytokine profiles in individual rats after eFSE Following eFSE, ~40% of rats develop epilepsy (Dubé et al., 2010; Choy et al., 2014). If inflammatory molecule activation contributes to epileptogenesis after eFSE, the prediction is that there will be strong individual variation in cytokine expression, with robust changes in ~40% of eFSE-experiencing rodents. We tested this possibility by delineating the inflammatory cytokine profile of individual rats.

The expression of different cytokines peaks at different time points; therefore, the timepoint for maximal expression of each cytokine was included in the composite molecular profile of each eFSE-experiencing rat (Figure 6). By 3 hours after the end of eFSE, mRNA levels of COX2, GFAP, TNFα, IL-1β and IL-1r1 were significantly augmented (Fig. 6A). In individual animals, expression levels of these cytokines tended to co-vary: animals with high expression of one cytokine tended to have higher expression of the others, whereas animals with low expression of one cytokine had depressed levels of the others. This trend was also found at the 24-hour time point, when IL-1r1, COX2, and TLR4 were significantly upregulated in a subset of rats (Fig. 6B).

Figure 4.6: Inter-animal variation of inflammatory mediator expression after eFSE: (A) 3-hours after eFSE, COX2, GFAP TNFα and IL-1r1 were significantly increased. When an individual rat's expression profile is examined across these mediators, trends in expression appear (n=4). For example, rat 1 has the highest expression across all explored mediators, while rat 4 has virtually no inflammatory response after eFSE. Rats 2 and 3 both fall in between rats 1 and 4, with moderate expression profiles. (B) A similar pattern is found 24-hours after eFSE as well (n=6). COX2, IL-1r1, TLR4 and GFAP were all significantly upregulated at this timepoint. As seen with the 3-hour timepoint, rats with high expression in one mediator, have high expression in all others, and vice- versa. Rat 6 has the highest expression of all examined mediators, while Rat 5 is a non-responder.

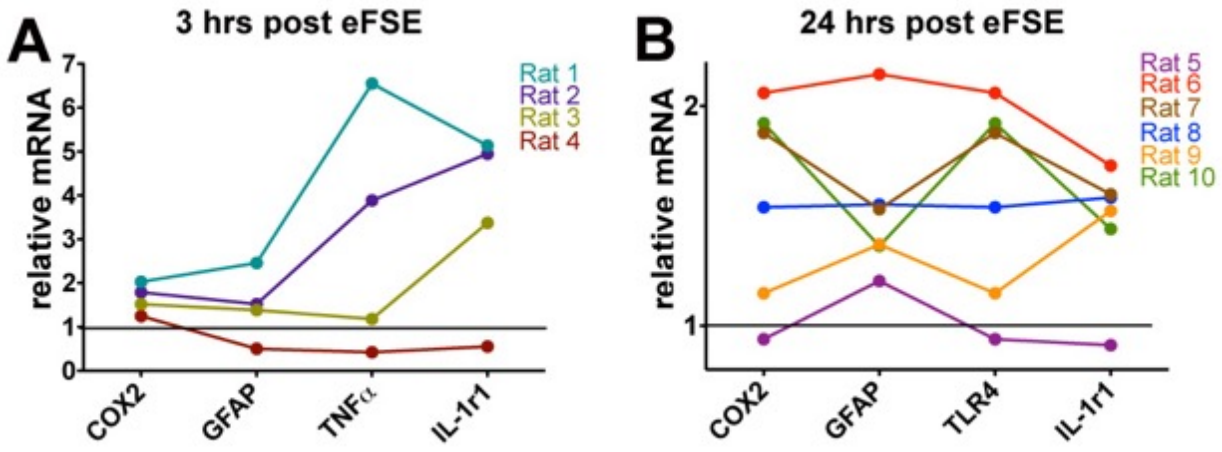
A
3 hrs post eFSE
relative mRNA
0
1
2
3
4
5
6
7
Rat 1
Rat 2
Rat 3
Rat 4
COX2
GFAP
TNFα
IL-1r1
B
24 hrs post eFSE
relative mRNA
1
2
Rat 5
Rat 6
Rat 7
Rat 8
Rat 9
Rat 10
COX2
GFAP
TLR4
IL-1r1

Expression levels in hippocampus and amygdala of a subset of inflammatory mediators correlate with a predictive marker of post eFSE epilepsy We previously investigated potential non-invasive predictive markers for the epileptogenesis that, in a subset of rats, follows eFSE. We found that decreased MRI T2 relaxation times in the amygdala 2-4 hours after eFSE predicted whether or not an individual animal developed spontaneous seizures that involved, and seem to originate from, the hippocampus (Choy et al., 2014). Here we capitalized on the epilepsy-predicting MRI signal change, and studied if augmented expression of hippocampal cytokines in individual rats correlated in the same animal with reduced T2 values. In this cohort, MRI T2 relaxation time was reduced in a subset of eFSE rats 6 hours after insult compared to controls (Fig. 7A). Three of 6 eFSE rats in this cohort had T2 relaxation times that were lower than 2 standard deviations from the control mean, the cut-off for considering the signal abnormal and predictive of later life epilepsy (Fig. 7B). We assessed hippocampal cytokine expression in the same rats 24-hours after eFSE. The expression of a number of inflammatory mediators tended to be higher in the rats in which MRI signal changes were found (Fig. 7C). In addition, expression of a number of individual inflammatory mediators correlated significantly and inversely with T2 relaxation times. This correlation was largely limited to inflammatory molecules that were upregulated in hippocampus 24 hours after the insult including: IL-1r1 and COX2 (Fig. 7D-E).

Because the epilepsy-predicting change in T2 relaxation time took place in the amygdala complex, we examined in an additional cohort of animals if cytokine expression in the amygdala correlated with T2 signal changes in the same animal. In

this cohort, 7 of 11 eFSE animals had T2 relaxation times lower than 2 standard deviations of control ('affected'; Fig. 7F). Amygdala cytokine mRNA levels at 24 hours after eFSE are shown in Figure 7G, dividing the cohort into 'affected' and non-affected. As apparent, a subgroup of inflammatory mediators including IL-1r1, TLR4 and IL-6 seemed to distinguish between the groups. When amygdalar cytokine mRNA levels were plotted against T2 relaxation times, only IL-1r1 was significantly correlated (Fig. 7H). Comparing the correlations of hippocampal and amygdala cytokine levels and the predictive T2 signal change, IL-1r1 was common to both regions. In addition, COX2 correlated with the MRI changes in hippocampus only. A weak correlation between mRNA levels of TLR4, a target of HMGB1with MRI changes was observed ($p = 0.15$, spearman $r = -0.33$) (Fig. 7I). Together, these data suggest that individual differences among rats in the type and degree of inflammatory response to eFSE in at least two limbic regions implicated in epileptogenesis, may underlie MRI signal changes that predict the eventual development of epilepsy in the same rats. The data support the notion that specific subsets of inflammatory molecules contribute to epileptogenesis following eFSE in individual animals.

Figure 4.7: Inflammation profiles of individual animals correlates with predictive measure of post eFSE epilepsy. (A) Representative color-coded quantitative T2 maps 4-6-hours after the end of eFSE from a control animal (n=9) an eFSE animal not expected to become epileptic (eFSE Not Affected; n=5) and an eFSE animal expected to become epileptic (eFSE Affected; n=7). Basolateral amygdala (whose T2 relaxation time is used to predict epilepsy) is highlighted in enlarged pictures below. Cooler colors (blues) represent faster T2 relaxation times while warmer colors (greens and oranges) indicate slower T2 relaxation times. (B) Prediction of epilepsy after eFSE is determined when T2 relaxation times of eFSE falls 2 standard deviations below the control mean, represented here by a black line across the y-axis. In hippocampus, expression of inflammatory molecules is higher in animals expected to become epileptic (affected-A) compared to those not expected to become epileptic (not affected- NA) (C). Inverse correlations are found between T2 relaxation times and IL-1r1 (D) and COX2 (E) (CTL n = 4, eFSE n = 6). (F) For cytokine correlations in amygdala, 7 of 11 eFSE animals had T2 values low enough to consider them “affected”. (G) Cytokine mRNA data from amygdalar punches 24 hours after the ends of eFSE demonstrate lower discrimination between affected and non-affected animals. Correlations between predictive MRI signal changes were present with IL-1r1 mRNA (H) a weak correlation existed between T2 levels and *T*LR4 (I) (CTL n= 9, eFSE n= 12). Data are presented as mean±SEM. *Statistically significant at $p<0.05$.

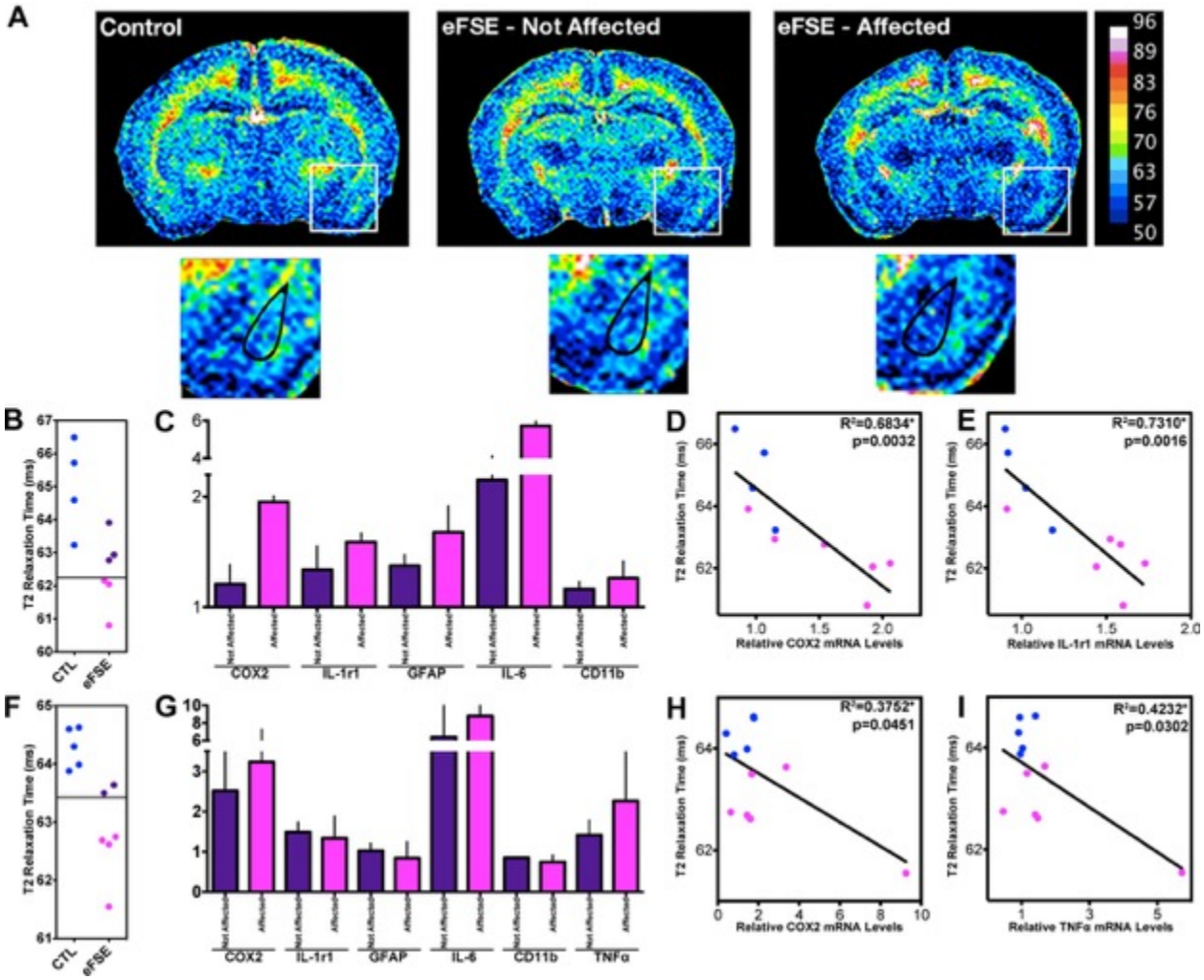
A
Control
eFSE - Not Affected
eFSE - Affected
96
89
83
76
70
63
57
50
B
T2 Relaxation Time (ms)
CTL
eFSE
C
COX2
IL-1r1
GFAP
IL-6
CD11b
D
R²=0.6834*
p=0.0032
Relative COX2 mRNA Levels
E
R²=0.7310*
p=0.0016
Relative IL-1r1 mRNA Levels
F
G
TNFα
H
R²=0.3752*
p=0.0451
I
R²=0.4232*
p=0.0302
Relative TNFα mRNA Levels

Discussion

The principal findings of this series of experiments are: (1) Rapid and coordinate upregulated expression of a subset of inflammatory molecules takes place in hippocampus and amygdala within hours after eFSE. (2) Inflammatory mediator expression profiles vary significantly among individual eFSE-experiencing rats, and only partial overlap exists between hippocampal and amygdala expression patterns. (3) Inflammatory profiles of individual rats correlate with MRI T2 signal changes that predict epileptogenesis.

The earliest change detected in a subgroup of eFSE experiencing immature rats was the translocation of the cellular-stress sensitive protein HMGB1 from nucleus to cytoplasm (Rovere-Querini et al., 2004). This event, taking place within minutes to hours suggests that while eFSE does not seem to kill cells it does provokes major cellular stress in hippocampal neurons (Toth et al., 1998; Dubé et al., 2010; Choy et al., 2014). HMGB1 translocation to the cytoplasm is typically followed by release from the cell and activation of receptors on microglia and astrocytes (including TLR4) to promote the synthesis of multiple inflammatory cytokines (Rovere-Querini et al., 2004). It should be noted that a number of other activators of TLR4 receptors (such as degradation products of the cellular matrix and heat shock proteins) have been reported by several groups. However, cellular debris and heat shock proteins have not been found in the eFSE model (Toth et al., 1998; Bender et al., 2004; Baram et al., 2011). In addition, whereas HMGB1 translocation in adult models of epilepsy has typically been reported in astrocytes and microglia (Maroso et al., 2010), in the eFSE model we find the

translocation exclusively in neurons during the first few hours (Choy et al., 2014). This cell-specificity might be a result of the seizure-inciting insult, the age of the animals, or both (Baram, 2012).

Here we found that, in hippocampus, expression of IL-1β, its receptor (IL-1r1), TNFα, COX2 and GFAP were upregulated during the hours and days following eFSE. Most cytokines were transiently upregulated with levels resembling those in controls by 96 hours after eFSE. Only COX2 remained upregulated at this time point. Looking within the amygdala (at the 24 hour timepoint) demonstrated similar findings, with IL-6, COX2 and TNFα expression augmented. These quantitative analyses of cytokine expression were complemented by immunohistochemical evidence for significant astrocytosis and microglia activation 24-hours after eFSE, indicative of an active inflammatory response in the hippocampus. Thus, whereas the expression of the cytokines measured here was transient, it might well set in motion additional downstream processes, potentially via activation of NF-κb and other transcriptional regulators (Crespel et al., 2002; Aronica et al., 2010). These downstream consequences of the original wave of select inflammatory processes might contribute to the development of epilepsy.

An important question for both clinical FSE and eFSE is *why* some individuals go on to become epileptic while others do not. Whereas difficult to test in humans, we have tried to identify factors that might contribute to epilepsy during or after eFSE. There were no discernable differences in the initial eFSE, where the seizure duration, time to onset and intensity were similar among rats that eventually became epileptic and those that did not

(Dubé et al., 2010; Choy et al., 2014). As demonstrated here, it is unlikely that the hyperthermia alone caused toxic physiological consequences because core temperatures never elevated above 41.5°C during eFSE. In addition, whereas there was no inter-litter variability in reaction to the inciting event, inter-animal variability was found in each litter both in the expression of inflammatory mediators and potential seizure outcome. The studies described here suggest that an insult across genetically similar animals might result in markedly varied inflammatory profiles. These might derive from prior inflammatory or immune challenge (Riazi et al., 2010; Galic et al., 2012) or other, as yet undiscovered reasons. The current data tempt us to speculate that the divergent inflammatory responses in eFSE-experiencing rats might, in turn, lead to divergent epileptogenic outcomes.

Interestingly, while in hippocampus both COX2 and IL-1r1 levels correlated with the epilepsy-predictive MRI signal change after eFSE, in amygdala the correlation was with IL-1r1 mRNA levels only. The divergence between regions may suggest regional inflammatory differences in the limbic system that are important for epileptogenesis. The involvement of IL-1r1 in both regions is intriguing, suggesting that this specific cytokine may be instrumental in epilepsy generated by eFSE. Previous work has demonstrated that this cytokine pathway was required for the generation of eFSE (Dubé et al., 2005). Further work suggested that IL-1β levels distinguished adult epileptic rats from those that did not develop epilepsy following eFSE (Dubé et al., 2010). The current work provides additional support for the notion that augmentation of this cascade in a subset of rats contributes to epileptogenesis in the same rats. Notably, blocking the interleukin-

1 cascade in epileptic animals has anti-convulsive effects, but the role if this cascade in epileptogenesis is presently unclear (Maroso et al., 2011; Noe et al., 2013). This role might vary among models because of differences in animal ages and other parameters.

In summary, these correlative studies demonstrate a potential relationship between selective augmentation of subsets of inflammatory mediators after eFSE and epilepsy. Blocking inflammation as a whole (Holtman et al., 2014) has proven unhelpful for aborting epilepsy, as have a number of studies targeting specific pathways in the inflammatory molecular-network (Noe et al., 2013; Vezzani et al, 2011; Holtman et al., 2009). Indeed, rather than being pathogenic, it is possible that some observed inflammatory responses may be neuroprotective against the epileptogenic process, as described for other disorders (Schwartz & Kipnis, 2005). Future studies will focus on dissecting out which of the inflammatory cytokines and mediators described here are epileptogenic and which might be important for restoring normal neuronal function.

CHAPTER 5

Blocking inflammation after eFSE prevents hippocampal hyper-excitability

Overview

Temporal lobe epilepsy (TLE) is an epilepsy that involves the limbic circuit associated with cognitive and emotional deficits The antecedents or risk factors for TLE include long (>30 minutes) fever-associated seizures in childhood known as febrile status epilepticus (FSE) (Cendes et al.,1993; Berg & Shinnar, 1996; Berg et al., 1997French et al., 1993; Dubé et al., 2007). Mounting evidence suggests that FSE leads to temporal lobe epilepsy (TLE) in a subset of individuals (Annegers et al., 1987; Cendes et al.,1993; Dubé et al., 2007; Seinfeld et al., 2014; Lewis et al., 2014). To elucidate potential mechanisms by which FSE promotes epilepsy, an immature rat model of experimental (e)FSE has been created and extensively studied (Baram et al., 1997; Dubé et al., 2010). In this model, ~40% of eFSE rats go on to become epileptic, in accord with the human condition.

Fever, the initiator of FSE, intrinsically involves inflammation and inflammation is implicated in many animal models of epileptogenesis. Our work has demonstrated that the cytokine interleukin- 1β (IL-1β) is a crucial component in eFSE generation (Dubé et al., 2005). Further, higher levels of IL-1β are found in the hippocampus of animals that become epileptic (Riazi et al., 2010; Heida et al., 2005, 2009; Luheshi, Stefferl & Turnbull, 1997; Eskilsson et al., 2014; Dubé et al., 2005, 2010). Finally, animals destined to become epileptic after eFSE have a more robust inflammatory response in

both hippocampus and amygdala (Patterson et al., 2015). For these reasons, inflammation has become an attractive target for anti-epileptogenic therapies, the goal of which would be to abort the epileptogenic process before spontaneous seizures begin. (De Simoni et al., 2000; Dedeurwaerdere et al., 2012; Pollut, Dudek & Dingledine, 2013; Ollikainen et al., 2004; Vezzani et al., 2010; Patterson et al., 2014).

Here, we used the global anti-inflammatory agent dexamethasone (DEX) immediately after eFSE to suppress inflammation. DEX is a readily available anti-inflammatory glucocorticoid, which inhibits the gene expression of many cytokines, including IL-1β (Jeon et al., 2000; Jang et al., 2007). Glucocorticoids, including DEX, act by inducing transcriptional changes through the glucocorticoid receptor (Bruccoleri et al., 1999). While there are varied downstream effects of this interaction (Sorrells & Sapolsky, 2007) the inhibition of NF-κB by DEX specifically prevents inflammation (Auphan et al., 1995). NF-κB is a heterodimer kept inactive in the cytoplasm until stimulation when it is rapidly degraded and specific subunits travel into the nucleus to promote the transcription of many pro-inflammatory cytokines and mediators (Gilmore, 2006). DEX prevents the degradation of NF-κB and thus the stimulation of broad inflammatory cascades (Auphan et al., 1995).

We found that acute, transient DEX administration after experimental FSE suppresses hippocampal hyper-excitability apparent as spike series for at least a month after eFSE, a finding with potential clinical relevance.

Methods and Materials

Induction of experimental Febrile Status Epilepticus (eFSE) All animal procedures were performed in accordance with the University of California-Irvine animal care committee's regulations. The induction of eFSE has been detailed previously and is briefly described here (Baram & Gerth 1997; Dubè et al., 2010; Patterson et al., 2015). Postnatal day 10-11 male Sprague-Dawley rat pups were used for all studies. Pups were placed, two at a time, inside a 3-liter flask the bottom of which was lined with absorbent paper. Pups were subjected to a continuous stream of warm air until behaviors indicating seizures began. These behaviors were identified as arrest of hyperthermia-induced hyperkinesis (freezing) followed by chewing automatisms. Core temperatures at the onset of these seizures were then rapidly measured, and seizure-onset time noted. Once seizures commenced, elevated core temperature and seizures were maintained via the warm air stream for 40-60 minutes. Seizure behaviors typically progressed over the hyperthermia period, including chewing of an extremity, clonic movements and eventual tonic extension. Pups' core temperature was measured every 2 minutes during the eFSE. If the pups' core temperature exceeded 41.5C they were removed from the chamber and placed on a cool metal surface for the next two minutes. After hyperthermia eFSE pups were briefly immersed in cool water (~23.0°C) to aid in return of core temperature to normothermia and promote seizure cessation. Pups were then placed on a euthermic pad maintained at 37ÆC for 30 minutes then returned to their home cage and dam. In this study, all pups subjected to hyperthermia experienced eFSE and there was no mortality.

Experimental overview Three distinct cohorts of rats were generated for this study:

1. The first cohort was established to test the relationship between eFSE, spike series and epilepsy. Both eFSE and control rata were generated in mixed litters and implanted 2 months after insult. Starting at ~P100 rats were chronically recorded using video/EEG to detect spike series and seizures. Rats were recorded in this manner until they were ~1 year of age when they were sacrificed.
2. Another cohort of rats was produced to assess the effects DEX on hippocampal excitability after eFSE. This cohort was implanted with EEG electrodes within 3 days after eFSE and video/EEG monitored for 4 weeks after surgery.
3. The third cohort of rats was employe to eamine eFSE-induced inflammation nand the effects of DEX. Rats were sacrificed 3 hours after the end of eFSE to measure mRNA levels of cytokines in the hippocampus.

DEX administration Immediately after the end of eFSE (after immersion in cool water to cease febrile seizures) rats were injected I.P. with 3 mg/kg DEX (sigma-alderich). Rats used for video/EEG monitoring for the presence of spike series (cohort 2) were given sequential tapering doses of DEX over the next 48 hours as well as aldosterone (0.2 µg/100mg SC) to provide mineralocortioicid functions which were suppressed by DEX. Rats used in the third cohort were sacrificed 3 hours after the end of eFSE and only received a singular dose of DEX. Vehicle treated animals received an I.P. injection of saline the volume of which was calculated as if the animal were receiving treatment. This paradigm yielded four experimental groups: 1) control (non-eFSE) rats injected with vehicle (CTL-VEH). 2) control (non-eFSE) rats injected with DEX (CTL-DEX). 3)

eFSE rats injected with vehicle (eFSE-VEH) and 4) eFSE rats injected with DEX (eFSE-DEX). Abbreviations of experimental groups will be used for the duration of the manuscript.

EEG electrode implantation 3 days or 2 months after eFSE (depending on experimental group), rats were implanted with bipolar electrodes (Plastics One) in both dorsal hippocampi (AP: 2.7; L: 1.8; V: -2.2 mm with reference to bregma) and a cortical electrode was placed over the parietal cortex (AP: 2.0; L: -1.5 mm). An additional ground electrode was inserted over the cerebellar cortex and the whole cap was secured with acrylic (Plastics One). Rats were kept on a warm pad for one hour after surgery and then returned to their home cage.

Video/EEG Recordings and Analysis Rats were recorded with video/EEG to study alterations in hippocampal brain wave activity. The first cohort of rats were chronically recorded from approximately ~100 days after eFSE until the rats were one year of age. EEG recordings from the second cohort of rats were obtained the day after electrode implantation (P14) for 4 weeks. Rats were recorded for 2 hours a day in amply bedded cages until the completion of the experiment. Short recording times were necessary to ensure that the pups received sufficient nutrition from their mothers. Hippocampal electroencephalograms were acquired from freely moving pups. EEGs were obtained and analyzed using Chart7 software (LabChart). Video/EEG was analyzed without knowledge of treatment group by a trained investigator.

qRT-PCR Whole hippocampi were rapidly dissected on ice 3 hours after the end of eFSE using RNAse free instruments. Tissue was immediately transferred to pre- chilled centrifuge tubes kept on dry ice. Samples were stored at -80C until use. Total RNA was extracted from hippocampi using the mirVana miRNA Isolation Kit according to the manufacturer's instructions (Ambion, New York, USA). Double- stranded cDNA was synthesized from total RNA using Roche 1st strand cDNA synthesis kit (Cat # 04379012001; Roche) with random hexamer primers. Analysis of the PCR products was executed using cDNA samples in triplicate on a Roche LIghtcycler 96 system (Roche). Samples were normalized to β-˘Actin and quantified using the cycle threshold method (2^ΔΔCt). Primers used in this study are shown in Table 4.1.

Statistics Appropriate statistical tests were run using Prism6 software (Graphpad). The D'Agostino & Pearson omnibus normality test was conducted to determine if data were Gaussian in nature. If data were Gasussian, a parametric statistical test was run. If the data was not Gaussian a non-parametric test was run. The numbers of rats needed for each experiment were determined using Power Analysis before experiments began.

Results

Spike series precede the occurrence of spontaneous seizures after eFSE eFSE result in spontaneous seizures in ~40% of rodents. The seizures are sparse (<1/week, Choy et al., 2014, Dubé et al., 2010), and their onset is in in late adolescence or adulthood. Whereas these features resemble the long latency between FSE and TLE in children, and the development of epilepsy in ~40% of individuals with FSE (Annegers et al.,

1987), they present challenges in addressing potential antiepileptogeneic effects of drugs.

To identify early predictors of epileptogenesis, we examined the relationship of spike series and spontaneous seizures after eFSE (Staley et al., 2011). As shown in figure 1, EEG recordings from dorsal hippocampus of control and eFSE rats (n=18) demonstrated both spike series and seizures (Fig. 1B-C). Notably, spike series were never found in control animals (n=5), supporting previous work (Raol et al., 2003; Dubé et al., 2000, 2006, 2010; Choy et al., 2014). In eFSE- experiencing rats, 69.2% of rats developed spike series and 38.5% (62.5% of these) progressed to spontaneous seizures. Neither spike series nor seizures were detected in about a third (30.8%) of eFSE-experiencing rats (Fig. 1D).

Thus, spike series were abnormal, and always preceded the development of spontaneous seizures after eFSE in this series, with a latency of one to 86 days (Fig. 1E-F). In addition, 65% of spike series-exhibiting rats progressed to overt seizures. Together, these data suggest that spike series indicate a hyperexcitable hippocampal network state after eFSE, that commonly portends future spontaneous seizures. Accordingly, spike series provide an early and useful target for assessing efficacy of anti-epileptogenic interventions

Figure 5.1: The relationship between spike series and seizures after eFSE. Representative traces showing baseline (A), spike series (B) and seizures (C) during EEG recordings from eFSE rats. eFSE rats fall into one of three categories: they are either epileptic (Epi; with spike series and spontaneous seizures), non-epileptic but hyperexcitable (Sp Ser; with spike series but no seizures) or non-epileptic (Non-Epi; no spike series or seizrues) (D). (E) The difference in the onset of spike series and seizures ranges from one day to 87 days and spike series always come first. (F) The onset of spike series always precedes the onset of seizures after eFSE. eFSE n=13, CTL n=5. Black arrows indicate spikes. EEG scale= 1 mV/5s

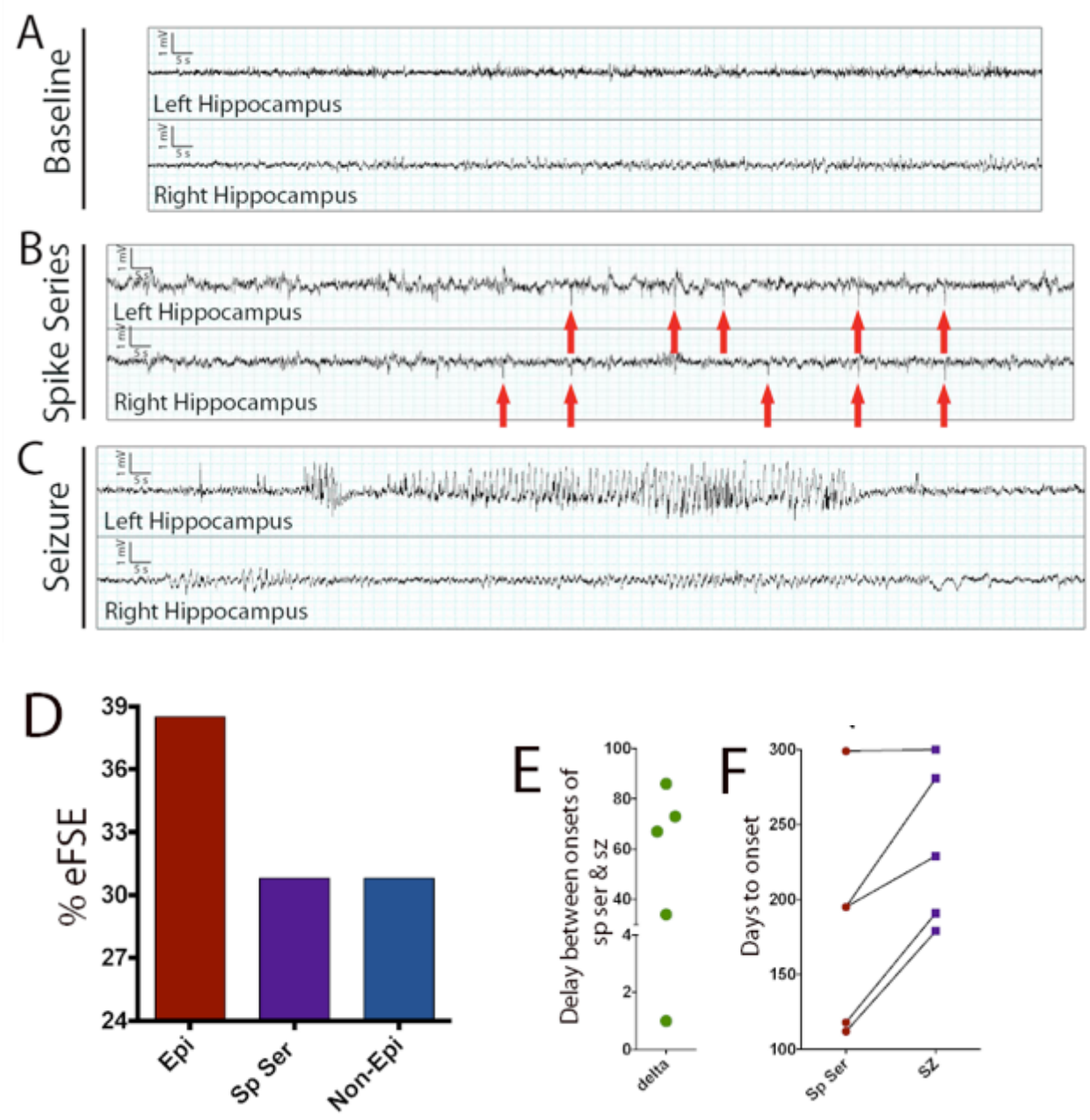
A
Baseline
Left Hippocampus
Right Hippocampus
B
Spike Series
Left Hippocampus
Right Hippocampus
C
Seizure
Left Hippocampus
Right Hippocampus
D
% eFSE
39
36
33
30
27
24
Epi
Sp Ser
Non-Epi
E
Delay between onsets of sp ser & sz
100
80
60
40
4
2
0
delta
F
Days to onset
300
250
200
150
100
Sp Ser
SZ

Dexamethasone reduces spike series after eFSE To test whether eFSE-induced inflammation contributed to hippocampal hyper-excitability we administrated the anti-inflammatory synthetic glucocorticoid DEX (Figure 2). We then investigated the onset, number and duration of spike series in eFSE rats compared with controls, and the effect of DEX on these parameters.

Figure 5.2: Schematic of experimental design. eFSE was induced in P10 rats. Rats were given DEX immediately, 24 hours and 48 hours after eFSE. Surgery to implant electrodes into dorsal hippocampus was conducted on P13. Daily EEG recordings were obtained from P14-P43.

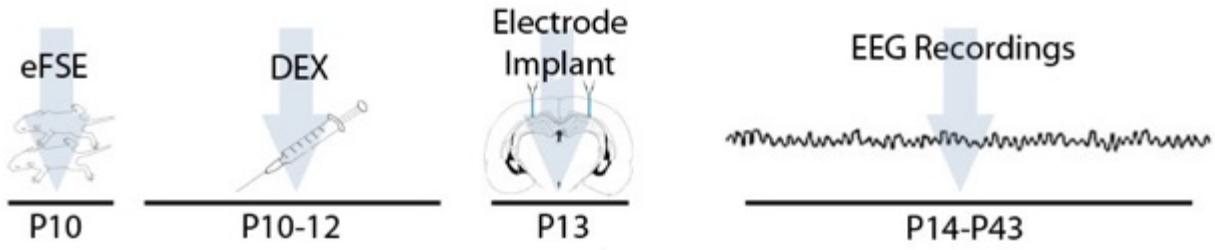
eFSE
DEX
Electrode Implant
EEG Recordings
P10
P10-12
P13
P14-P43

Representative EEG from eFSE rats without spike series (Fig. 3A) and with spike series (Fig. 3B) are shown. Neither CTL-VEH nor CTL-DEX rats had spike series throughout the recording period (Fig. 3C). Among eFSE-VEH rats, 57.1% (8/14) had at least one spike series in the month after eFSE. In contrast, only 23.1% (3 out of 13) eFSE-DEX rats had at least one spike series during the same recording time. The total number of all spike series was significantly different between eFSE-VEH and eFSE-DEX groups (Mann-Whitney U=50.50, p=0.03). Notably, the probability of having at least one spike series was not higher than zero in the eFSE-DEX rats (one sample t-test; t_{12}=1.9, p=0.08; Fig. 3B). Interestingly, DEX did not influence the duration of spike series (eFSE-DEX vs eFSE-VEH; mean duration eFSE-VEH=37.56 seconds and eFSE-DEX=39.39 seconds; Mann-Whitney U=12; p>0.99; Figure 3D).

Together these data demonstrate that administration of DEX transiently following eFSE reduces the probability of the development of a hyperexcitable hippocampus, measured as a spike series.

Figure 5.3: DEX reduces spike series after eFSE. Representative EEG traces show baseline hippocampal activity (A) and spike series (B). (C) DEX reduces the number of spike series recorded after eFSE in rats and neither CTL-VEH nor CTL-DEX rats have spike series (ANOVA, Kruskal-Wallis=8.05, p=0.04). (D) DEX reduces the probability of spike series after eFSE, while the likely-hood of spike series with vehicle treatment is high (eFSE-VEH, t_{13}=4, p=0.001; eFSE-DEX, t_{12}=1.9, p=0.08). (E) DEX does not later the length of spike series when they occur as compared to the average length of spike series in eFSE-VEH rats (Mann-Whitney U=12, P>0.99). CTL-VEH n=4, CTL-DEX n=4, eFSE-VEH n=14, eFSE-DEX n=13. Data are presented as mean ± SEM. *Statistically significant at p<0.05. Black arrows indicate spikes. EEG scale= 1 mV/5s

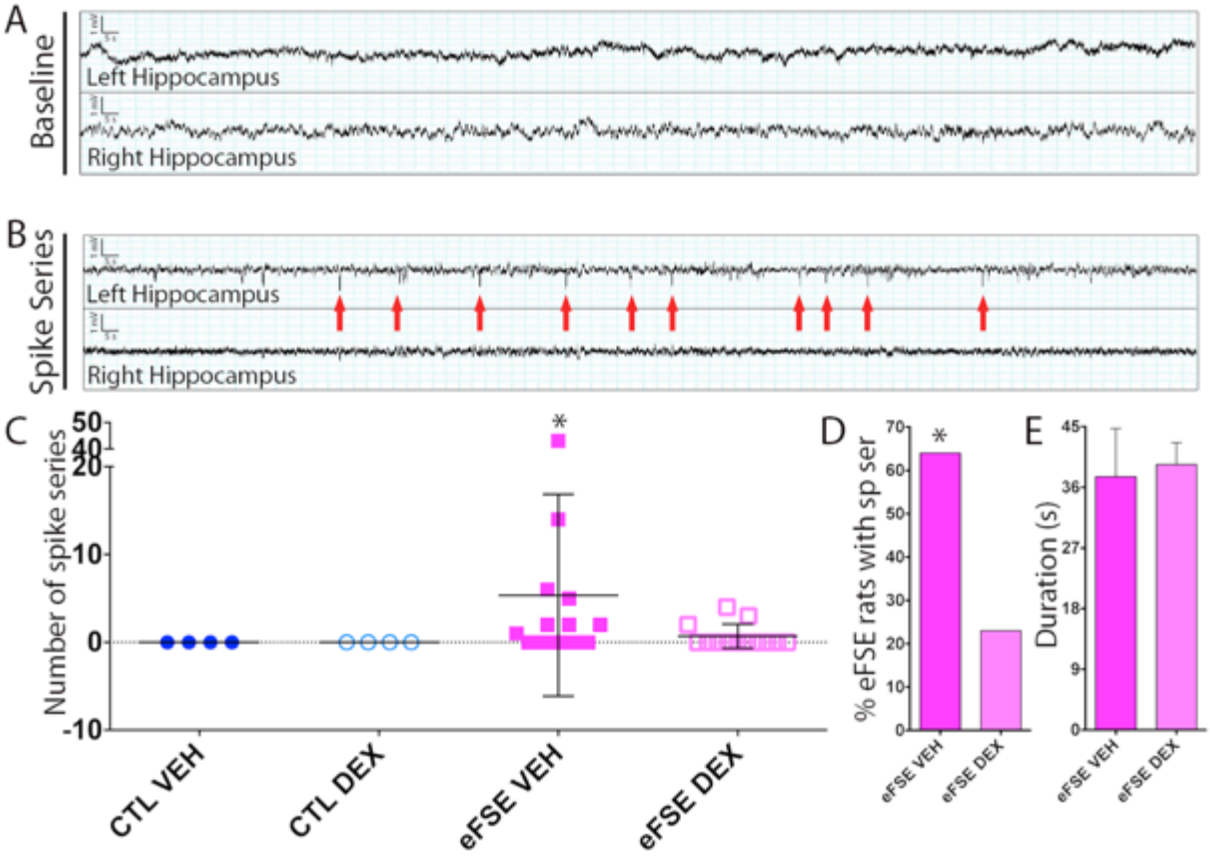
A
Baseline
Left Hippocampus
Right Hippocampus
B
Spike Series
Left Hippocampus
Right Hippocampus
C
Number of spike series
50
40
20
10
0
-10
*
CTL VEH
CTL DEX
eFSE VEH
eFSE DEX
D
% eFSE rats with sp ser
70
60
50
40
30
20
10
0
*
eFSE VEH
eFSE DEX
E
Duration (s)
45
36
27
18
9
0
eFSE VEH
eFSE DEX

Dexamethasone administration immediately after eFSE prevents upregulation of pro-inflammatory mRNA transcripts The levels of several inflammatory mediators shown to be augmented by eFSE (Patterson et al., 2015, Dubé et al., 2005), as well as other types of status epilepticus (De Simoni et al., 2000; Pouliot et al., 2013) were analyzed three hours after the eFSE, and the effects of DEX on the expression of these inflammatory mediators were assessed using qRT-PCR. We focused on molecules that are upregulated rapidly after eFSE, and that, in addition, have been implicated in epileptogenesis (Maroso et al., 2010; Noe et al., 2013).

Group effects in the levels of IL-1β mRNA were detected in the hippocampi of experimental rats 3 hours after the end of eFSE compared with controls (Fig 4A; one-way ANOVA; $F=9.98$, $p=0.0002$). Whereas IL-1β mRNA levels in both control groups were similar (CTL-VEH, mean=1.00 versus CTL-DEX, mean=1.18; $t_{22}=0.48$, $p>0.05$; Bonferroni's multiple comparisons test) there was a significant increase in IL-1β mRNA in eFSE-VEH hippocampi (CTL-VEH versus eFSE-VEH, mean=1.52; 3 $t_{22}=4.22$, $p<0.05$). DEX administration after eFSE rendered the levels of hippocampal IL-1β mRNA statistically similar from those of CTL-VEH rats (CTL-VEH versus eFSE-DEX, mean=0.56, $t_{22}=0.32$, $p>0.05$).

Group effects in the mRNA expression for the IL-1β receptor, IL-1r1 are also found (Fig. 4B; one-way ANOVA; $F=10.91$, $p=0.0002$). Again DEX did not influence control rats (CTL-VEH, mean=1.09 vs CTL-DEX, mean=0.56 $t_{20}=2.66$, $p>0.05$ Bonferroni's multiple comparisons test). IL-1r1 levels in eFSE-VEH rats (mean=1.55) are higher than in CTL-

VEH and significantly higher than in CTL-DEX (t_{20}=5.16, p<0.05). Notably, treatment with DEX reduced hippocampal levels of IL-1r1 mRNA in FSE-DEX group (mean=0.36) to levels indistinguishable from CTL-VEH rats (CTL-VEH versus eFSE-DEX; t_{20}=2.03, p>0.05) and significantly lower than eFSE-VEH rats (eFSE-VEH versus eFSE-DEX; t_{20}=4.6, p<0.05).

COX2 mRNA did not reveal statistically significant group differences (Fig. 4C; one-way ANOVA; F=2.65, p=0.08). No difference in mRNA expression exists between control groups (CTL-VEH, mean=1.00 versus CTL-DEX, mean=0.89; t_{19}=0.12, p>0.05; Bonferroni's multiple comparisons test) but some eFSE-VEH rats had 4-6 times the amount of COX2 mRNA (CTL-VEH versus eFSE-VEH, mean=3.56; t_{19}=2.13, p>0.05). eFSE-DEX rats are indistinguishable from either control group (eFSE-DEX, mean=1.45 versus CTL-VEH; t19=0.36, p>0.05).

Together these data suggest that DEX administration after eFSE prevents the upregulation of multiple inflammatory pathways after insult. DEX administration alone (as demonstrated in CTL-DEX rats) does not have any appreciable influence on nascent cytokine transcripts.

Figure 5.4: DEX prevents inflammation after eFSE. (A) IL-1β mRNA is upregulated after eFSE (mean=2.75) as compared to CTL-VEH (mean=1.0) rats while eFSE-DEX (mean=0.9) rats are similar to control (one-way ANOVA; F=9.83, p=0.0002: CTL-VEH vs CTL-DEX, t_{22}=0.48, p>0.05; CTL-VEH vs eFSE-VEH, t22=4.$_{22}$, p<0.05; CTL-VEH vs eFSE-DEX, t_{22}=0.32, p>0.05; eFSE-VEH vs eFSE-DEX, t_{22}=4.93, p<0.05; Bonferroni's multiple comparisons test). (B) The receptor for IL-1β, IL-1r1 is also marginally upregulated after eFSE (mean=1.55) as compared to CTL-VEH (1.09) rats (one-way ANOVA, F=10.91, p=0.0002: CTL-VEH vs CTL-DEX, t_{20}=2.66, p>0.05; CTL-VEH vs eFSE-VEH, t_{20}=2.26, p>0.05; CTL-VEH vs eFSE-DEX, t_{20}=2.03, p>0.05; eFSE-VEH vs eFSE-DEX, t_{20}=4.6, p<0.05; Bonferroni's multiple comparisons test). eFSE-DEX (mean=0.7) rats have similar levels of IL-1r1 to CTL-VEH rats. (C) COX2 expression in eFSE-VEH (mean=3.56) is heterogeneic in nature, but upregulated in many rats compared to CTL-VEH (mean=1.0) (one-way ANOVA, F=2.65, p=0.08: CTL-VEH vs CTL-DEX, t19=0.12, p>0.05; CTL-VEH vs eSFE-VEH, t19=2.13, p>0.05; CTL-VEH vs eFSE-DEX, t19=0.36, p>0.05; eFSE-VEH vs eSFE-DEX, t19=2.07, p>0.05; Bonferroni's multiple comparisons test). Data are presented as mean ± SEM. *Statistically significant at p<0.05.

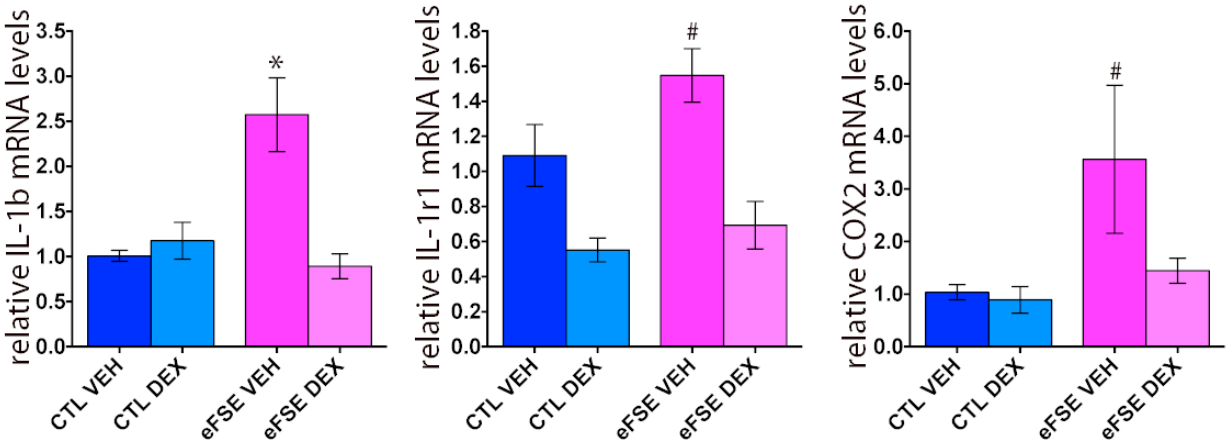
relative IL-1b mRNA levels
3.5
3.0
2.5
2.0
1.5
1.0
0.5
0.0
*
CTL VEH
CTL DEX
eFSE VEH
eFSE DEX
relative IL-1r1 mRNA levels
1.8
1.6
1.4
1.2
1.0
0.8
0.6
0.4
0.2
0.0
#
CTL VEH
CTL DEX
eFSE VEH
eFSE DEX
relative COX2 mRNA levels
6.0
5.0
4.0
3.0
2.0
1.0
0.0
#
CTL VEH
CTL DEX
eFSE VEH
eFSE DEX

Discussion

The main findings of the present study are as follows: 1) Spike series often precede seizures and are a good indicator of a hyperexcitable hippocampal network after eFSE 2) DEX administration after eFSE rapidly and completely blocks the transcription of several pro-inflammatory mediators 3) Acute, transient DEX administration greatly reduces the probability of developing spike series in eFSE-esperienceing rats. These findings suggest that inflammation contributes to early-stages of epileptogenesis that follow eFSE, with potential for translational relevance.

DEX was specifically selected for this study for a multitude of reasons. It is a powerful anti-inflammatory agent on the order of ~5 times more potent than prednisone already used in children in the age range with FSE are prevalent. DEX is known to rapidly cross the blood brain barrier, a concern whenever dealing with therapeutics in the brain. Additionally, DEX is already clinically available, rendering its potential effects more immediate and cost efficient compared to the development of targeted, novel small molecules which are not yet to market.

Much research has focused on the relationship between inflammation and epileptogenesis. Numerous prior studies in several models failed to show that blocking inflammation prevents the development of spontaneous seizures (Holtman et al., 2009, 2010, 2014; Pouliot et al., 2013: Noe et al., 2013). Differences between those studies and the present one may lie in the animal models used to study epileptogenesis. Traditional models of epileptogenesis use powerful chemoconvulsants including kainic

acid or pilocarpine. These models induce epilepsy in close to 100% of rodents, providing excellent statistical power to demonstrate a reduction in epileptogenesis. However, they provoke cell death and may be too robust for reversion or amelioration by most interventions. In contrast, our model of eFSE which provokes epilepsy in only 40% of rats. This is a disadvantage in high-throughput studies, but provides significant advantages. Molecular and cellular changes that occur in rats who progress to epilepsy can be compare with the same processes in rats that do not become epileptic, providing insight into relevant mechanisms. In addition, the absence of cell death in the model obviates confusion between mechanisms that are involved with cell death and repair and those that are involved in epileptogenesis.

Many questions remain after this initial research finding. The first and obvious one is whether eFSE-DEX rats go on to epilepsy in a similar or different manner than eFSE-VEH treated rats. While unlikely, it is possible that eFSE-DEX rats might not have spike series but do ultimately have spontaneous seizures. Secondly, a very high dose of DEX was used in this study. While no obvious deleterious effect was noted in DEX treated rats, it is always advantageous to use the lowest effective dose of a therapeutic. Finally, whether DEX treatment after FSE in children prevents later life limbic hyperexcitability is unclear. These queries will be focus of future research.

Chapter 6

Enduring cognitive deficits following eFSE are mediated by functional and structural effects of the neuronal repressive silencing factor (NRSF/REST1)

Overview

Epilepsy describes a broad category of disorders defined by spontaneous seizures. Whereas seizures have been the central focus of epilepsy research, they are commonly accompanied by cognitive deficits including memory and decision-making problems that contribute to poor quality of life in these individuals (Berg, 2011; Lucas et al., 2011). In the specific example of temporal lobe epilepsy (TLE), where the disorder involves the hippocampal-limbic circuit, cognitive problems are especially prominent (Mueller et al., 2012; Jokeit & Ebner, 1999; Helmstaedter et al., 2003; Brown et al., 2014), yet the mechanisms underlying their onset remain unclear (Elger, et al., 2004).

Many individuals with TLE have a history of long childhood febrile seizures (FS). While FS are common and benign in most cases, long febrile seizures, known as febrile status epilepticus (FSE) may cause hyperexcitability and epilepsy after an extended phase of network remodeling known as the “silent period” (Berg & Shinnar, 1996; French et al., 1993; Dubé et al., 2007; Lewis et al., 2014). A rodent model of experimental (e)FSE has been characterized and employed extensively to elucidate the mechanisms that underlie the generation of epilepsy after eFSE (Baram et al., 1997; Dubé et al., 2010; Patterson et al., 2015). Further, eFSE provoked enduring deficits in learning and memory (Barry et al., 2015; Barry et al., 2016; Dube et al., 2009), as found in some

children after FSE (Martinos et al., 2013; Shinnar et al., 2001; Tsai et al., 2015; Roy et al., 2011; Visser et al., 2012)

Although refractory TLE can be associated with cognitive decline (Jokeit and Ebner, 1999;Helmstaedter et al., 2003), there is evidence that cognitive deficits may arise before the onset of spontaneous seizures, or be independent from them (Hoppe et al., 2007; Elger et al., 2004;Hermann et al., 1997). These facts indicate that seizures and memory problems may engage the same limbic/hippocampal networks via independent or partially overlapping processes involving the hippocampal network

We have recently identified some of the mechanisms underlying functional changes in the hippocampal network that promote seizure-development after eFSE. Specifically, we uncovered coordinated transcriptionally-regulated changes in the expression of multiple genes that govern neuronal behavior. These changes, including enduring repression of the ion channel HCN1, were common to several insults promoting TLE, and replicated across laboratories (Jung et al., 2007, 2011; Brewster et al., 2002, 2005; Huang et al., 2009; Shin et al., 2008). Importantly, this large-scale, pro-epileptogenic transcriptional program involved the transcription factor Neuron Restrictive Silencing Factor (NRSF) (McClelland et al., 2011, 2014). NRSF is canonically expressed in non-neuronal tissues where it suppresses neuron-specific genes (Schoenherr & Anderson, 1995). Conversely, NRSF is found at low levels in mature neurons, where the expression of NRSF-regulated genes that contribute to neuronal maturation including the development of excitatory synapses is necessary (Rodenas-Ruano et al., 2012; McClelland 2014; Chen et al., 1998). After an epilepsy-inducing insult, including status

epilepticus, NRSF levels and activity are augmented (Palm et al., 1998; McClelland et al., 2011;2014), likely via insult-induced activation of sirtuins and repression of micro-RNA124 (Brennan et al., 2016). This important role of increased NRSF activity in mediating hippocampal network transformation after status epilepticus was identified because blocking NRSF binding to the chromatin attenuated the ensuing epilepsy (McClelland et al., 2011).

NRSF also plays a role in the regulation of gene expression programs during specific stages of neuronal maturation (Lunyak & Rosenfeld, 2005; Hsieh & Gage, 2004). During the developmental epoch when FSE takes place (infancy and early childhood in human, P10-11 in the rat model), most neurons are fully mature, but specific neuronal populations including dentate gyrus granule cells (GCs), are still differentiating and maturing (Schlessinger et al., 1975; Gao et al., 2011; Hester et al., 2013, 2014). These granule cells should be influenced by aberrantly increased levels of NRSF. Interestingly, abnormal maturation of GCs following status epilepticus has been shown to contribute to the formation of aberrant hippocampal networks (Thind et al., 2008; Goldberg & Coulter, 2013).

These dual roles render NRSF a promising candidate for contributing to abnormal structure and function of the hippocampal network following eFSE that might contribute to cognitive deficits. Here tested this hypothesis by transiently blocking NRSF binding to the chromatin after eFSE, then performing cognitive testing later in life. We analyzed the hippocampal oscillations underlying memory encoding and retrieval, and assessed structural integrity of the hippocampal network and the effects of eFSE and of blocking

NRSF function on both functional and structural underpinnings of hippocampus-dependent memory.

Methods and Materials

All experiments were conducted with approval of the institutional animal care committee (IACUC) and conformed to NIH guidelines. Experimental design, performance and analysis aimed to adopt guidelines for rigor and reproducibility in science (Landis et al., 2012). Group sizes were determined a priori, and animals were randomly assigned to experimental groups. All analyses were performed without knowledge of treatment group.

Induction of eFSE Induction of eFSE has been previously described (Baram, Gerth & Schultz 1997; Dubé 2010; Patterson et al., 2015). P10-11 male rats weighing 20-25 grams were used for all studies. Before hyperthermia, measures were taken to avoid burns to sensitive areas like the paws, ears and tails. Specifically, damage to the delicate tails of P10 rats was avoided by adhering the tail to a small, thin piece of wood. The edge of a larger, square piece of gauze was glued to the opposite side of the wood. Once the glue had dried, a generous amount of a glycerin-based hydrating ointment was applied to the tail. The gauze was then wrapped three times around the tail and the whole bandage was held into place with tape. Ears and paws were also coated with the glycerin-based hydrating ointment before hyperthermia. Using this method, no damage was incurred to these sensitive areas during or after hyperthermia. After protection was applied, rats were placed two at a time inside a 3-liter flask and subjected to a

continuous stream of warm air. The beginning of the seizure was determined by the onset of seizure-like behaviors such as freezing followed by chewing automatisms. Core temperature was noted at this time and this was considered seizures onset. Once seizures began, hyperthermia was maintained and thusly seizures which were noted by continued behavioral manifestations. Core temperatures were quickly checked every 2 minutes to ensure body temperature was maintained between 39.5 and 41.5°C during eFSE. This paradigm was continued for the duration of desired seizure length which for this study was 60 minutes. At the end of eFSE, animals were removed from the hyperthermia chamber and their bodies were briefly immersed in room temperature water, bringing their core temperatures down towards basal levels, and ensuring the cessation of seizures. Tail protection was easily removed and the pups were returned to their home cages and dams. In our hands, no mortality of pups from eFSE was observed.

ICV infusions of oligonucleotides An intact NRSE or a scrambled (SCR) NRSE sequence oligonucleotide (ODN) was infused ICV 3 hours after the end of eFSE (Sigma Aldrich). Four experimental groups were employed in these experiments. The first was a non-eFSE control animal that received a scrambled sequence of NRSE (CTL-SCR). The second was a non-eFSE control who received the NRSE sequenced ODN (CTL-NRSE). Third, were eFSE animals infused with scrambled ODN (eFSE-SCR). Finally, there was a group of eFSE animals infused with NRSE ODNs (eFSE-NRSE). These groups will be identified by their respective acronyms. A sharp-tipped cannula was created using a 30 gauge hyperthermic needle with the depth delineated for the

ventricles of a P10 rat pup (3mm) by a small amount of solder. The cannula was attached to microtubing and the tubing was attached to a 10μL Hamilton syringe. The syringe cannula was then loaded with either NRSE or SCR ODNs and placed into a syringe pump (KD Scientific). ICV infusions were done free-hand by using bregma demarcations, which are visible through the skin in a P10 rat pup. The needle was inserted through the skin and skull and into the brain up until the stopper was reached. 2.5 nmol of either NRSE or SCR ODN were infused bilaterally into the ventricles at a rate of 0.5 μL/minute and a volume of 2.5 μL/hemispheres. ICV infusions were repeated exactly as described again 24 hours after eFSE to ensure complete abatement of NRSF during noted times of augmentation after seizures.

Surgery At 3-5 months of age rats underwent implantation of a bilateral array of recording electrodes. The rats were anesthetized with inhaled isoflurane and placed in a stereotaxic frame. The skull was exposed and four screws inserted, two anterior to the left and right ends of bregma and two left and right over the cerebellum. Grounding was achieved via the right cerebellar screw.

Rats were chronically implanted with a custom implant that allowed for LFP (Local Field Potential) recordings from a 2 x 8 array of 50 μm stainless steel electrodes (California Fine Wire, CA) divided between the left and right hippocampus (- 3.8 AP, ± 3.8 ML). The electrode tips ranged from 2.5 – 3.5 mm in length from the skull surface. All implants were fixed to the skull via the skull screws (FHC Inc) and Grip Cement

(Dentsply Inc.). The wound was sutured and topical antibiotic applied. The interval between surgery and the beginning of electrophysiological recording was 1 week.

Active avoidance Animals underwent testing in the active place avoidance task (Biosignal; Brooklyn, New York). In this task, animals learn to associate an unmarked region of space with a mild shock on a constantly rotating arena. The rats must attend to their ever-changing position in the room frame lest they be rotated into a pre-determined shock zone where they receive a mildly painful electrical shock.

Rats were lightly anesthetized and implanted with a stainless steel swivel in the skin between the shoulders. This allowed attachment of a cable with an LED at the end that allows for automated tracking and also the delivery of shock. Experimenters were blind as to which animals were control and FSE.

The arena consists of a steel disc 82 cm in diameter and is lighted from both above and below. The arena is centered in a room where it is approximately 50 cm from black curtains on the S and E sides and 50 cm from white walls on the N and W sides. The N and W walls have an 11 cm gray power-strip that forms a continuous line 50 cm above the floor of the arena. Two rectangular spatial cues (30 cm high x 43 cm wide) depicting a red star (centered at W position) and a black circle (centered at N position), both on a white background, were placed 18 cm above the arena floor. An additional rectangular polarizing cue (53 cm high x 84 cm wide) made of white paper (Color-Aid 2.5 grey) with five 2.5 cm wide diagonal black stripes (Color-Aid 9.5 gray) was centered at the N position, 5 cm above the gray power strip.

On day one of training, the animal was connected to the shock cable and introduced to the rotating arena for a 10 min habituation without shock. On all subsequent sessions on training days 1 and 2, rats received a 0.4 ma shock in an unmarked 876 cm^2 wedge-shaped sector covering a 60° arc in the NE sector of the arena. The shock zone was stable in the room frame while the arena rotated. The entrance latency of the shock was 1ms, the shock duration was 0.5 sec and the inter-shock latency was 2 sec. Mixed groups of eFSE and control rats were trained in 8 ten-minute sessions per day for two days (16 sessions). Performance measures were recorded and analyzed using custom software (Biosignal; Brooklyn, New York).

Electrophysiology and recording protocols Rats were tethered to a recording cable while exploring the stable arena or during the active avoidance task. EEG signals were pre-amplified X 1 at the headstage and channeled through the tether cable to the signal amplifiers and computer interface. LFPs were sampled at 30 KHz and filtered at 1-9000 Hz (Neuralynx, Montana). All signals were referenced against a tetrode wire above the cerebellum.

The rat's location in the arena was sampled at 60 Hz (Biosignal, Brooklyn, USA) using a digital camera that detected a light emitting diode (LED) placed near the animal's head. Position and electrophysiology timestamps were synchronized offline using custom software. An additional LED fixed to the rotating arena was also detected and in register with the animal LED allowed for accurate calculation of speed when the arena was moving.

Recording sessions during exploration of the stable platform was used to assess baseline hippocampal EEG properties in the absence of cognitive demand. Two consecutive recording sessions were then made during performance of the active avoidance task. Rats were connected to the shock tether via a pin on the animal's neck. Two minutes later the arena would begin to rotate and the recording session in the active avoidance context would last for 10 min. The alternation from stable arena exploration to avoidance was typically separated by 5-10 min.

Signal processing of LFPs LFP signals were analyzed using the Matlab Signal Processing Toolbox (Mathworks, Inc.) and the Chronux toolbox (Mitra and Bokil, 2008). Spectrograms (1s window, 1s overlap, [3,5] tapers, 1-140 Hz) computed from fast Fourier transforms were performed over time course of the recording sessions. Only segments where the animal's speed was equal or greater to 5 cm/s were included in the analysis. The mean frequency and power (normalized by the sum of the spectrum) of the signal was calculated in theta (5-12 Hz) and slow gamma (25-50 Hz) bands. We also analyzed the relationship between animal speed and theta frequency in a similar manner to previous work (Richard et al., 2013).

Only one channel from the left and right hippocampus was used for analysis. In the case of multiple suitable electrodes, the electrode signal with the largest mean theta/delta ratio was selected for analysis.

Chromatin Immunoprecipitation (ChIP) 3 hours after ODN infusion, pups were rapidly decapitated and their hippocampi were removed and stored at -80°C. Hippocampi were thawed, cross linked with methanol-free formaldehyde for 10 min at room temperature in PBS. Neutralization of cross-linking was achieved with the addition of glycine. Tissue was added to homogenization buffer (50 mM HEPES pH 8.0, 140 mM NaCl,1 mM EDTA, 0.4% Igepel CA-630, 0.2% Triton X-100, and a cocktail of protease inhibitors) and centrification aided in nuclei collection. Nuclei were sonicated for 30 min using Diagenode sonicator (Denville, NJ) to an average size of 500 bp. After cellular debris was removed, lysate was precleared overnight with Protein-A/G (Santa Cruz, Dallas, TX) at 4 ^{o}C and then incubated with 10 µg of either control non-immune serum (IgG) (Cell Signaling, Danvers, MA) or anti-NRSF (Santa Cruz, Dallas, TX), overnight at 4^{o}C in buffer containing 20 mM Tris-HCl (pH 7.4), 150 mM NaCl, 1 mM EDTA and protease inhibitors. Protein A/G beads precleared with salmon sperm DNA (400 µg/ml) were added to lysate for 2 hours. The beads were washed several times and then eluted using a buffer containing 2% SDS and 0.2 M sodium bicarbonate. After reversal of cross-linking at 65 ^{o}C overnight, the bound DNA was purified and eluted using the QiaQuick MinElute PCR purification kit (Qiagen, Valencia, CA). Quantitative PCR (qPCR) amplification was done using SYBR Green chemistry (Roche) on a Lightcycler 96 (Roche) with primers specific for *Hcn1*.

Golgi Impregnation Rats were deeply anesthetized with 10 mg/kg pentobarbital. When they were unreactive to a toe pinch, rats were transcardically perfused with aldehyde fixative provided in the sliceGolgi Kit (Bioenno). After perfusion, brains were

immediately removed and drop- fixed in aldehyde for 48 hours. The sliceGolg Kit and protocol was used to impregnate neurons for structural analysis (Bioenno Tech, 003760). Brains were sectioned into 200 μM coronal slices on a vibratome and slices were immersed in impregnation solution for 7 days at room temperature in the dark. Sections were rinsed with 0.01 M PBS-T and transferred into a staining solution for 8 minutes followed by a 1 minute 0.01 M PBS-t wash. Slices were then treated with post-staining solution for 4 minutes followed by 4, 5 minute PBS washes. Slices were mounted onto gelatin coated slides, allowed to dry over night, dehydrated with 100% alcohol and xylenes and finally coverslipped with permount (Fisher).

Analysis of Golgi impregnated cells All Golgi analysis was conducted without knowledge of treatment groups. Analysis was completed at the same level in dorsal hippocampus for all animals and groups. Dentate Granule Cells (DGC) were selected based on their structure (small soma with fan-like apical processes and few basal processes) and their location in the upper and lower blade of the hlius. Total number of DGC were counted in both the upper and lower blades of the hilus over ~11,500 μM of dorsal hippocampus per animal. Hilar basal dendrites were categorized as a process on a DGC pointing into the hilus that is on the order of ~5 times thicker than a visible axon.

Sholl analysis of dorsal hippocampal CA1 cells were completed on fully impregnated cells between the crest and distal to the midline. Only long- shaft CA1 neurons were selected for this study. A total of 93 neurons were chosen for analysis with an average of 10 neurons selected for each animal. Sholl of DG neurons was completed on 263

neurons with an average of 65 neurons per group. Specifically, 4x microscope pictures were taken of dorsal CA1 or dorsal DG and masks of fully impregnated neurons were created in Photoshop. Concentric circles with increasing radiuses of 20 μM were centered with the smallest circle over the soma. A line was drawn horizontally across the soma to delineate apical and basal processes. Counts of processes crossing at each circle were completed to assess dendritic complexity and length.

Hippocampal Organotypic Slice Culture To test the direct effects epilepsy inducing insults has on the structure of developing DGCs, an in vitro system of DGC maturation was employed. Homozygous Thy1- YFP male mice were bred to C57bl6 female mice to produce heterozygote litters. These pups all expressed yellow fluorescent protein (YFP) on the neuron specific Thy1 promoter, which allowed for easy visualization of DGCs with fluorescent microscopy. At P7, pups were rapidly decapitated and their brains were removed under sterile conditions and in ice cold prep media ((MEM (Gibco), L-Glutamine (Gibco), HEPES Buffer (Fisher Scientific), Magnesium sulphate (Sigma) and cell culture grade water (GE Healthcare). Brains were cut in half and coronal hippocampi slices 200 μM in thickness were obtained using a McIllwain Tissue Chopper. Dorsal sections of hippocampi were isolated from the rest of the slice and placed four at a time on a 0.4 μM, 30 mm diameter cell culture insert (Merk Millipore) where they were maintained for the duration of culturing. Inserts were then placed in 6 well plates and into all ready prepared media (MEM, HBSS (Gibco), L-Glutamine, Magnesium sulfate, Sodium bicarbonate (Gibco), HEPES, heat inactivated horse serum (Gibco), ascorbic acid (Sigma) and cell culture grade water). 6- well plates were moved

to and maintained in a CO_2 enriched incubator (Thermo). On DIV 7, seizure- like activity was achieved in cultures by transferring inserts into culture media containing 6 μM Kainic Acid (Abcam) for 24 hours. Seizure-like activity was ceased by transferring cultures to fresh media. A time course of structural abnormalities conceived from seizure-like activity was completed by fixing cultures with ice cold paraformaldehyde at various time points after KA induction. Hippocampi were then removed from inserts and mounted on gelatin coated slides. Endogenous YFP in the processes of DGC was readily visible allowing for appropriate analysis.

Hippocampal Neuron culture Hippocampal neuron cultures were derived from postnatal day 0 rats. Hippocampi were quickly removed and incubated for 30 min in buffered salt solution containing 10 units/ml papain (Worthington). Cells were then mechanically triturated and plated at a density of 400–60 cells/mm^2 on 12-mm coverslips that were precoated with poly-D-lysine (Sigma). Cultures began incubation with Neurobasal Medium with B-27 supplement (Invitrogen) at 36 °C and 5% CO2. 3 hours later, half of the culture medium was replaced with a Neurobasal Medium/B-27-based medium that was preconditioned with 1–2-week old non-neuronal cell culture prepared from P3-P4 rat cortices. Cultures were refreshed approximately every 72 hours with conditioned medium. On DIV 7, cultures were exposed to 100 nM BODIPY linked ODNS (NRSE or SCR). BODIPY is a small, fluorescent molecule which allows for visualization of the ODN without structurally interfering with its transportation across membranes. New ODNs were added to cultures each time they were refreshed. Cultures were collected

on DIV 28 by fixing them with fresh ice-cold 4% paraformaldehyde (Fisher) and affixing coverslips to pre-coated microscope slices with mounting media (Southern Biotech).

Statistical considerations All rats were assigned randomly to groups, and group sizes were determined a priori based on expected effect size and variance. All analyses were performed without knowledge of treatment group. We used several a priori determined comparisons, and aimed to apply the appropriate statistical tests. For example, because the behavioral and place cell datasets contained data from multiple sessions in single animals and the LFP dataset contained data from up to 3 recording sessions from each animal, the observations for each of these measures within single animals are likely to be correlated, and these data can be represented as a cluster. In this case, the existence of a relationship between each measure of interest within an individual animal may then be assumed (Ziegler et al., 1998). In this study we used generalized estimating equations (GEE) (SPSS; Armonk, NY), a class of regression marginal model, for exploring multivariable relationships between clustered response data in control and FSE animals in the active avoidance task. At the behavioral level we tested for differences in the number of shocks, the number of entrances into the shock zone and the amount of time spent opposite the shock zone. We used one-way ANOVA to compare multiple groups, and two-way ANOVA for the Sholl analyses, involving treatment and distance from soma. Paired t-tests were used to compare performance of individual rats over time. Unless noted otherwise, Prism 6 was used to conduct all statistics (GraphPad Software) and data are presented as group means with standard errors.

Results

NRSF binding to the chromatin is augmented after eFSE, and can be abrogated post-hoc using a decoy strategy NRSF protein levels in hippocampus from eFSE rats were augmented 2 days post eFSE compared with controls (p=0.04), and this increase was apparent also at 7(p=0.06), 19 (p=0.04) and 60 days later (p=0.02) (Fig. 1A-B). To interfere with NRSF function after eFSE, we employed a decoy strategy using oligodeoxynucleotides (ODNs). Specifically, we designed synthetic, protected ODNs with a sequence of the NRSE and used a scrambled sequence (SCR) as a control. NRSE-ODNs bind NRSF, sequestering the protein and preventing it from binding to chromatin and repressing gene expression. To demonstrate the ODNs' ability to travel into neurons we employed bodipy-tagged ODNs, and determined that ODNs entered hippocampal neurons and accumulated inside nuclei, the location of chromatin (Fig. 1C).

Chromatin immunoprecipitation (ChIP) demonstrated that using the doses and administration regimens employed here resulted in group differences in the binding of NRSF to chromatin (One-way ANOVA, F=6.57, p=0.003; Fig. 1D). To assess the functional binding of NRSF to target gene chromatin, we utilized *hcn1,* a gene that encodes for hyperpolarization-activated cyclic nucleotide-gate channel 1, as a marker gene for NRSF chromatin-binding, because NRSF has previously been shown to bind and repress this gene after status epilepticus (McClelland et al., 2011, 2014). NRSF occupancy at the HCN1 gene was not different in CTL-SCR and CTL-NRSE rats (Bonferroni's multiple comparisons tests). However, NRSF binding to *hcn1* was

significantly augmented in hippocampi of eFSE-SCR rats 3 hours after insult ($p<0.05$; CTL-SCR vs. eFSE-SCR). Administration of the NRSE ODN after eFSE significantly reduced NRSF binding in the eFSE-NRSE group compared to eFSE-SCR ($p<0.05$) and this binding was not significantly different than in controls (eFSE-NRSE vs. CTL-SCR, $p>0.05$).

Figure 6.1: Binding of augmented NRSF to chromatin after eFSE is prevented using a decoy system. (A) Representative Westernblot depicting augmented levels of NRSF protein 7-days post eFSE. (B) Quantification of NRSF protein expression at select days after eFSE shows statistically significant upregulation of NRSF protein 2-days (unpaired t-test; t_6=2.49; p=0.047; CTL n=4, eFSE n=4), trends towards significance by 7 days (unpaired t-test, t_5=2.30; p=0.07; CTL n=3, eFSE=4) is significantly upregulated again by 19 days (unpaired t-test; t_7=2.50; p=0.041; CTL n=4, eFSE=5) and is still upregulated 60 days after eFSE (unpaired t-test; t_7=2.88; p=0.024; CTL=5, eFSE=4). (C) Representative bright field and fluorescent photomicrographs depicting NRSE ODNs ability to aggregate inside the nuclei of cultured hippocampal neurons using bodipy tagged ODNs. Quantification of ChIP of NRSF to the *Hcn1* gene reveals NRSE ODN's block NRSF's ability to bind to bind to chromatin after eFSE (One-way ANOVA; F=6.56; p=0.003; bonferroni's multiple comparisons post tests: CTL-SCR vs. CTL-NRSE t_{20}=1.04, p>0.05; CTL SCR vs. eFSE-SCR t_{20}=3.12, p<0.05; CTL-SCR vs. eFSE-NRSE t_{20}=1.37, p>0.05; CTL-NRSE vs. eFSE-NRSE t_{20}=0.15, p>0.05; CTL-SCR n=9, CTL-NRSE n=4, eFSE-SCR n=5, eFSE-NRSE n=6). Data are presented as mean±SEM. *Statistically significant at p<0.05.

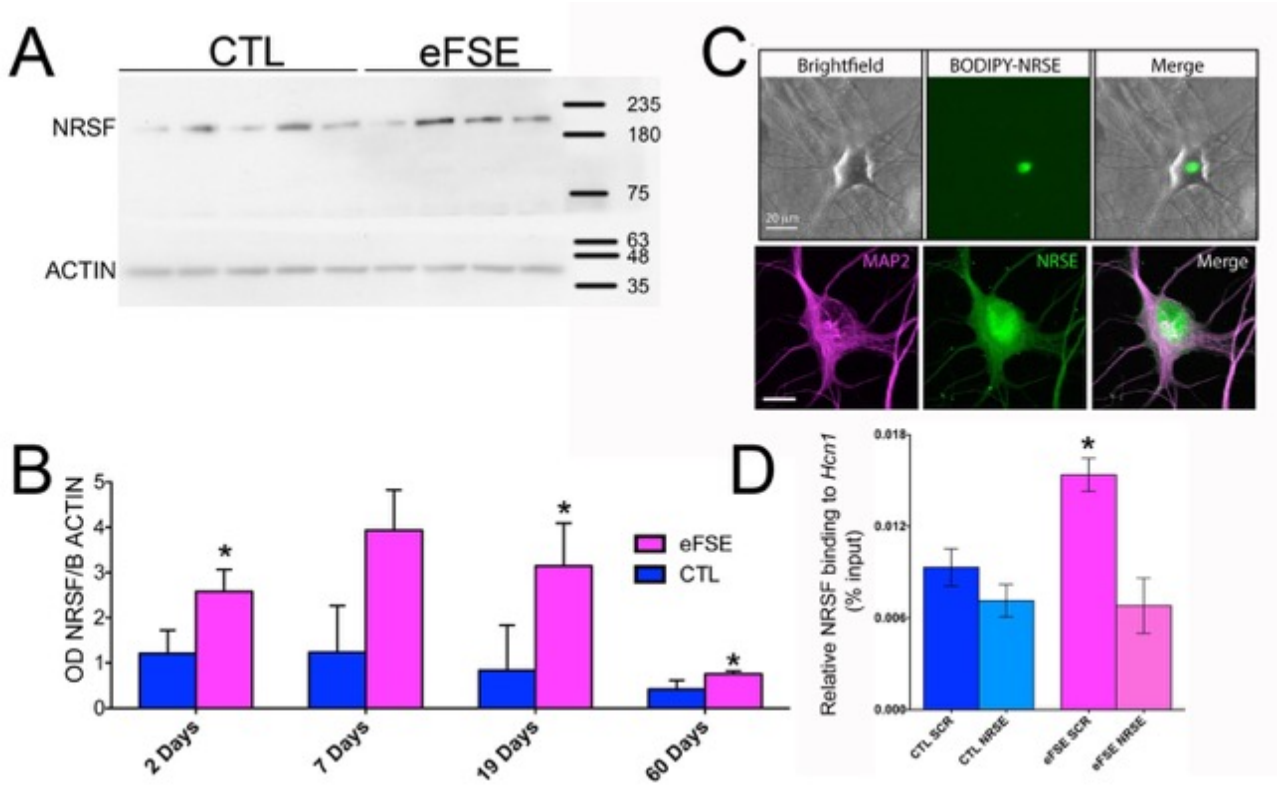
A
CTL
eFSE
NRSF
ACTIN
235
180
75
63
48
35
C
Brightfield
BODIPY-NRSE
Merge
20 µm
MAP2
NRSE
Merge
B
OD NRSF/B ACTIN
eFSE
CTL
2 Days
7 Days
19 Days
60 Days
D
Relative NRSF binding to Hcn1 (% input)
CTL SCR
CTL NRSE
eFSE SCR
eFSE NRSE

Blocking NRSF function after eFSE prevents cognitive deficits months later

Approximately 3 months after the eFSE and the interventions, rats were subjected to the active placement avoidance task. During this behavioral test, rats are exposed to a rotating arena containing a shock-zone quadrant. Rats are scored on their ability to encode and remember the location of the shock zone using unique visual cues placed around the arena. Behavior in this task was scored over two days with 8 trials per day. We compared performance in this task of four experimental groups, control (CTL) rats that received either SCR or NRSE ODNs, and rats that were subjected to eFSE and received either SCR or NRSE-ODNs *post-hoc*.

On the first day, eFSE-SCR rats received significantly more shocks (15.48±2.685) than each of the other three groups (CTL-SCR, 9.03±2.287; CTL-NRSE, 7.708±1.833; eFSE-NRSE 5.708±0.9523), suggesting that they were not able to learn the location of the shock quadrant (one-way ANOVA, $F=4.82$, $p=0.003$; Bonferroni's multiple comparisons tests between CTL-SCR and. eFSE-SCR, $p<0.05$). A second measure of spatial learning in this task is the duration of time a rat spends in the quadrant opposite the shock zone. eFSE-SCR rats spent significantly less time in the opposite quadrant (214.7±11.64) as compared to the other three groups, indicating they could not form a memory strategy to avoid shocks (CTL-SCR, 261.0±17.81, CTL-NRSE 287.6±16.7; eFSE-NRSE 282.5±16.77; one-way ANOVA $p=0.0014$; CTL-SCR vs. eFSE-SCR $p<0.05$). By the second day, the differences among groups were larger. eFSE-SCR rats received more shocks ($p<0.0001$; CTL-SCR vs. eFSE-SCR, $p<0.05$) and entered the shock zone quadrant more times than any other group (Fig. 2A; $p<0.0001$; CTL-SCR vs.

eFSE-SCR, $p<0.05$). eFSE-SCR rats again spent significantly less time in the opposite quadrant than any group. Strikingly, eFSE-NRSE rats were indistinguishable from either control group on any measure used to detect spatial memory (CTL-SCR vs eFSE-NRSE, $p>0.05$ for number of shocks and time spent in opposite quadrant), suggesting that transiently blocking the function of NRSF after eFSE rescues from cognitive deficits provoked by eFSE (Fig. 2A).

Over the two days of testing, CTL-SCR animals improved significantly in this task, with less shocks on day two as compared to day one (paired t-test; $t_{31}=3.67$, $p=0.0009$), less entrances into the shock zone ($p<0.00001$) and more time spent in the opposite quadrant ($p=0.0006$). CTL-NRSE rats were indistinguishable from the CTL-SCR group in improved performance in the three memory parameters (number of shocks $p=0.0002$; number of entrances, $p<0.00001$; time spent in the opposite quadrant, $p=0.001$). In contrast, eFSE-SCR rats did not improve over the two days. While they received fewer shocks on the second day, they entered the shock zone equally on both days ($p=0.08$) and spent the same amount of time opposite the shock zone ($p=0.7$). Notably, treatment with the NRSE-ODN enabled the eFSE-NRSE group to perform as well as controls on the three measures of the active avoidance test. They received less shocks on day two as compared to day one ($p<0.0001$), entered the shock zone less on day two ($p<0.0001$) and spent more time opposite the shock zone ($p=0.01$; Fig. 2B).

Finally, retesting the rats one month later, assessing the longevity of this memory, demonstrated the enduring memory of the CTL groups as well as of the eFSE-NRSE

group (One-way ANOVA, F=3.45, p=0.017; Fig. 2C). In contrast, the eFSE-SCR group failed to remember the location of the shock zone, as evident from large numbers of entries into it as compared to control animals (Bonferroni's multiple comparisons testsCTL-SCR vs. eFSE-SCR $p<0.05$), shocks; (CTL-SCR vs. eFSE-SCR, $p<0.05$) and reduced time in the opposite quadrant ($p<0.05$). Blocking the action of NRSF after eFSE enabled rats to retain memories from the active avoidance test rendering them indistinguishable from controls. This was evident in the number of shocks they received, entrances into the shock zone and time spent in the opposite quadrant (for all, Bonferroni's multiple comparisons tests CTL-SCR vs. eFSE-NRSE $p>0.05$; Fig. 2C).

Together, these data indicate that eFSE greatly reduced a rat's ability to create a spatial memory during the active avoidance test. Importantly, blocking NRSF activity after eFSE allowed NRSE-ODNs rats to learn and perform the active avoidance task. However, the mechanisms for both of these striking observations remained unclear.

Figure 6.2: Blocking NRSF binding to chromatin after eFSE has long term influences in learning and memory. (A) eFSE-SCR rats receive more shocks than CTL-SCR, CTL-NRSE or eFSE-NRSE while eFSE-NRSE rats are indistinguishable from control groups on day two of the active avoidance test (One-way ANOVA; $F=11.11$; $p<0.0001$; bonferroni's multiple comparisons post tests: CTL-SCR vs. CTL-NRSE $t_{148}=0.72$, $p>0.05$; CTL-SCR vs eFSE-SCR $t_{148}=4.65$, $p<0.05$; CTL-SCR vs eFSE-NRSE $t_{148}=0.16$, $p>0.05$; eFSE-SCR vs. eFSE-NRSE $t_{148}=5.02$, $p<0.05$). eFSE-SCR rats enter into the shock zone more than any other experimental group, while eFSE-NRSE rats are indistinguishable from either CTL group (One-way ANOVA; F10.21, $p<0.0001$; bonferroni's multiple comparisons post tests: CTL-SCR vs CTL-NRSE $t_{148}=1.02$, $p>0.05$; CTL-SCR vs eFSE-SCR $t_{148}=4.54$, $p<0.05$; CTL-SCR vs. eFSE-NRSE $t_{148}=0.23$, $p>0.05$; eFSE-SCR vs eFSE-NRSE $t_{148}=4.81$, $p<0.05$). eFSE-SCR rats spend less time in the opposite quadrant of the active avoidance test compared to all other groups on day two of testing (one-way ANOVA; F=9.44l $p<0.0001$; bonferroni's multiple comparisons post tests: CTL-SCR vs CTL-NRSE $t_{148}=0.31$, $p>0.05$; CTL-SCR vs eFSE-SCR $t_{148}=4.56$, $p<0.05$; CTL-SCR vs. eFSE-NRSE $t_{148}=0.80$, $p>0.05$' eFSE-SCR vs. eFSE-NRSE $t_{148}=3.86$, $p<0.05$). (B) eFSE-SCR rats receive less shocks over the course of training, but do not fair as well as other experimental groups (paired t-tests, day 1 vs day 2: CTL-SCR, $t_{31}=3.67$, $p=0.0009$; CTL-NRSE, $t_{23}=4.34$, $p=0.0002$; eFSE-SCR, $t_{47}=3.45$, $p=0.0012$; eFSE-NRSE, $t_{47}=5.23$, $p<0.0001$). eFSE-SCR rats enter into the shock zone an indistinguishable amount of times over two days of training, while other experimental groups enter less on day two as compared to day one (paired t-tests, day 1 vs day 2: CTL- SCR $t_{31}=5.07$, $p<0.0001$;

CTL-NRSE t_{23}=5.19, p<0.0001; eFSE-SCR t_{47}=1.82, p=0.076; eFSE-NRSE t_{47}=7.31, p<0.0001). eFSE-SCR rats spend a similar amount of time in the opposite side of the quadrant while the other three experimental groups spend more time in the opposite quadrant on day two as compared to day one (paired t-tests, day 1 vs day 2: CTL-SCR t_{31}=3.81, p=0.0006; CTL-NRSE t_{23}=3.77, p=0.001; eFSE-SCR t_{47}=0.40, p=0.69; eFSE-NRSE t_{47}=2.65, p=0.01). (C) eFSE-SCR animals did worse on the three outcome measures compared to other groups when retested in the active avoidance test one month after initial testing (one-way ANOVA F=3.49, p=0.04). (D) representative traces depicting rat's movement around the active avoidance test of cognition in each experimental group. Data are presented as mean± SEM. CTL-SCR n=4, CTL-NRSRE n=4, eFSE-SCR n=6, eFSE-NRSE n=6. *Statistically significant at p<0.05.

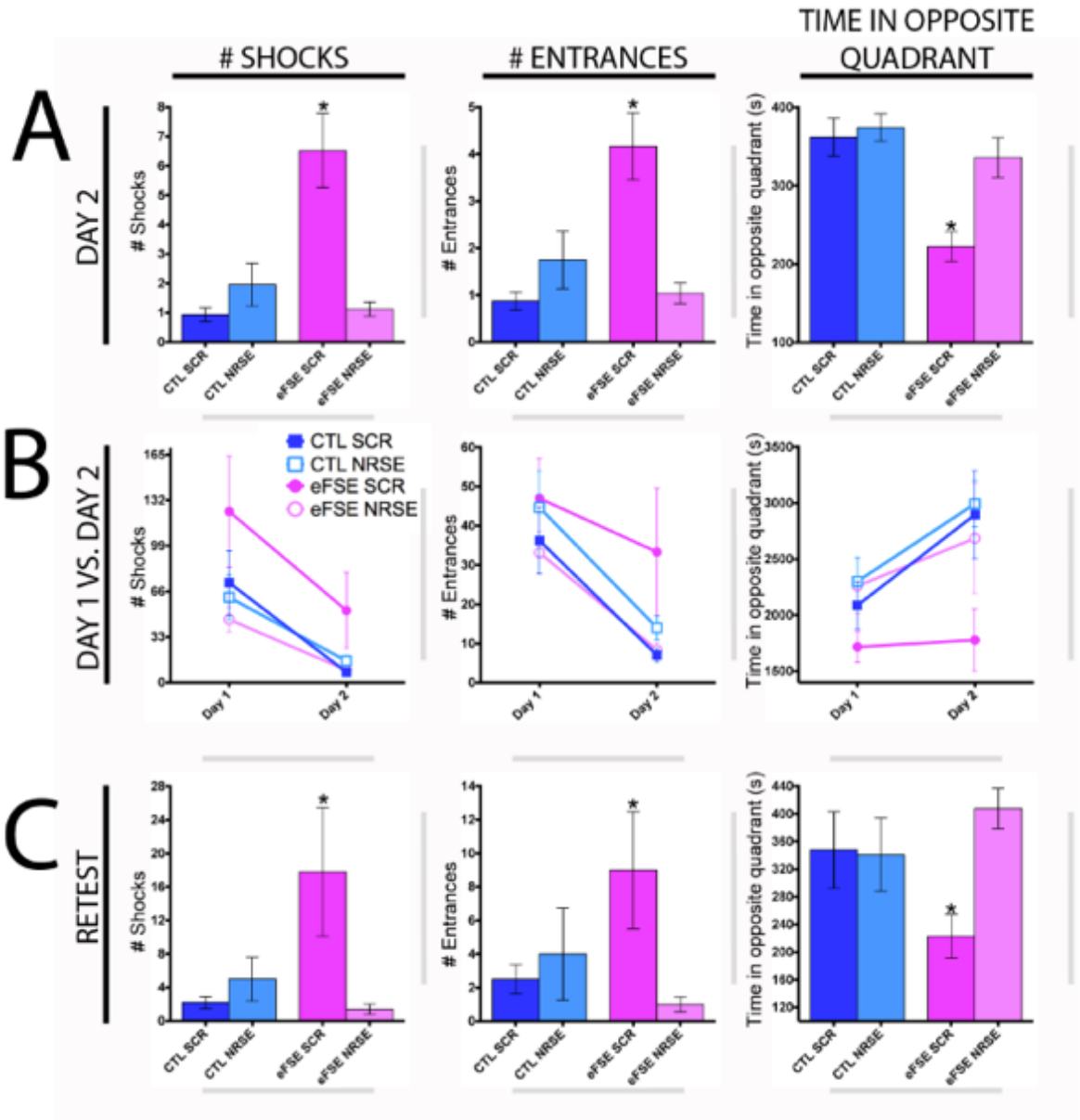
A
DAY 2
SHOCKS
ENTRANCES
TIME IN OPPOSITE QUADRANT
Shocks
Entrances
Time in opposite quadrant (s)
CTL SCR
CTL NRSE
eFSE SCR
eFSE NRSE
B
DAY 1 VS. DAY 2
CTL SCR
CTL NRSE
eFSE SCR
eFSE NRSE
Day 1
Day 2
C
RETEST

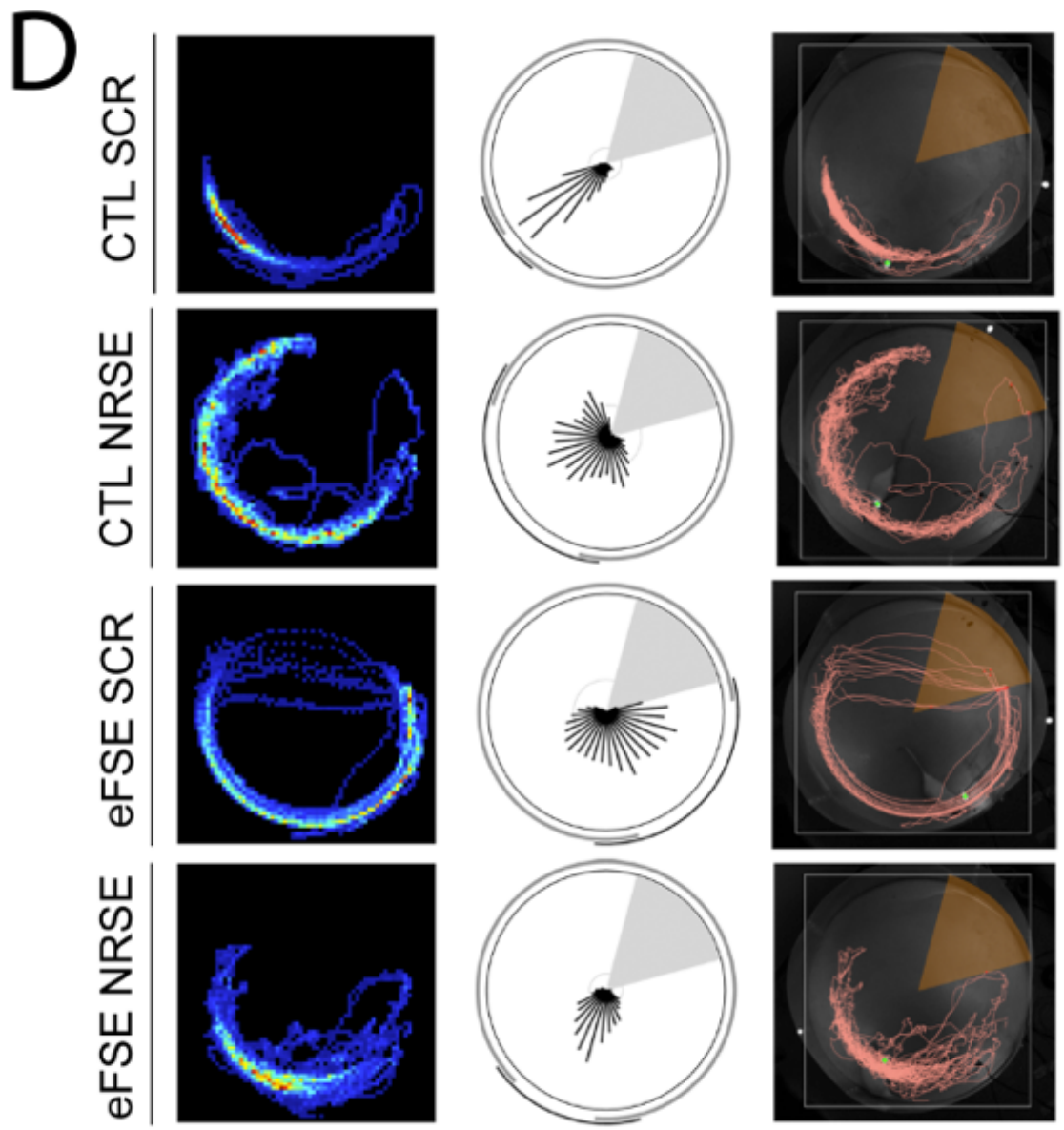
D
CTL SCR
CTL NRSE
eFSE SCR
eFSE NRSE

Brain oscillations underlying spatial memory are altered after eFSE and further modulated by the administration of NRSE ODNs To probe the functional mechanisms of the cognitive deficits caused by eFSE, and their reversal by *post-hoc* blocking of NRSF function, rats were implanted with a bilateral array of recording electrodes in hippocampal region CA1. We focused on oscillations well associated with spatial memory (Colgin, 2015; Bieri et al., 2014), such as theta and slow and fast gamma oscillations. These rhythms have distinct origins and roles: slow gamma is often considered to involve CA3-CA1 pathways and contribute to memory retrieval, whereas fast gamma reflecting information flow in the entorhinal cortex-CA1 node of the hippocampal network (Colgin et al., 2009). Significant alterations provoked by eFSE in each of these rhythms were found, indicating profound changes in the hippocampal network (Fig. 3). Several of these alterations were no longer present in the eFSE-NRSE-groups. In addition unique network changes were found in the NRSE-ODN eFSE animals that were associated with improved outcomes on the active avoidance task.

We investigated these oscillations during exploration in the stable arena to obtain measures of the baseline network available for learning. We then recorded in the rotating arena during active avoidance, when the rats have a need to remember the location of the shock zone. During exploration (foraging) in the stable arena, we detected a significant effect of group on rats' mean movement speed ($p=0.001$). Specifically, mean speed of eFSE-SCR (14.87±0.668) was significantly faster than that of CTL-SCR (11.52±0.68, $p<0.001$), CTL-NRSE (11.13±1.04, $p=0.002$) and eFSE-NRSE (12.17±0.64, $p=0.003$). This finding is notable because increased mean speed should correlate with an increased speed/theta relationship (Richard et al., 2013), yet

animals in the eFSE group that received scrambled ODNs tended to have the lowest speed/theta correlations, implying circuit dysfunction (Barry et. al., 2016). Importantly, the speed of the eFSE-experiencing group that was treated transiently with NRSF-blocking NRSE-ODNs was indistinguishable from those of either control groups.

The influence of both eFSE and NRSF blockade on theta rhythm was complex. Theta frequency itself was not altered by either. However, GEE analysis revealed a significant group effect ($p=0.018$) regarding the linear relationship between motor speed and CA1 theta frequency. Speed/theta correlation coefficients were robust in the CTL-SCR group (0.25 ± 0.041) and was reduced drastically by eFSE (to 0.068 ± 0.058 in the eFSE-SCR group). The correlation coefficient was partially restored in the eFSE-NRSE group (0.136 ± 0.016) though, surprisingly, preventing NRSF function in controls (CTL-NRSE: 0.103 ± 0.03) worsened speed/theta correlations compared to control receiving scrambled ODN ($p=0.004$; Fig 3A-C).

In the stable arena, eFSE accelerated fast gamma mean frequency, which was significantly higher in eFSE-SCR rats (81.64 ± 3.02; Fig. 3D) compared with both control groups: CTRL-SCR (77.62 ± 1.88), and CTL-NRSE (78.57 ± 0.882). Remarkably, blocking NRSF function after eFSE abolished the acceleration of mean frequency of the fast gamma in the eFSE-NRSE group (74.09 ± 0.53). There was also a significant group effect ($p=0.003$) on the normalized mean amplitude of fast gamma oscillations. Compared with the CTL-SCR group (0.502 ± 0.0028), mean amplitudes were slightly higher after eFSE (eFSE-SCR: 0.505 ± 0.0029), reverted to control levels by blocking

NRSF (eFSE-NRSE: 0.4966±0.0014) and were surprisingly slightly increased in CTL-NRSE rats (0.502±0.0010).

Thus, eFSE influenced baseline measures of both mean amplitude and mean frequency of fast gamma oscillations and frequency measures in the active avoidance context, in a manner that was congruent with the ability of the rat to remember the location of the shock zone during the active avoidance test. Faster and larger fast-gamma oscillations were associated with worse performance in the active avoidance task. The inability to filter fast gamma oscillations (i.e., information flow between hippocampus and neocortex) during exploration might interfere with the acquisition of spatial information processes involving slow gamma rhythms and information flow in the CA3-CA1 node of the hippocampal network. Accordingly, we examined the effects of eFSE and of blocking of NRSF function, on slow gamma rhythms in hippocampal CA1.

In the stable arena, normalized mean amplitudes of slow gamma were lowest in the eFSE-SCR group (0.187±0.0015). The amplitude was significantly higher ($p<0.001$) in eFSE rats that were treated with NRSE-ODN (0.192±0.0005) and in this group was actually higher than those of controls (CTL-NRSE: 0.188±0.00066 and CTL-SCR: 0.19015±0.00144; Fig 3E). There was a strong trend for group effect for slow gamma frequencies ($p=0.07$). Notably, compared to CTL-SCR (32.56±0.327) and the CTL–NRSE (32.25±0.059) groups, slow gamma frequency in eFSE rats was lower (31.69±0.401) but this was no longer observed in the eFSE-NRSE group (32.44±0.072). Thus, eFSE altered hippocampal network properties by augmenting amplitude and

frequency of fast gamma oscillation and attenuating these parameters in the slow gamma band which underlies information flow required for encoding spatial information.

Indeed, during the active avoidance test, when a demand for encoding and retrieval of spatial memory was great, similar and enhanced effects of eFSE on slow gamma oscillation properties were noted: Slow gamma frequencies were lowest in rats experiencing eFSE (eFSE-SCR: 31.37±0.399). Frequency was restored by the early administration of NRSE-ODN to eFSE rats (eFSE-NRSE: 33.37±0.555), yielding slow gamma frequencies similar to those of both control groups (CTL-NRSE: 32.03±0.5; CTL-SCR: 32.10±0.663; Fig 3F). As found in the stable arena, normalized mean amplitudes of slow gamma were lowest in the eFSE-SCR group (0.1878±0.0006). The amplitude was significantly higher in eFSE rats that were treated with NRSE-ODN (0.1913±0.0008), and in this group was actually higher than those of controls (CTL-NRSE: 0.1884±0.0005 and CTL-SCR: 0.1899±0.00107). The frequencies of fast gamma oscillations recorded during the active avoidance tests varied by group ($p=0.016$). Specifically, compared with CTL-SCR (77.67±1.78) and CTL-NRSE (75.99±0.106), frequency of eFSE-SCR rats (78.47±2.15) was higher. This was no longer observed in eFSE rats treated with NRSE-ODNs (74.34±0.574). Notably, there was no significant group effect for fast gamma amplitude during active avoidance ($p=0.255$).

Together, these findings point at potential mechanisms for both the deleterious effects of eFSE on spatial memory, and for the ameliorating actions of blocking NRSF function transiently. They suggest that eFSE somehow results in faster and higher-amplitude

fast gamma oscillations, consistent with failure of filtering this cortical input within CA1 place cells. This might derive from deficits in the filtering properties of apical dendrites within CA1 (Takahashi & Magee, 2009; Magee, 2001; Noam et al., 2011). In addition, eFSE lead to attenuation of amplitudes and frequencies of slow gamma oscillations, and these may derive from abnormal functions of inputs to CA3 and CA1. Transient treatment with NRSE-ODN enables the FSE-NRSE group to form spatial memories, associated with modulation of gamma oscillations.

Figure 6.3: eFSE modulates hippocampal rhythms The relationship between rat speed and theta properties of amplitude and frequency for a hippocampal electrode in a CTL-SCR animal during a single active avoidance session. (A) Spectrogram showing signal amplitude over a 10-minute avoidance session in relation to signal frequency (Top) and rat speed (Bottom). Segments where the speed plot is above 0 indicate several seconds of recording before and after the active avoidance session. (B) Speed filtered spectrogram shown in A. Together, the plot shows that the power and frequency of theta increases in relation to rat speed. (C) Relationship between speed of movement and theta frequency (blue dots) throughout the active avoidance session shown in A-D for the CTRL-SCR animal (Top). The line of best fit (black line) and the corresponding correlation coefficient between theta frequency and speed indicate a significant linear relationship. The significant r-value (r and p values indicated above plot) indicates that as animal speed increases, so does theta frequency. While the eFSE-SCR animal did not exhibit a significant linear relationship between speed and frequency (Middle), there was a significant speed/frequency relationship for the eFSE-NRSE animal (Bottom). (F) eFSE increases rat speed during active avoidance (cm/s) and NRSF blockade reduces speed to rates comparable to control groups. (G) Fast gamma frequency is increased in eFSE-SCR rats and restored to control levels in eFSE-NRSF rats. (F) eFSE decreases slow gamma frequency in rats in both the open field and active avoidance task. Slow gamma frequency is restored when NRSF activity is blocked after eFSE.

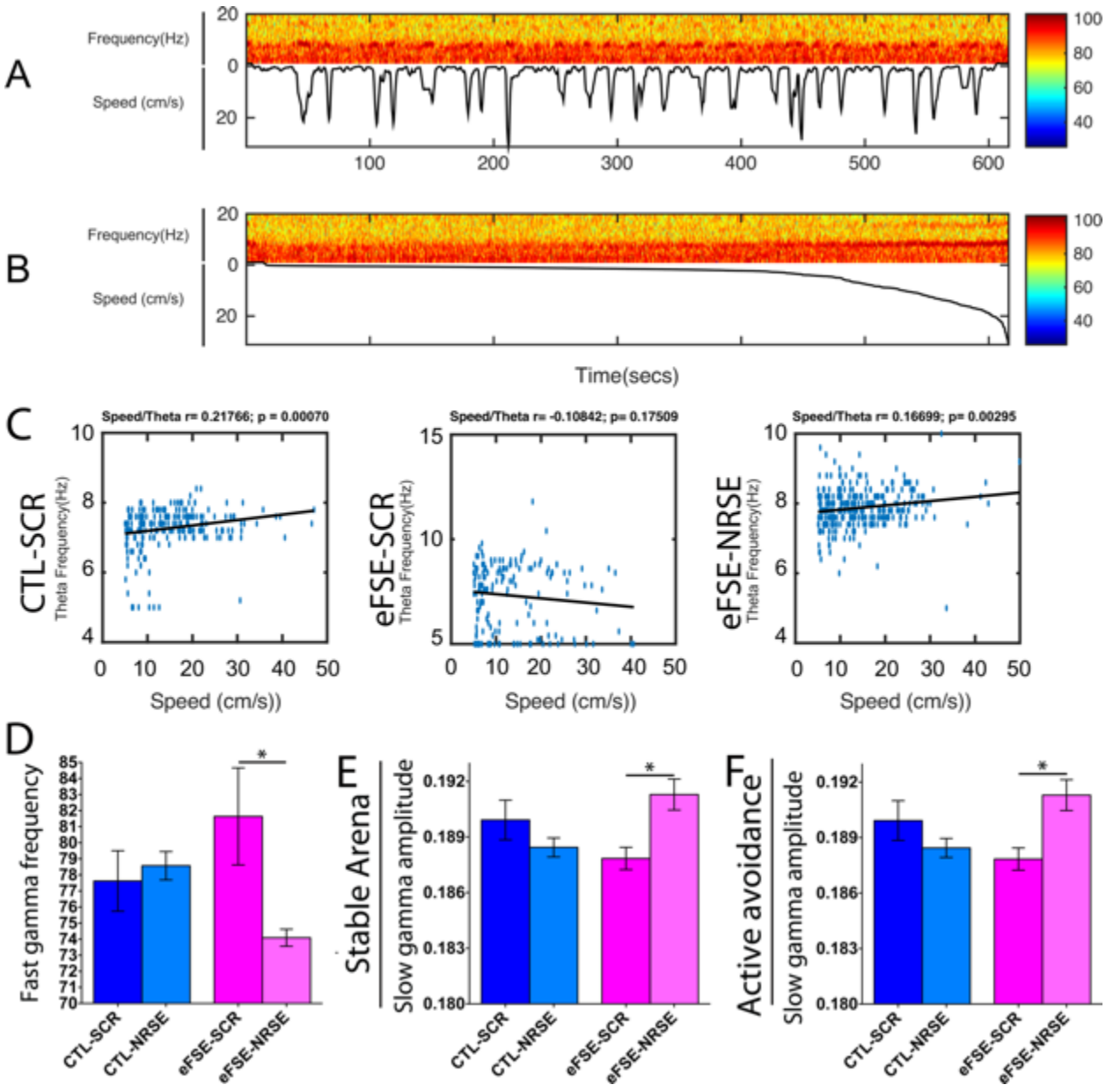
A
Frequency(Hz)
Speed (cm/s)
B
Time(secs)
C
Speed/Theta r= 0.21766; p = 0.00070
Speed/Theta r= -0.10842; p= 0.17509
Speed/Theta r= 0.16699; p= 0.00295
CTL-SCR
eFSE-SCR
eFSE-NRSE
Theta Frequency(Hz)
Speed (cm/s))
D
Fast gamma frequency
E
Stable Arena
Slow gamma amplitude
F
Active avoidance
CTL-SCR
CTL-NRSE
eFSE-SCR
eFSE-NRSE

Blocking NRSF after eFSE ameliorates aberrant excitatory synaptogenesis in dentate gyrus granule cells The results above suggested that eFSE influences several properties of brain oscillations that underlie encoding and retrieval of spatial information. These included the correlation of theta rhythms recorded from CA1 neurons with animal speed, as well as amplitudes and frequencies of slow and fast gamma oscillations, which involve neurotransmission throughout the hippocampal formation. Interestingly, blockade of NRSF function in the eFSE-NRSE rats enabled them to encode and retain spatial memories, associated with modulation of both fast gamma and slow gamma amplitude and frequency. Because it is believed that these two types of oscillations involve somewhat distinct neuronal ensembles, we proceeded to examine separately the effects of both eFSE and NRSF on the structural integrity of principal neurons in the hippocampal formation.

We first examined excitatory synapses within the dentate gyrus (DG), which gates input onto CA3 and CA1 (Goldberg & Coulter, 2013). Seizures have been shown to augment the numbers of excitatory synapses onto GC via two mechanisms. An important effect of seizures is promoting retention of hilar basal dendrites (HBDs) that are normally lost with granule cell maturation (Kron et al., 2010). These basal dendrites are targets of both ectopic excitatory synapses as well as those from neighboring GCs (Thind et al., 2008). These aberrant loops alter excitability within the DG, and might disrupt information flow within the dentate gyrus ‘gate’ to CA3 and CA1. Thus, we examined whether eFSE promotes HBDs in DGCs and if there was an effect of blocking NRSF after the insult.

Granule cells were identified in dorsal hippocampal sections obtained post mortem from all four groups of rats based on the classic structural phenotype of this cell type (Figure 4A-D). The density of GCs *per se* did not vary among the groups (One-way ANOVA, $F=1.78$, $p=0.16$; Fig. 4F). The number of HBDs on GC was not different between CTL-SCR (1.04±0.44) or CTL-NRSE (0.65±0.5) animals (Bonferroni's multiple comparisons test CTL-SCR v. CTL-NRSE $p>0.05$) However the number of HBDs on GCs from eFSE-SCR rats were significantly increased (3.14±1.22; Bonferroni's multiple comparisons test CTL-SCR v. eFSE-SCR, $p<0.05$). Blocking NRSF activity after eFSE abolished the difference in the number of HBDs on GCs (1.21±0.18; CTL-SCR v. eFSE-NRSE, $p>0.05$; Figure 4G). The results persisted when data were analyzed as the percentage of GCs with retained HBDs: CTL-SCR (1.38±0.22%); CTL-NRSE (0.79±0.59%), and eFSE-NRSE (1.68±0.56%) did not differ ($p=0.15$), whereas the percent of dysmature GCs with persistent HBDs was significantly higher in the eFSE-SCR group (4.57±0.79%; Fig. 4E).

The presence of dysmature basal dendrites provides a source for excitatory synapses that disrupt circuit function in the dentate gyrus. A second possible source for aberrant synapses involves exuberant branching of apical GC dendrites as recently reported after eFS (Raijmakers et al., 2016). Therefore, we examined the structure of GC apical dendrites in all groups. Sholl analyses revealed a group effect (Two-way ANOVA; interaction, $F=12.49$ $p<0.00001$; distance from soma, $F=627.3$ $p<0.00001$; experimental condition, $F=209.3$, $p<0.00001$). Branching in eFSE-SCR GCs was higher compared to those from CTL-SCR (Bonferroni's multiple comparisons test, 10-110 μM from soma,

$p<0.05$), indicating augmented arborization primarily in the GC layer rather than the outer molecular layer (Fig. 4H). eFSE-NRSE GCs were indistinguishable from both control groups at all distances from the soma. For dendritic length, a group difference was found (one-way ANOVA, $p=0.05$). It derived from a significant increase in the eFSE-SCR group (519.5±67.05) vs. all others (CTL-SCR: 415±10.80; CTL-NRSE: 387.4±19.71; eFSE-NRSE: 323.5±44.1; Fig. 4I).

Taken together, these data indicate that eFSE increased excitatory synapses of GCs via two mechanisms: dysmaturation, apparent as retention of HBDs and their synapses, as well as hyper-branching of apical dendrites, that then form excitatory synapses on other GCs and cell types within the DG, disrupting information flow.

Figure 6.4: Blocking NRSF activity post eFSE reduces augmented dendritic arborization of dentate gyrus granule cells (A-D) Representative photomicrographs of the dentate gyrus in each experimental group. Inserts are magnified GCs with intact Golgi-cox filling for appropriate analysis. Red arrows indicate HBD. (A'-D') Representative masks of GC from each experimental group created for analysis. (E) eFSE-SCR rats have a higher percentage of GCs with HBDs as compared to other groups, while eFSE-NRSE rats are indistinguishable from either CTL groups (one-way ANOVA $F=25.56$, $p=0.0002$; bonferroni's multiple comparisons post tests: CTL-SCR vs CTL-NRSE $t_8=1.25$, $p>0.05$; CTL-SCR vs eFSE-SCR $t_8=6.77$, $p<0.05$; CTL-SCR vs eFSE-NRSE $t_8=0.63$, $p>0.05$; eFSE-SCR vs eFSE-NRSE $t_8=6.14$, $p<0.05$). (F) There are no group difference in the total number of GCs between experimental groups (one-way ANOVA $F=1.78$, $p=0.16$). (G) The number of granule cells with HBDs is increased in eFSE-SCR animals and indistinguishable among CTL-SCR, CTL-NRSE and eFSE-NRSE (one-way ANOVA $F=7.6$, $p=0.01$; bonferroni's multiple comparisons post tests: CTL-SCR vs CTL-NRSE $t_8=0.69$, $p>0.05$; CTL-SCR vs eFSE SCR $t_8=3.68$, $p<0.05$; CTL-SCR vs eFSE-NRSE $t_8=0.28$, $p>0.05$; eFSE-SCR vs eFSE-NRSE $t_8=3.39$, $p>0.05$). (H) eFSE-SCR animals have augmented dendritic arborization in the granule cell layer of the dentate gyrus compared to other experimental groups, while eFSE-NRSE rats are indistinguishable from either CTL groups (two-way ANOVA; Interaction $p<0.0001$; Micrometers from the soma $p<0.0001$; Experimental group $p<0.0001$). (I) Total dendritic length is augmented in eFSE-SCR rats, but not in other experimental groups (one-way ANOVA $F=48.73$, $p<0.0001$; bonferroni's multiple comparisons post tests: CTL-SCR vs CTL-NRSE $t_{257}=1.25$, $p>0.05$; CTL-SCR vs eFSE-SCR $t_{257}=7.47$, $p<0.05$; CTL-SCR vs

eFSE-NRSE t_{257}=5.46, p<0.05; eFSE-SCR vs eFSE-NRSE t_{257}=11.92, p<0.05). Data are presented as mean±SEM. CTL-SCR n=3 (rats) n=89 (neurons), CTL-NRSRE n=3 (rats) n=47 (neurons), eFSE-SCR n=4 (rats) n=58 (neurons), eFSE-NRSE n=4 (rats) n=65 (neurons). *Statistically significant at p<0.05.

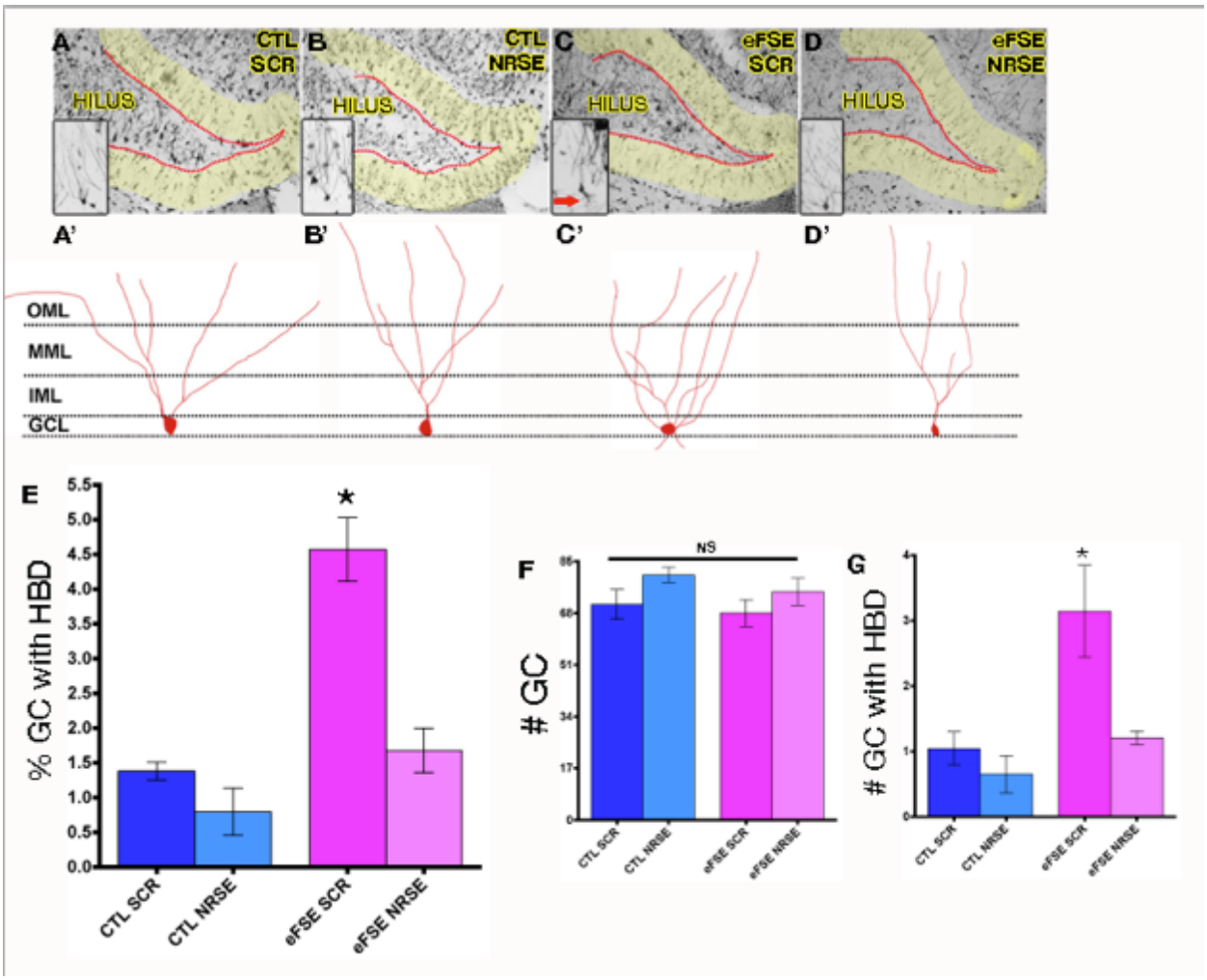
A
CTL SCR
HILUS
B
CTL NRSE
HILUS
C
eFSE SCR
HILUS
D
eFSE NRSE
HILUS
A'
B'
C'
D'
OML
MML
IML
GCL
E
% GC with HBD
CTL SCR
CTL NRSE
eFSE SCR
eFSE NRSE
F
GC
NS
G
GC with HBD

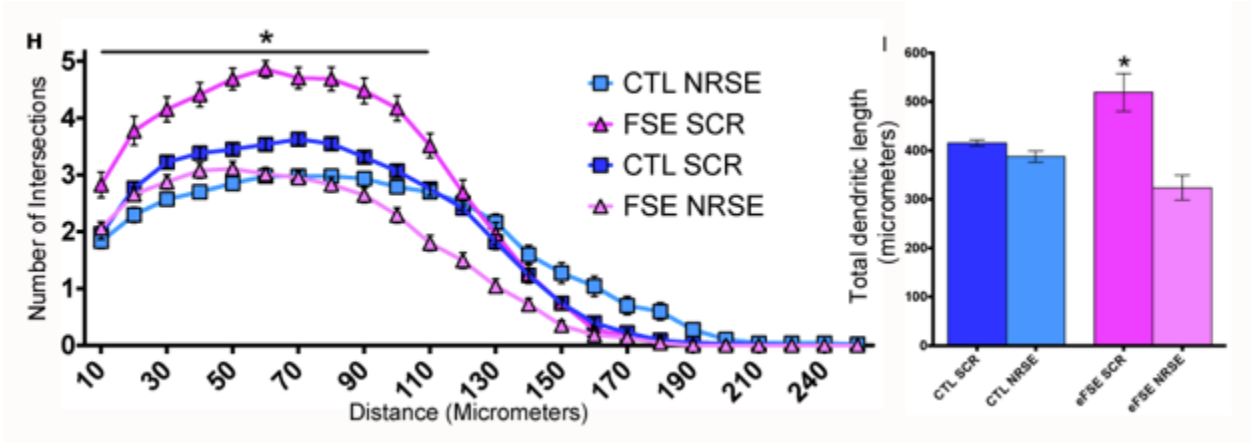
H
Number of Intersections
Distance (Micrometers)
CTL NRSE
FSE SCR
CTL SCR
FSE NRSE
I
Total dendritic length (micrometers)

Blocking NRSF does not ameliorate eFSE-induced dendritic defects in CA1 pyramidal cells eFSE generated impairments of spatial memory, associated with abnormal rhythms recorded from CA1 pyramidal cells. The higher amplitude and frequencies of fast gamma oscillations suggested an impaired filtering capacity of these cortical-hippocampal oscillations by CA1 pyramidal cell apical dendrites. Therefore, we examined the structural integrity of these dendrites, as well as the consequences of blocking NRSF function after FSE, a treatment that effectively restored memory functions.

We studied CA1 neurons from the same animals employed for the cognitive studies, and employed Sholl analyses of Golgi-impregnated neurons taken without knowledge of group (Fig. 5A-D). One-way ANOVA revealed a group effect $F=13.74$, $p<0.0001$). Notably, no differences in arborization or in total dendritic length were found between control animals infused with either the SCR (838.9±66.04) or the NRSE (986.7±47.60) ODNs (unpaired t-test, $t=1.84$, $DF=38$, $p=0.07$). In the eFSE-SCR group there was a reduction of total dendritic length (666.3±38.36). Interference with the function of NRSF in the eFSE-NRSE group had little effect on the structural deficits provoked by the early-life seizures (590.6±42.92). There were no discernable differences in dendritic length between the eFSE groups (unpaired t-test, $t=1.178$, $DF=51$, $p=0.24$; Fig. 4E). Together, these data indicated that eFSE reduced overall apical dendritic integrity in CA1 pyramidal cells, consistent with the observed filtering deficits observed in the eFSE groups. Importantly, the data suggested that the improved cognitive function afforded by

early NRSE-ODN treatment did not take place by prevention of the CA1 dendritic defects.

Figure 6.5: eFSE-induced dendritic defects in CA1 pyramidal cells are independent of NRSF (A-D) Representative photomicrographs of area CA1 of dorsal hippocampus with Golgi-cox filled neurons. (A'-D') Representative masks generated from CA1 pyramidal cells for analysis. (E) Quantification of total dendritic length demonstrates NRSF is unable to rescue reduced dendritic arborization after eFSE (one-way ANOVA $F=13.74$, $p<0.0001$; bonferroni's multiple comparisons post tests: CTL-SCR $t_{89}=1.97$, $p>0.05$; CTL-SCR vs eFSE-SCR $t_{89}=2.24$, $p>0.05$; CTL-SCR vs eFSE-NRSE $t_{89}=3.65$, $p<0.05$; eFSE-SCR vs eFSE-NRSE $t_{89}=1.11$, $p>0.05$). Data are presented as mean±SEM. CTL-SCR n=3 (rats) n=19 (neurons), CTL-NRSRE n=3 (rats) n=21 (neurons), eFSE-SCR n=4 (rats) n=20 (neurons), eFSE-NRSE n=4 (rats) n=34 (neurons). *Statistically significant at $p<0.05$.

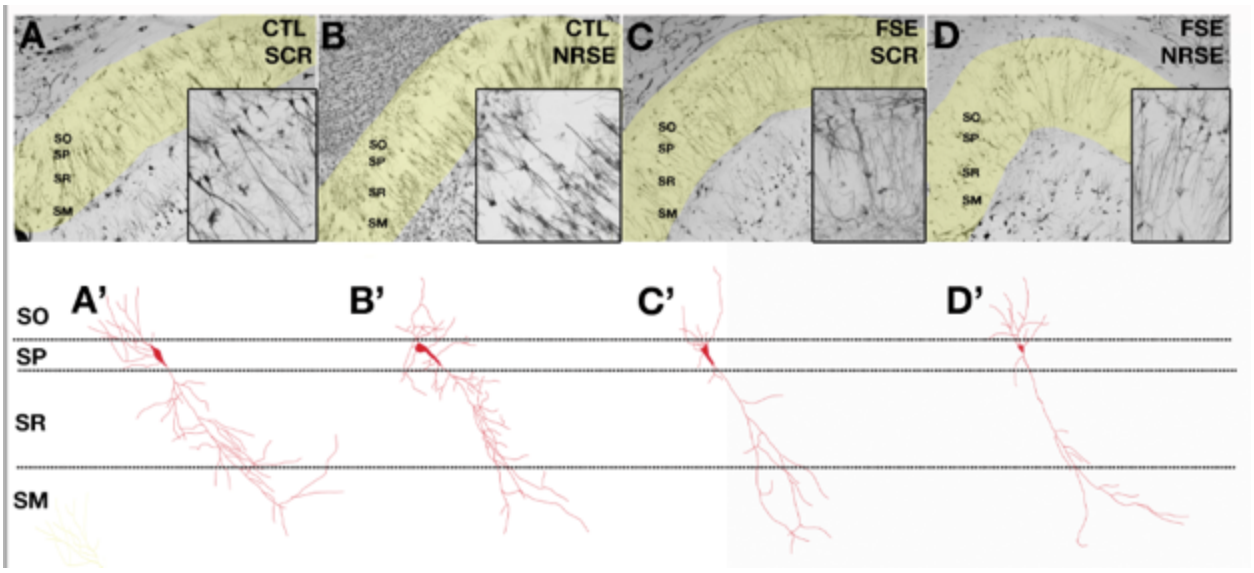
A
CTL
SCR
B
CTL
NRSE
C
FSE
SCR
D
FSE
NRSE
SO
SP
SR
SM
A'
B'
C'
D'

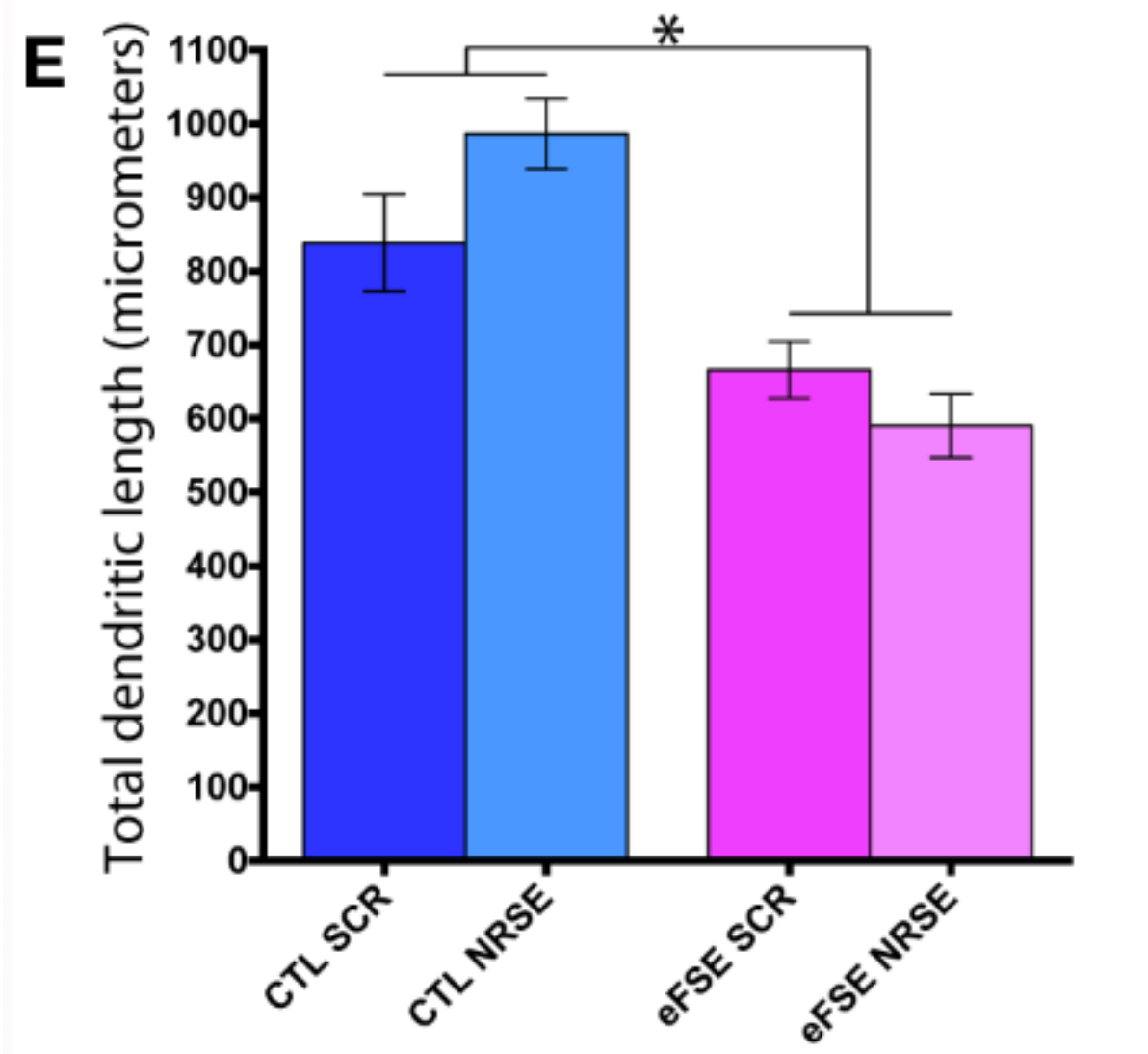
E
Total dendritic length (micrometers)
1100
1000
900
800
700
600
500
400
300
200
100
0
*
CTL SCR
CTL NRSE
eFSE SCR
eFSE NRSE

NRSF acts within the dentate gyrus to mediate the disruptive effects of eFSE on granule cells maturation and connectivity The data shown up to now suggested that eFSE promotes aberrant retention of excitatory synapses on basal dendrites of GCs, as well as the formation of supernumerary apical dendritic branching, and that these effects might be abrogated by blocking NRSF function during a critical period that follow eFSE. However, *in vivo*, we infused the NRSE-ODN throughout the whole brain, and it is possible that the effects of the ODNs was indirect, influencing gene expression and neuronal structure in areas connecting to the DG rather than acting to prevent the effects of NRSF within the dentate gyrus of P10-11 rats experiencing eFSE.

To study the direct effects of NRSF on the structure of developing dentate gyrus granule cells, we employed an *in vitro* organotypic slice culture system. Hippocampi cultured from P7 Thy1-YFP expressing mice enabled direct visualization of granule cells and their development (Fig. 6A). Notably, *in vitro*, the organotypic cultures follow patterns of *in vivo* development relatively faithfully (Bender et al, 2007; Fig. 6B-C). Hippocampi were exposed to seizure-like activity (Richichi et al., 2008) at an age parallel to eFSE *in vivo*, using bath administration of kainic acid (KA) at doses shown to provoke epileptiform discharges but not cell death (Richichi et al., 2008). The seizure-like events induced a robust increase in NRSF protein in dentate gyrus extracts 24 hours later (Fig. 6D), and cultures were sampled periodically to examine granule cell maturation. Three weeks after KA exposure, most granule cells in control and KA cultures appeared structurally mature with a typical tuft of apical dendrites radiating into the DG molecular layer. However, in hippocampi exposed to seizure-like activity at DIV 7, immature-

looking GCs with a retained basal dendrite (HBD) were found (4.5±1.3). Post-hoc treatment with a random ODN did not present the retention of HBDs in hippocampi exposed to KA: KA-SCR= 3.6±2.3; Fig. 6G). In contrast, in KA-GCs where NRSF function was blocked using NRSE ODNs for 72 hours following the seizure-like activity, the number of HBDs was reduced (0.86±0.9; One-way ANOVA; p=0.0119; Fig. 6E). When calculated as the percentage of GCs that retained HBDs, the same result obtained (Fig. 5D; p=0.049; Figure 6E).

Together, these data indicate that GC maturation within the DG is perturbed by early-life seizures, and that NRSF contributes crucially and directly to these disturbances to the normal formation and connectivity of the DG network.

Figure 6.6: NRSF acts directly on dentate gyrus granule cells that are disrupted by seizure-like activity. (A) Representative low magnification photomicrograph of the DG of DIV28 hippocampal slice culture generated from Thy1-YFP mice. (B) Representative high magnification image of YFP-filled GCs with typical dendritic arborization from a CTL hippocampus. (C) Representative high magnification image of YFP- Filled GC with atypical dendrites, specifically HBDs extending down into the hilus. Red arrows indicate HBDs. (D) Western blot from both control (C1-C3) and kainic acid (K1-K4) for NRSF and actin demonstrates augmented NRSF protein after seizure-like activity. Quantification of optical density of NRSF over β-actin reveals statistically significant upregulation of NRSF protein (unpaired t-test; t_5=192, p=0.009; CTL=3, KA=4). (E) The percentage of HBD on GC reveals seizure like activity increase the instance of HBDs on GCs (one-way ANOVA F=7.47, p=0.003; bonferroni's multiple comparisons post tests: CTL vs KA t_{15}=3.35, p<0.05; CTL vs KA-SCR t_{15}=2.68, p>0.05; CTL vs KA-NRSE t_{15}=0.18, p>0.05; KA vs KA-NRSE t_{15}=3.88, p<0.05. (F) There are no group differences in the total number of GCs in this *in vitro* system (one-way ANOVA F2.29, p=0.12). (G) There were group differences in the total number of GC after seizure-like activity and after NRSE-ODN administration (one-way ANOVA F=7.47, p=0.003; bonferroni's multiple comparisons post tests: CTL vs KA t15=3.35, p<0.05; CTL vs KA-SCR t15=2.68, p>0.05; CTL vs KA-NRSE t15=0.18, p>0.05; KA vs KA-NRSE t15=3.88, p<0.05; KA-SCR vs KA-NRSE t15=3.12, p<0.05). Scale bars, 20 μM. Data are presented as mean±SEM. CTL n= 55 (neurons) n= 3 (hippocampi), KA n=217 (neurons) n=4 (hippocampi), KA-SCR n=174 (neurons) n=5 (hippocampi), KA-NRSE n=162 (neurons) n=7 (hippocampi). *Statistically significant at p<0.05.

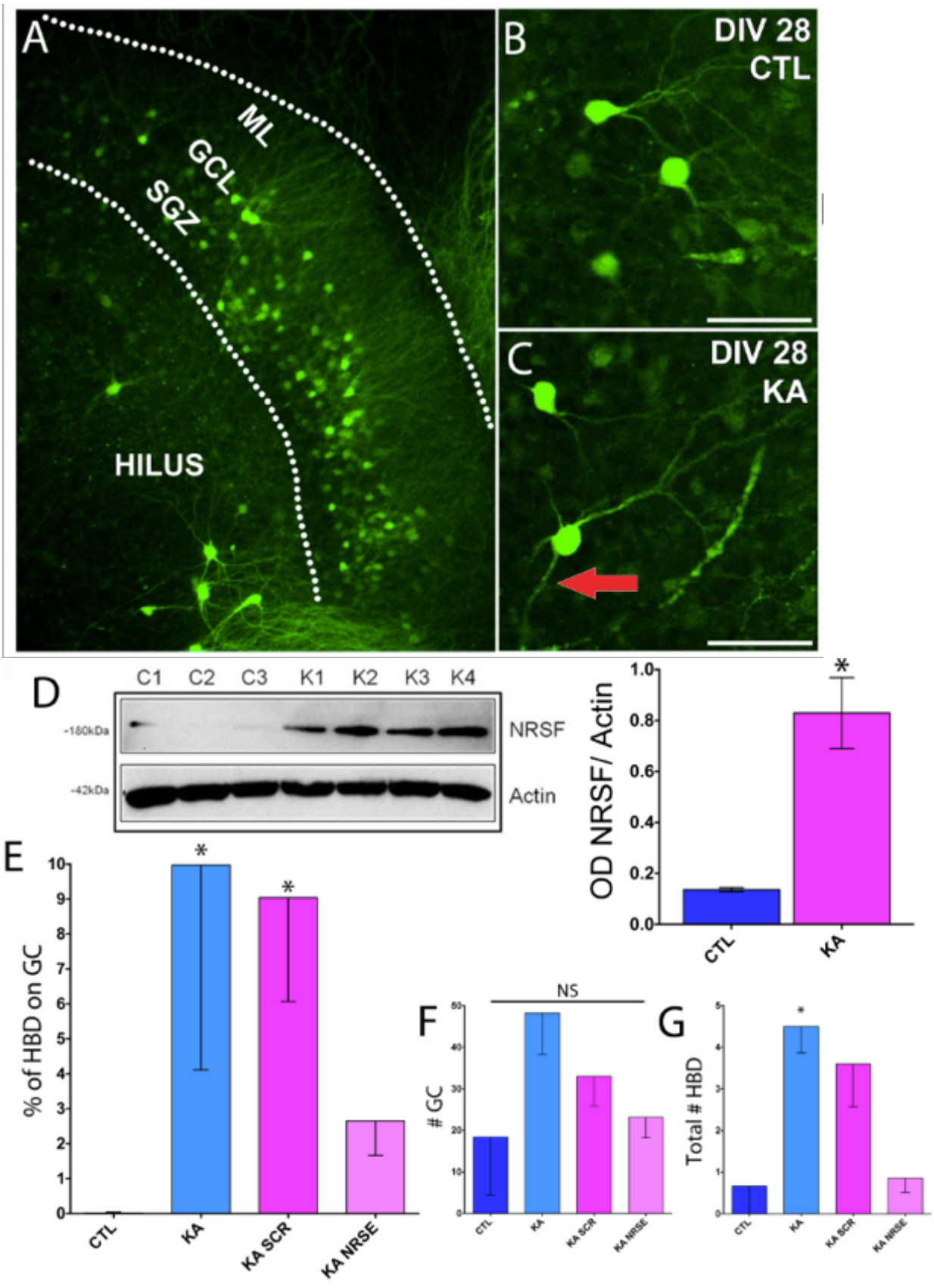
A
ML
GCL
SGZ
HILUS
B
DIV 28
CTL
C
DIV 28
KA
D
C1 C2 C3 K1 K2 K3 K4
~180kDa
~42kDa
NRSF
Actin
OD NRSF/ Actin
CTL
KA
E
% of HBD on GC
CTL
KA
KA SCR
KA NRSE
F
NS
GC
G
Total # HBD

Discussion

The principal findings of the current experiments are: long, early-life seizures in a model of febrile status epilepticus lead to profound and enduring memory impairments. Remarkably, these deficits are abrogated by transient, *post hoc* interference with the transcriptional repressor NRSF, known to contribute to neuronal differentiation and programmed gene expression. The mechanisms of the memory problems involve abnormal rhythms within the hippocampal formation. These likely derive from impaired dendritic and synaptic function, resulting from regionally specific dendritic loss and aberrant generation of excitatory synapses. Blocking NRSF function prevents aberrant structural plasticity in the dentate gyrus, which is sufficient to allow eFSE-NRSE rats to encode and retrieve spatial memories. Together, these studies provide novel information about the development of memory processing and the mechanisms by which disease may influence them. Importantly, the findings suggest approaches to prevent cognitive problems after early-life seizures, with strong translational promise.

Spatial memory deficits after eFSE arise from profound disturbances of the hippocampal network eFSE rats had severe difficulties in locating the shock zone in an arena decorated with spatial cues. This was apparent from numerous entries to the shock zone and increased shock numbers. The problems involved both short term memory (avoiding additional shocks in the same session), as well as long-term memory (poor improvement on the second day of the series and in the retest a month later). The current findings are in line with other reports of memory difficulties after early-life

seizures in rodents (Lugo et al., 2014; Liu et al., 1999). Interestingly, the duration of the inciting eFSE profoundly worsened cognitive outcomes as compared with our previous work in a model of short FS (Dubé et al., 2009; Barry et al., 2015). Importantly, they support the notion that repeated or long seizures in children might disrupt memory function as well.

Probing the structural and functional underpinnings of memory deficits, we surveyed the hippocampal network using *in vivo* electrophysiology and neuroanatomical tools. We identified perturbations of hippocampal oscillations including enhanced amplitude and frequency of fast gamma oscillations and reduced parameters of slow gamma rhythms, as well as disrupted theta/speed relationships. These defects might arise via numerous mechanisms, including loss or 'dropout' of rhythm-generating pyramidal cells, or of interneurons that tune the network (Barry et al., 2015;2016). There is strong evidence that neuronal loss is minimal in the model used here (Toth et al.,1998; Dubé et al., 2007; Dubé et al., 2010; Baram et al., 2011), and therefore we investigated potential structural or functional changes in the remaining neurons. We found significant structural deficits in existing neurons that might explain the physiological deficits: the observed paucity of apical dendritic branches and reduced dendritic length should influence filtering properties of the CA1 apical dendrites, augmenting oscillations involving input from cortical regions such as fast gamma. New, aberrant excitatory synapses in the DG might disrupt the gating function of DG onto CA3, influencing amplitude and frequency of slow gamma, as found here.

Convergent studies of hippocampal oscillations and neuronal structure are instructive about the mechanisms of spatial memory problems and memory rescue by NRSF blockers. How do we explain the profound effects of a long early-life seizure in the eFSE-SCR group and the remarkable improvement induced by the short treatment with NRSF-blockers in the eFSE-NRSE group? These questions are particularly intriguing, because both groups had significant perturbation of CA1 apical dendritic trees, crucial for place-cell and hippocampal network function.

The electrophysiological findings in both the stable arena and during active avoidance are informative here: During baseline conditions on the stable arena, the eFSE-SCR rats had larger and faster fast gamma oscillations in CA1 than controls. Fast gamma rhythms are considered to reflect input to CA1 from cortical regions including the entorhinal cortex via the temporoammonic pathway. Increased amplitude and frequency of these oscillations might indicate poor filtering of this input, and might repress intrinsic hippocampal oscillations such as slow gamma. Indeed, during active avoidance, when the memory demand was greatest, eFSE-rats had low frequency and amplitude of slow gamma oscillations, considered to reflect CA3-CA1 input that is influenced by dentate gyrus gating (Colgin et al., 2009). Together, we found that the balance of routed neural information to CA1 from the EC (fast gamma) and CA3 (slow gamma) seems to have been disrupted by the eFSE, interfering with both the acquisition of spatial information believed to be associated with entorhinal inputs as well as the recall of spatial information believed to be associated with CA3 inputs.

In this context, blocking NRSF had remarkable effects: in the active avoidance arena, eFSE-NRSE rats had larger and faster slow gamma oscillations than all other groups and the amplitude of these oscillations was significantly higher than even that of the control groups. The restoration of slow gamma properties, considered crucial for memory retrieval, in the eFSE-NRSE rats suggested that the treatment with NRSF blockers might have ameliorated the effects of eFSE on the DG-CA3 pathway, and this hypothesis was therefore tested.

NRSF employs several mechanisms to mediate seizure-induced disruption of hippocampal processes underlying memory Long seizures including eFSE increase the expression and chromatin binding of NRSF. This transient augmentation of NRSF function seems to disturb hippocampal networks enduringly via
several, region specific mechanisms.

In mature CA1 neurons in adult hippocampus there are ~400 potential targets for NRSF, namely genes containing the recognition site NRSE (Johnson et al., 2007, McClelland et al., 2011; 2014), However, only 30-40 of these genes are actually repressed by the augmentation of NRSF levels that takes place following status epilepticus (McClelland et al., 2014). Notably, these genes comprise crucial components of neuronal function including glutamate receptors, calcium dependent signaling molecules and ion channels.

Focusing on the filtering properties of CA1 apical dendrites, NRSF directly repressed the expression of HCN1, the principal contributor to the dendritic current I_h in hippocampus (McClelland et al., 2011). Indeed, reduced I_h after long seizures in the adult have found by several groups (Noam et al., 2011), and the current was restored by blocking NRSF (McClelland et al., 2011). HCN1 is also reduced after early-life seizures including eFSE (Brewster et al., 2002). In the current studies, blocking NRSF function shortly after eFSE reversed the increases in fast gamma properties without reversing the structural defects in CA1 dendrites. This suggests that NRSF-mediated changes in gene expression including HCN1 were involved. In support of this notion, blocking NRSF function in control rats influences the amplitude of fast gamma, without modifying dendritic trees in CA1. Whereas the mechanisms are unclear, interference with the carefully regulated levels of HCN1 and of I_h and its co-regulation with other ion channels might be at play (Santoro & Baram, 2003; George et al., 2013).

Major effects of eFSE-induced upregulation of NRSF clearly took place in the dentate gyrus. Both *in vivo* and in the organotypic cultures, early-life seizures provoked major anomalous production of excitatory synapses, and these were reversed by NRSF. Specifically, dysmaturation of granule cells, apparent as retention of basal dendrites which form excitatory synapses on neighboring granule cells was observed after eFSE and prevented by NRSF. It has been well documented that the persistent HBD are found on cells that are immature during the seizures (Parent et al., 1997; Kron et al., 2010; Hester et al., 2013,2014; Murphy et al., 2012; Singh et al., 2013), a population of GCs known to be strongly influenced by NRSF. NRSF regulates numerous genes

involved in structural and synaptic maturation of neurons (Johnson et al., 2007, Gao et al., 2011), and immature GCs are those primarily subject to maladaptive plasticity following early-life insults. Thus, it is reasonable to consider NRSF as a potent mediator of seizure-induced defects in the dentate gyrus network that is crucial for gating information flow to the hippocampus proper. Indeed, our *in vitro* studies using the organotypic cultures demonstrate that NRSF levels are augmented within the DG, influence and result in dysmaturation of GCs apparent as both retention of basal dendrites and exuberant growth of apical dendrites. Further, both of anomalies are prevented by blocking NRSF function during a critical developmental period in the life cycle of granule cells. Remarkably, preventing dysregulation of DG maturation was sufficient to influence hippocampal oscillations and to allow memory encoding processing and retrieval in the eFSE-NRSE rats.

In summary, long febrile seizures in an immature rat model provoke profound and enduring spatial memory problems. The mechanisms of these problems involve complex disruption of memory-related oscillations within the hippocampal network, likely deriving from impaired dendritic filtering and synaptic function in CA1 and DG, respectively. Remarkably, these deficits are abrogated by transient, *post hoc* interference with chromatin binding of the transcriptional repressor NRSF, with significant translational potential.

Summary and Conclusions

TLE is a devastating and chronic brain disorder that may result from FSE. Understanding mechanisms which cause TLE after FSE would facilitate the development of novel, anti-epileptogenic treatments. There were three challenges to understanding this relationship.

1. An appropriate animal model needed to be developed to study processes that occur after FSE and lead to TLE.
2. Not all children with FSE develop TLE; thus it was necessary to identify a way of predicting which individuals go on to have spontaneous seizures after FSE. This approach not only allows for individually-focused treatments but also enables research of which post FSE processes are important for epileptogenesis.
3. Mechanisms that mediate epileptogenesis and cognitive dysfunction must be identified and studied.

Therefore, we set out to meet these challenges using modern scientific approaches. Our results are:

1. We created a model of experimental (e)FSE in immature rats which reflects human phenomenology. Long (~60 minute) febrile seizures are maintained in P10 rats, meeting the criteria for status epilepticus. Using this model, we were able to ascertain epilepsy in ~40% of rats; cognitive dysfunction, including spatial memory deficits were identified as well.
2. We created a novel, non-invasive MRI technique that predicts withing hours after the insult, which eFSE individuals will become epileptic months later.

3. Multiple pro-inflammatory mediators are activated after eFSE with inter-rat variability. The probability of spontaneous limbic seizures increased with the levels of certain inflammatory mediators
4. Blocking inflammation greatly reduced the probability of hippocampal hyperexcitability after eFSE
5. NRSF expression and function are augmented after eFSE and contributes to the development of cognitive deficits later in life. Preventing NRSF binding to chromatin post hoc, after the eFSE rescues memory functions.

Together, these results offer a comprehensive examination of how eFSE provokes both TLE and cognitive deficits. These results have significant translational potential.

References

Ablah E, Hesdorffer DC, Liu Y, Paschal AM, Hawley S, Thurman D & Hauser WA (2014) Prevalence of epilepsy in rural Kansas. *Epilepsy Research*. 4:729-801.

Annegers JF, Hauser WA, Shirts SB & Kurland LT (1987) Factors prognostic of unprovoked seizures after febrile convulsions. *New England Journal of Medicine* 316:493–498.

Aronica E, Fluiter K, Iyer A, Zurolo E, Vreijlin E, van Vliet EA, Baayen JC & Gorter JA (2010) Expression pattern of miR-146a, an inflammation-associated microRNA, in experimental and human temporal lobe epilepsy. *European Journal of Neuroscience.* 31:1100-1107.

Andermann E, Robitaille Y, Lopes-Cendes I (1993b) Early childhood prolonged febrile convulsions, atrophy and sclerosis of mesial structures, and temporal lobe epilepsy: an MRI volumetric study. *Neurology.* 43:1083–1087.

Auphan N; DiDonato JA, Rosette C, Helmberg A, Karin M (1995) Immunosuppression by glucocorticoids: Inhibition of NF-kappaB activity through induction of IkappaB synthesis. *Science*. 270; 286.

Baram TZ (2012) The brain, seizures and epilepsy throughout life: understanding a moving target. *Epilepsy Currents.* 12:7-12.

Baram TZ, Jensen FE & Brooks-Kayal A (2011) Does acquired epileptogenesis in the immature brain require neuronal death? *Epilepsy Currents.* 11:21-26.

Baram TZ, Gerth A, & Schultz L (1997) Febrile seizures: an appropriate-aged model suitable for long-term studies. *Developmental Brain Research*. 98:265-270.

Barry JM, Choy M, Dubé C, Robbins A, Obenaus A, Lenck-Santini PP, Scott RC, Baram TZ & Holmes GL (2015) T2 relaxation time post febrile status epilepticus predicts cognitive outcome. *Experimental Neurology*. 269:242-252.

Barry JM, Sakkaki S, Barriere SJ, Patterson KP, Lenck-Santini P, Scott RC, Baram T Z & Holmes GL (2016) Temporal Coordination of hippocampal neurons reflects cognitive outcome post-febrile status epilepticus. *EBioMedicine*. 7:175-190.

Barry JM, Tian C, Spinella A, Page M & Holmes, GL. (2016) Spatial cognition following early-life seizures in rats: Performance deficits are dependent on task demands. *Epilepsy & Behavior*. 60:1-6.

Bender RA, Dubé C & Baram TZ (2004) Febrile seizures and mechanisms of epileptogenesis: Insights from an animal model. *Advances in Experimental Medicine and Biology*. 548:213-225.

Bender RA, Dubé C, Gonzalez-Vega R, Mina EW, Baram TZ (2003). Mossy fiber plasticity and enhanced hippocampal excitability, without hippocampal cell loss or altered neurogenesis, in an animal model of prolonged febrile seizures. *Hippocampus* 13:399-412.

Bender RA, Galindo R, Mameli M, Gonzalez-Vega R, Valenzuela CF, Baram TZ (2005) Synchronized network activity in developing rat hippocampus involves regional hyperpolarization-activated cyclic nucleotide-gated (HCN) channel function. *European Journal of Neuroscience*. 22:2669-2674.

Bender RA, Kirschstein T, Kretz O, Brewster AL, Richichi C, Rüschenschmidt C, Shigemoto R, Beck H, Frotscher M, Baram TZ (2007) Localization of HCN1 channels to presynaptic compartments: novel plasticity that may contribute to hippocampal maturation. *Journal of Neuroscience*. 27:4697-4706

Berg AT (2011) Epilepsy, cognition, and behavior: the clinical picture. *Epilepsia*, 52:7–12.

Berg AT & Shinnar S (1996) Complex febrile seizures. *Epilepsia*. 37:126-133.

Berg AT, Shinnar S, Darefsky AS, Holford TR, Shapiro ED, Salomon ME, Crain EF & Hauser AW (1997) Predictors of recurrent febrile seizures: A prospective cohort study. *Archives of Pediatrics & Adolescent Medicine*. 151:371-378.

Berg AT & Shinnar S (1996) Complex febrile seizures. *Epilepsia*. 37:126-133.

Bieri KW, Bobbitt KN & Colgin LL (2014) Slow and fast gamma rhythms coordinate different spatial coding modes in hippocampal place cells. *Neuron*. 82:670-681.

Bernhardt BC, Bernasconi N, Kim H, Bernasconi A (2012) Mapping thalamocortical network pathology in temporal lobe epilepsy. *Neurology.* 78:129–136.

Blumenfeld H (2004) Positive and Negative Network Correlations in Temporal Lobe Epilepsy. *Cerebral Cortex*. 14:892–902.

Bouilleret V, Nehlig A, Marescaux C, Namer IJ (2000) Magnetic resonance imaging follow-up of progressive hippocampal changes in a mouse model of mesial temporal lobe epilepsy. *Epilepsia* 41:642–650.

Brennan GP, Dey D, Chen Y, Patterson KP, Magnetta EJ, Hall AM, Dubé CM, Mei TY & Baram TZ (2016) Dual and opposing roles of microRNA-124 in epilepsy are mediated through Inflammatory and NRSF-dependent gene networks. *Cell Reports*. 14:2402-2412.

Brewster A, Bender RA, Chen Y, Dubè C, Eghbal-Ahmadi M & Baram TZ (2002) Developmental febrile seizures modulate hippocampal gene expression of

hyperpolarization-activated channels in an isoform- and cell-specific manner. *The Journal of Neuroscience*. 22:4591-4599.

Brewster AL, Bernard JA, Gall CM & Baram TZ (2005) Formation of heteromeric hyperpolarization-activated cyclic nucleotide-gated (HCN) channels in the hippocampus is regulated by developmental seizures. *Neurobiology of Disease*. 19:200-207.

Brown FC, Westerveld M, Langfitt JT, Hamberger M, Hamid H, Shinnar S, Sperling MR, Devinsky O, Barr W, Tracy J, Masur D, Bazil CW, Spencer SS (2014) Influence of anxiety on memory performance in temporal lobe epilepsy. *Epilepsy and Behavior*. 31:19-24.

Bruccoleri A, Pennypacker KR & Harry GJ (1999) Effect of dexamethasone on elevated cytokine mRNA levels in chemical-induced hippocampal injury. *Journal of Neuroscience Research.* 57:916-926.

Calamante F, Lythgoe MF, Pell GS, Thomas DL, King MD, Busza AL, Sotak CH, Williams SR, Ordidge RJ, Gadian DG (1999) Early changes in water diffusion, perfusion, T1, and T2 during focal cerebral ischemia in the rat studied at 8.5 T. *Magnetic Resonance in Medicine.* 41:479–485.

Cassidy RM, Gale K (1998) Mediodorsal thalamus plays a critical role in the development of limbic motor seizures. *Journal of Neuroscience*. 18:9002–9009.

Cendes F, Andermann F, Gloor P, Lopes-Cendes I, Andermann E, Melanson D, Jones-Gotman M, Robitaille Y, Evans A, Peters T (1993a) Atrophy of mesial structures in patients with temporal lobe epilepsy: cause or consequence of repeated seizures? *Annals of Neurology*. 34:795–801.

Cendes F, Andermann F, Dubeau F, Gloor P, Evans A, Jones-Gotman M, Olivier A, Chen ZF, Paquette AJ & Anderson, DJ (1998) NRSF/REST is required in vivo for repression of multiple neuronal target genes during embryogenesis. *Nature genetics*. 20:136-142.

Chen K, Baram TZ, Soltesz I (1999) Febrile seizures in the developing brain result in persistent modification of neuronal excitability in limbic circuits. *Nature Medicine*. 5:888–894.

Chen Y, Bender RA, Brunson KL, Pomper JK, Grigoriadis DE, Wurst W, Baram TZ (2004) Modulation of dendritic differentiation by corticotropin-releasing factor in the developing hippocampus. *Proceedings of the National Academy of Sciences*. 101:15782–15787.

Chong J, Hesdorffer DC, Thurman DJ, Lopez D, Harris RB, Hauser WA, Labiner ET, Velarde A, Labiner DM (2013) The prevalence of epilepsy along the Arizona-Mexico border. *Epilepsy Research*. 105:206–215.

Choy, M, Dubé, CM, Patterson KP, Barnes SR, Maras P, Blood A B, Hasso An, Obenaus A & Baram TZ (2014) A novel, noninvasive, predictive epilepsy biomarker with clinical potential. *Journal of Neuroscience*. 34:8672–8684.

Clarke DD and Sokoloff L (1999) Regulation of Cerebral Metabolic Rate. In: Basic Neurochemistry: Molecular, Cellular and Medical Aspects. 6th edition (Siegel GJ, Agranoff BW, Albers RW, et al., editors), pp637-670. Philadelphia: Lippinott-Raven.

Colgin LL (2016) Rhythms of the hippocampal network. *Nature Reviews Neuroscience*. 17:239-249.

Colgin LL, Denninger T, Fyhm M, Hafting T, Jensen O, Moser MB & Moser EI (2009) Frequency of gamma oscillations routes flow of information in the hippocampus. *Nature*. 19:353-357.

Crespel A, Coubes P, Rousset MC, Brana C, Rougier A, Rondouin G, Bockaert J, Baldy-Moulinier M & Lerner-Natoli M (2002) Inflammatory reactions in human medial temporal lobe epilepsy with hippocampal sclerosis. *Brain Research.* 952:159-169.

Dedeurwerdere S, Friedman A, Fabene PF, Mazarati A, Murashima YL, Vezzani A & Baram TZ (2012) Finding a better drug for epilepsy: Antiinflammatory targets. *Epilepsia*. 1-6.

de Graaf RA, Brown PB, McIntyre S, Nixon TW, Behar KL, Rothman DL (2006) High magnetic field water and metabolite proton T1 and T2 relaxation in rat brain in vivo. *Magnetic Resonance in Medicine*. 56:386–394.

De Landrot RI, Minokoshi M, Silveira DC, Cha BH & Holmes GL (2001) Recurrent neonatal seizures: relationship of pathology to the electroencephalogram and cognition. *Developmental Brain Research.* 129:27-38.

DeSalvo MN, Schridde U, Mishra AM, Motelow JE, Purcaro MJ, Danielson N, Bai X, Hyder F, Blumenfeld H (2010) Focal BOLD fMRI changes in bicuculline-induced tonic–clonic seizures in the rat. *Neuroimage* 50:1–8.

De Simoni MG, Perego C, Ravizza T, Moneta D, Conti M, Marchesi F, De Luigi, A, Garattini S & Vezzani A (2000) Inflammatory cytokines and related genes are induced in the rat hippocampus by limbic status epilepticus. *European Journal of Neuroscience.* 12:2623-2633.

Ding X-Q, Kucinski T, Wittkugel O, Goebell E, Grzyska U, Görg M, Kohlschütter A, Zeumer H (2004) Normal brain maturation characterized with age-related T2 relaxation times: an attempt to develop a quantitative imaging measure for clinical use. *Investigative Radiology*. 39:740–746.

Dinstein I, Heeger DJ, Lorenzi L, Minshew NJ, Malach R, Behrmann M (2012)

Unreliable evoked responses in autism. *Neuron* 75:981–991.

Dosenbach NUF, Nardos B, Cohen AL, Fair DA, Power JD, Church JA, Nelson SM, Wig GS, Vogel AC, Lessov-Schlaggar CN, Barnes KA, Dubis JW, Feczko E, Coalson RS, Pruett JR, Barch DM, Petersen SE, Schlaggar BL (2010) Prediction of individual brain maturity using fMRI. *Science*. 329:1358–1361.

Dreifuss S, Vingerhoets FJ, Lazeyras F, Andino SG, Spinelli L, Delavelle J, Seeck M (2001) Volumetric measurements of subcortical nuclei in patients with temporal lobe epilepsy. *Neurology* 57:1636–1641.

Dubé CM, Brewster AL & Baram TZ (2009) Febrile seizures: mechanisms and relationship to epilepsy. *Brain & Development*. *31*:366–71.

Dubé C, Brunson KL, Eghbal-Ahmadi M, Gonzalez-Vega R, Baram TZ (2005b) Endogenous neuropeptide Y prevents recurrence of experimental febrile seizures by increasing seizure threshold. *Journal of Molecular Neuroscience*. 25:275–284.

Dubé CM, Brewster AL, Richichi C, Zha Q & Baram TZ (2007) Fever, febrile seizures and epilepsy. *Trends in Neurosciences*. *30*:490–496.

Dubé, C, Chen K, Eghbal-Ahmadi M, Brunson K, Soltesz I, & Baram TZ (2000) Prolonged febrile seizures in the immature rat model enhance hippocampal excitability long term. *Annals of Neurology*. 47:336–344.

Dubé, C., Yu, H., Nalcioglu, O., & Baram, T. Z. (2004) Serial MRI after experimental febrile seizures: altered T2 signal without neuronal death. *Annals of neurology*, 56:709–714.

Dubé CM, Ravizza T, Hamamura M, Zha Q, Keebaugh A, Fok K, Andres AL, Nalcioglu O, Obenaus A, Vezzani A & Baram TZ (2010) Epileptogenesis provoked by prolonged experimental febrile seizures: mechanisms and biomarkers. *The Journal of Neuroscience*. *30*: 7484–94.

Dubé C, Richichi C, Bender RA, Chung G, Litt B, Baram TZ (2006) Temporal lobe epilepsy after experimental prolonged febrile seizures: prospective analysis. *Brain.* 129:911–922.

Dubé C, Vezzani A, Behrens M, Bartfai T, & Baram TZ (2005) Interleukin-1beta contributes to the generation of experimental febrile seizures. *Annals of Neurology*. *57*:152–155.

Dubé CM, Zhou JL, Hamamura M, Zhao Q, Ring A, Abrahams J, McIntyre K, Nalcioglu O, Shatskih T, Baram TZ & Holmes GL (2009) Cognitive dysfunction after experimental febrile seizures. *Experimental Neurology*. 215:167-177.

Duffy BA, Choy M, Riegler J, Wells JA, Anthony DC, Scott RC, Lythgoe MF (2012)

Imaging seizure-induced inflammation using an antibody targeted iron oxide contrast agent. *Neuroimage.* 60:1149–1155.

Dunleavy M, Shinoda S, Schindler C, Ewart C, Dolan R, Gobbo OL, Kerskens CM, Henshall DC (2010) Experimental neonatal status epilepticus and the development of temporal lobe epilepsy with unilateral hippocampal sclerosis. *American Journal of Pathology*. 176:330–342.

Elger, CE, Helmstaedter, C, & Kurthen, M. (2004). Chronic epilepsy and cognition. *The Lancet Neurology*. 3:663-672.

Englot DJ, Modi B, Mishra AM, DeSalvo M, Hyder F, Blumenfeld H (2009) Cortical deactivation induced by subcortical network dysfunction in limbic seizures. *Journal of Neuroscience*. 29:13006–13018.

Eskilsson A, Mirrasekhian E & Dufour S (2014) Immune-induced fever is mediated by IL-6 receptors on brain endothelial cells coupled to STAT3-dependent induction of brain endothelial prostaglandin synthesis. *Journal of Neuroscience*. 34:15957-15961.

Folbergrová J, Ingvar M, Nevander G, Siesjo BK (1985) Cerebral metabolic changes during and following fluorothyl-induced seizures in ventilated rats*. Journal of Neurochemistry.* 44:1419–1426.

French JA, Williamson PD, Thadani VM, Darcey TM, Mattson RH, Spencer SS & Spencer DD (1993) Characteristics of medial temporal lobe epilepsy: I. Results of history and physical examination. *Annals of Neurology*. 34:774-780.

Fujikawa DG, Dwyer BE, Wasterlain CG (1986) Preferential blood flow to brainstem during generalized seizures in the newborn marmoset monkey. *Brain Research.* 397:61–72.

Galic MA, Riazi K & Pittman QJ (2012) Cytokines and brain excitability. *Frontiers in Neuroendocrinology.* 33:116-125.

Gao Z, Ure K, Ding P, Nashast M, Yuan L, Ma J, Hanner RE & Hsieh J (2011) The master negative regulator REST/NRSF controls adult neurogenesis by restraining the neurogenic program in quiescent stem cells. *The Journal of Neuroscience*. 31:9772-9786.

George MS, Abbott LF & Siegelbaum SA (2009) HCN hyperpolarization-activated cation channel inhibit EPSPs by interactions with M-type K(+) channel. *Nature Neuroscience*. 5:577:584.

Gilmore TD (2006) Introduction to NF-κB: Players, pathways, perspectives. *Oncogene*. 25:6680-6684.

Gloor P, Olivier A, Quesney LF, Andermann F, Horowitz S (1982) The role of the limbic

system in experiential phenomena of temporal lobe epilepsy. *Annals of Neurology*. 12:129–144.

Goddard GV, McIntyre DC, Leech CK (1969) A permanent change in brain function resulting from daily electrical stimulation. *Experimental Neurology*. 25:295–330.

Goense J, Merkle H, Logothetis NK (2012) High-Resolution fMRI Reveals Laminar Differences in Neurovascular Coupling between Positive and Negative BOLD Responses. *Neuron*. 76:629–639.

Goldberg EM & Coulter DA (2013) Mechanisms of epileptogenesis: a convergence on neural circuit dysfunction. *Nature Reviews: Neuroscience*. 14:337-349.

Greene NDE, Bamidele A, Choy M, de Castro SCP, Wait R, Leung K-Y, Begum S, Gadian DG, Scott RC, Lythgoe MF (2007) Proteome changes associated with hippocampal MRI abnormalities in the lithium pilocarpine-induced model of convulsive status epilepticus. *Proteomics.* 7:1336–1344.

Grohn O, Pitkänen A (2007) Magnetic resonance imaging in animal models of epilepsy—noninvasive detection of structural alterations. *Epilepsia.* 48, 3-10.

Haller Jm Mickis E & Makara GB (2008) The effects of non-genomic glucocorticoid mechanisms on bodily functions and the central enural system. A critical evaluation of findings. *Fronteirs in Neuroendocrinology*. 29:273-291.

Hascoet JM, Monin P, Vert P (2007) Persistence of impaired autoregulation of cerebral blood flow in the postictal period in piglets. *Epilepsia*. 29:743–747.

Hesdorffer DC, Logroscino G, Cascino GD, Hauser WA (2007) Recurrence of afebrile status epilepticus in a population-based study in Rochester, Minnesota. *Neurology*. 69:73–78.

Heida JG, Boissé L & Pittman QJ (2004) Lippopolysaccharide- induced febrile convulsions in the rat: Short-term sequelae. *Epilepsia*. 45:1317-1329.

Heida JG, Teskey GC & Pittman QJ (2005) Febrile convulsions induced by the combination of lipopolysaccharide and low-dose kainic acid enhance seizure susceptibility, not epileptogenesis, in rats. *Epilepsia*. 35:1898-1905.

Heida JG, Moshé SL & Pittman QJ (2009) The role of interleukin-1β in febrile seizures. *Brain & Development.* 388-393.

Heida JG & Pittman QJ (2005) Causal links between brain cytokines and experimental febrile convulsions in the rat. *Epilepsia*. 46:1906-1913.

Hellier JL, Patrylo PR, Buckmaster PS & Dudek FE (1998) Recurrent spontaneous motor seizures after repeated low-dose systemic treatment with kainite: assessment of a rate model of temporal lobe epilepsy. *Epilepsy Research*. 31:73-84.

Helmstaedter C, Kurthen M, Lux S, Reuber M & Elger CE (2003) Chronic epilepsy and cognition: a longitudinal study in temporal lobe epilepsy. *Annals of Neurology.* 54:425-432.

Hermann BP, Seidenberg M, Schoenfeld J & Davies K (1997) Neuropsychological characteristics of the syndrome of mesial temporal lobe epilepsy. *JAMA Neurology*. 54:369-376.

Hester MS & Danzer SC (2014) Hippocampal granule cell pathology in epilepsy- a possible structural basis for comorbidities of epilepsy? *Epilepsy & Behavior.* 38:105-116.

Hester MS & Danzer SC (2013) Accumulation of abnormal adult- generated hippocampal granule cells predicts seizure frequency and severity. *The Journal of Neuroscience*. 33:8926-8936.

Holmes GL (2015) Cognitive impairment in epilepsy: the role of network abnormalities. *Epileptic Disorders*. 2:101-116.

Holmes GL, Gairsa JL, Chevassus-Au-Louis N & Ben- Ari Y (1998) Consequences of neonatal seizures in the rat: morphological and behavioral effects. *Annals of Neurology*. 44:845-857.

Holmes GL, Thompson JL (1988) Effects of kainic acid on seizure susceptibility in the developing brain. *Brain Research.* 467:51-59.

Hoppe C, Elger CE & Helmstaedter C (2007) Long-term memory impairment in patients with focal epilepsy. *Epilepsia*. 9:26-29.

Holtman L, van Vliet EA, Appeldoorn C, Gaillard PJ, de Boer M, Dorland R, Wadman WJ & Gorter JA (2014) Glutathione pegylated liposomal methylprednisolone administration after the early phase of status epilepticus did not modify epileptogenesis in the rat. *Epilepsy Research*. 108:396-404.

Holtman L, van Vliet EA, Edelbroek PM, Aronica E & Gorter JA (2010) Cox-2 inhibition can lead to adverse effects in a rat model for temporal lobe epilepsy. *Epilepsy Research*. 91: 49-56.

Holtman L, van Vliet EA, van Schaik R, Queiroz CM, Aronica E & Gorter JA (2009) Effects of SC58236, a selective COX-2 inhibitor, on epileptogenesis and spontaneous seizures in a rat model for temporal lobe epilepsy. *Epilepsy Research*. 84:56-66.

Hsieh J & Gage FH (2004) Epigenetic control of neural stem cell fate. *Current opinion in genetics & development*. 14:461-469.

Huang Z, Walker MC & Shah MM (2009) Loss of dendritic HCN1 subunits enhances cortical excitability and epileptogenesis. *The Journal of Neuroscience*. 29:10979-10988.

Ivy AS, Rex CS, Chen Y, Dubé C, Maras PM, Grigoriadis DE, Gall CM, Lynch G, Baram TZ (2010) Hippocampal dysfunction and cognitive impairments provoked by chronic early-life stress involve excessive activation of CRH receptors. *Journal of Neuroscience*. 30:13005-15.

Jang BC, Lim KJ, Suh MH, Park JG & Suh SI (2007) Dexamethasone suppresses interleukin-1β-induced human-β-defensin 2 mRNA expression: involvement of p38 MAKP, JNK, MKP-1, and NF-κB transcriptional factor in A549 cells*. Immunology & Medical Microbiology* 51.171-184.

Jansen JFA, Lemmens EMP, Strijkers GJ, Prompers JJ, Schijns OEMG, Kooi ME, Beuls EAM, Nicolay K, Backes WH & Hoogland G (2008) Short- and long-term limbic abnormalities after experimental febrile seizures. *Neurobiology of Disease*. 32:293-301.

Jensen FE, Applegate CD, Holtzman D, Belin TR, Burchfiel JL (1991) Epileptogenic effect of hypoxia in the immature rodent brain. *Annals of Neurology*. 29:629–637.

Jeon YJ, Han SH, Lee YW, Lee M, Yang KH & Kim HM (2000) Dexamethasone inhibits IL-1β gene expression in LPS-stimulated RAW 264.7 cells by blocking NF-κB/Rel and AP-1 activation. *Immunopharmacology*. 48;173-183.

Johnson DS, Mortazavi A, Myers RM & Wold B (2007) Genome-wide mapping of in vivo protein-DNA interactions. *Science*. 316:1497-1502.

Jokeit H & Ebner A (1999) Long term effects of refractory temporal lobe epilepsy on cognitive abilities: a cross sectional study. *Journal of Neurology, Neurosurgery & Psychiatry*. 67:44-50.

Jones FS & Meech R (1999) Knockout of REST/NRSF shows that the protein is a potent repressor of neuronally expressed genes in non neural tissues. *Bioessays*. 21:372–376.

Jung S, Jones TD, Lugo JN, Sheerin AH, Miller JW, D'Ambrosio R, Anderson AE, Poolos NP (2007) Progressive dendritic HCN channelopathy during epileptogenesis in the rat pilocarpine model of epilepsy. *The Journal of Neuroscience*. 27:13012-13021.

Jung S, Warner LN, Pitsch J, Becker AJ & Poolos NP (2011) Rapid loss of dendritic HCN channel expression in hippocampal pyramidal neurons following status epilepticus. *The Journal of Neuroscience*. 31:14291-14295.

Jupp B, Williams JP, Tesiram YA, Vosmansky M, O'Brien TJ (2006) Hippocampal T2

signal change during amygdala kindling epileptogenesis. *Epilepsia.* 47:41–46.

Kelley MS, Jacobs MP, Lowenstein DH, NINDS Epilepsy Benchmark Stewards (2009) The NINDS epilepsy research benchmarks. *Epilepsia.* 50:579–582.

Kleen JK, Scott RC, Holmes GL & Lenck- Santini PP (2010) Hippocampal interictal spikes disrupt cognition in rats. *Annals of Neurology*. 67:250-257.

Kovac S, Domijan A-M, Walker MC, Abramov AY (2012) Prolonged seizure activity impairs mitochondrial bioenergetics and induces cell death. *Journal of Cell Science*. 125:1796–1806.

Koyama R, Tao K, Sasaki T, Ichikawa J, Miyamoto D, Muramatsu R, Matsuki N, Ikegaya Y (2012) GABAergic excitation after febrile seizures induces ectopic granule cells and adult epilepsy. *Nature Medicine*. 18:1271-1278.

Kron MM, Zhang H & Parent JM (2010) The developmental stage of dentate granule cells dictates their contribution to seizure-induced plasticity. *The Journal of Neuroscience*. 6:2051-2059.

Kubová H, Druga R, Lukasiuk K, Suchomelová L, Haugvicová R, Jirmanová I, Pitkänen A (2001) Status epilepticus causes necrotic damage in the mediodorsal nucleus of the thalamus in immature rats. *Journal of Neuroscience*. 21:3593–3599.

Landis SC, Amara SG, Asadullah K, Austin CP, Blumenstein R, Bradley EW, Crystal RG, Darnell RB, Ferrante RJ, Fillit H, Finkelstein F, Fisher M, Gendelman HE, Golub RM, Goudreau JL, Gross RA, Gubitz AK, Hesterlee SE, Howells DW, Huguenard J, Kelner K, Koroshetz W, Krainc D, Lazic SE, Levine MS, Macleod MR, McCall JM, Moxley III RT, Narasimhan K, Noble LJ, Perrin S, Porter JD, Steward O, Unger E, Utz U & Silberberg SD (2012) A call for transparent reporting to optimize the predictive value of preclinical research. *Nature*. 490:187-191.

Lee CL, Hannay J, Hrachovy R, Rashid S, Antalffy B, Swann JW (2001). Spatial learning deficits without hippocampal neuronal loss in a model of early-onset epilepsy. *Neuroscience.* 107:71–84.

Lenz KM, Nugent BM, Haliyur R, & McCarthy MM (2013) Microglia are essential to masculinization of brain and behavior. *The Journal of Neuroscience*. 33:2761–2772.

Lewis DV, Shinnar S, Hesdorffer DC, Bagiella E, Bello JA, Chan S, Xu Y, MacFall J, Gomes WA, Moshè SL, Mathern GW, Pellock JM, Nordi DR, Frank LM, Provenzale J, Shinnar RC, Epstein LG, Masur D, Litherland C, Sun S & the FEBSTAT study team (2014) Hippocampal Sclerosis after Febrile Status Epilepticus: the FEBSTAT Study. *Annals of Neurology*. 75:178-185.

Lewis DV, Shinnar S & Hesdorffer DC (2014) Hippocampal sclerosis after febrile status epilepticus: the FEBSTAT study. *Annals of Neurology.* 75:178-185.

Leppert IR, Almli CR, McKinstry RC, Mulkern RV, Pierpaoli C, Rivkin MJ, Pike GB, Brain Development Cooperative Group (2009) T2 relaxometry of normal pediatric brain development. *Journal of Magnetic Resonance Imaging*. 29:258–267.

Lewis DV, Shinnar S, Hesdorffer DC, Bagiella E, Bello JA, Chan S, Xu Y, Macfall J, Gomes WA, Moshé SL, Mathern GW, Pellock JM, Nordli DR Jr, Frank LM, Provenzale J, Shinnar RC, Epstein LG, Masur D, Litherland C, Sun S; FEBSTAT Study Team (2014) Hippocampal sclerosis after febrile status epilepticus: The FEBSTAT study. *Annals of Neurology*. 75:178–185.

Lindsay J, Ounsted C, Richards P (1979) Long-term outcome in children with temporal lobe seizures. I: Social outcome and childhood factors. *Developmental Medicine and Child Neurology*. 21:285–298.

Liu Z, Yang Y, Silveira DC, Sarkisian MR, Tandon P, Huang L-T, Stafstrom CE & Holmes CL (1999) Consequences of recurrent seizures during early brain development. *Neuroscience*. 92:1443-1454.

Lothman E (1990) The biochemical basis and pathophysiology of status epilepticus. *Neurology*. 40:13–23.

Luheshi GN, Stefferl A & Turnbull AV (1997) Febrile response to tissue inflammation involves both peripheral and brain IL-1 and TNF-alpha in the rat. *American Journal of Physiology*, 272:R862-R868.

Lugo JN, Swann JW & Anderson AE (2014) Early-life seizures result in deficits in social behavior and learning. *Experimental Neurology*. 256:74-80.

Lunyak, VV & Rosenfeld MG (2005) No rest for REST: REST/NRSF regulation of neurogenesis. *Cell*. 121:621-631.

Maroso M, Balosso S, Ravizza T, Liu J, Aronica, E, Iyer A. M, Rossetti, C, Molteni M, Casalgrandi M, Manfredi AA, Bianchi ME & Vezzani A (2010) Toll-like receptor 4 and high-mobility group box-1 are involved in ictogenesis and can be targeted to reduce seizures. *Nature Medicine*. *16*:413–419.

Maroso M, Balosso S, Ravizza T, Iori V, Wright CI, French J & Vezzani A (2011) Interleukin-1 biosynthesis inhibition reduces acute seizures and drug resistant chronic epileptic activity in mice. *Neurotherapeutics*. 8:304-315.

Martinos MM, Yoong M, Patil S, Chong WK, Mardari R, Chin RF, Neville BG, de HM & Scott RC (2013) Early developmental outcomes in children following convulsive status epilepticus: a longitudinal study. *Epilepsia* 54:1012-1019.

Mathern GW, Pretorius JK, Babb TL (1995) Influence of the type of initial precipitating injury and at what age it occurs on course and outcome in patients with temporal lobe

seizures. J Neurosurg 82:220–227.

Mirsattari SM, Sharpe MD, Young GB (2004) Treatment of refractory status epilepticus with inhalational anesthetic agents isoflurane and desflurane. *Archives of Neurology*. 61:1254–1259.

McClelland S, Brennan GP, Dubé C, Rajpara S, Iyer S, Richichi C, Bernard C & Baram TZ (2014) The transcription factor NRSF contributes to epileptogenesis by selective repression of a subset of target genes. *eLife*, *3*, e01267.

McClelland S, Flynn C, Dubé C, Richichi C, Zha Q, Ghestem A, Esclapez, M, Bernard C & Baram TZ (2011) Neuron-restrictive silencer factor-mediated hyperpolarization-activated cyclic nucleotide gated channelopathy in experimental temporal lobe epilepsy. *Annals of neurology*. *70*:454–64.

Mueller SG, Laxer KD, Scanlon C, Garcia P, McMullen WJ, Loring DW, Meador KJ, Weiner MW (2012) Different structural correlates for verbal memory impairment in temporal lobe epilepsy with and without mesial temporal lobe sclerosis. *Human Brain Mapping*. 33:489-499.

Murphy BL, Hofacer RD, Faulkner CN, Loepke AW & Danzer SC (2012) Abnormalities of granule cell dendritic structure are a prominent feature of the intrahippocampal kainic acid model of epilepsy despite reduced postinjury neurogenesis. *Epilepsia*. 53:908-921.

Natsume J, Bernasconi N, Miyauchi M, Naiki M, Yokotsuka T, Sofue A, Bernasconi A (2007) Hippocampal volumes and diffusion-weighted image findings in children with prolonged febrile seizures. *Acta Neurologica Scandinavica*. 186:25–28.

Nitecka L, Tremblay E, Charton G, Bouillot JP, Berger ML, Ben-Ari Y (1984) Maturation of kainic acid seizure-brain damage syndrome in the rat. II. Histopathological sequelae. *Neuroscience.* 13:1073–1094.

Noam Y, Bernard C & Baram TZ (2011) Towards an integrated view of HCN channel role in epilepsy. *Current Opinion in Neurobiology*. 21:873-879.

Noe FM, Polascheck N, Frigerio F, Bankstahl M, Ravizza T, Marchini S, Beltrame L, Reschke Bandero C, Losher W & Vezzani A (2013) Pharmacological blockade of IL-1β/IL-1 receptor type 1 axis during epileptogenesis provides neuroprotection in two rat models of temporal lobe epilepsy. *Neurobiology of Disease*. 59:183-193.

Ogawa S, Lee TM, Kay AR, Tank DW (1990) Brain magnetic resonance imaging with contrast dependent on blood oxygenation. *Proceedings of the National Academy of Sciences.* 87:9868–9872.

Oishi K, Faria AV, Yoshida S, Chang L, Mori S (2013) Quantitative evaluation of brain development using anatomical MRI and diffusion tensor imaging. *International Journal of Developmental Neuroscience*. 31:512–524.

Olafsson E, Ludvigsson P, Gudmundsson G, Hesdorffer D, Kjartansson O, Hauser WA (2005) Incidence of unprovoked seizures and epilepsy in Iceland and assessment of the epilepsy syndrome classification: a prospective study. *Lancet Neurology* 4:627–634.

Ollikainen J, Honkaniemi J, Palmio J & Peltola J (2004) Regulation of IL-6 system in cerebrospinal fluid and serum compartments by seizures: the effect of seizure type and duration. *Journal of Neuroimmunology.* 152:121-125.

Parent JM, Yu TW, Leibowitz RT, Geschwind DH, Sloviter RS & Lowenstein DH (1997) Dentate granule cell neurogenesis is increased by seizures and contributes to aberrant network reorganization in the adult rat hippocampus. *The Journal of Neuroscience*. 10:3727-3738.

Patterson K P, Baram T Z & Shinnar S (2014) Origins of temporal lobe epilepsy: febrile seizures and febrile status epilepticus. *Neurotherapeutics.* 11: 242–50.

Pereira de Vasconcelos A, Ferrandon A, Nehlig A (2002) Local cerebral blood flow during lithium-pilocarpine seizures in the developing and adult rat: role of coupling between blood flow and metabolism in the genesis of neuronal damage. *Journal of Cerebral Blood Flow and Metabolism.* 22:196–205.

Pouliot, WA, Dudek, FE & Dingledine R (2013) Inhibition of the prostaglandin receptor EP2 following status epilepticus reduces delayed mortality and brain inflammation. *Proceedings of the National Academy of Sciences.* 110:3591-3596.

Racine RJ (1972) Modification of seizure activity by electrical stimulation. II. Motor seizure. *Electroencephalography and Clinical Neurophysiology*. 32: 281–294.

Raol YS, Budreck EC, Brooks-Kayal AR (2003) Epilepsy after early-life seizures can be independent of hippocampal injury. *Annals of Neurology*. 53:503–511.

Raijmakers M, Clynen E, Smisdom N, Nelissen S, Brône D, Rigo JM, Hoogland G & Swijsen A (2016) Experimental febrile seizures increase dendritic complexity of newborn dentate granule cells. *Epilepsia*, 5:717-726.

Ravizza T, Gagliardi B, Francesco N, Boer K, Aronica E & Vezzani A (2008) Innate and adaptive immunity during epileptogenesis and spontaneous seizures: Evidence from experimental models and human temporal lobe epilepsy. *Neurobiology of Disease*. 142-160.

Riazi K, Galic MA & Pittman QJ (2010) Contributions of peripheral inflammation to seizure susceptibility: Cytokines and brain excitability. *Epilepsy Research*. 89:34-42.

Roch CEA (2002) Predictive Value of Cortical Injury for the Development of Temporal Lobe Epilepsy in 21-day-old Rats: An MRI Approach Using the Lithium-pilocarpine Model. *Epilepsia*. 43:1129–1136.

Richard GR, Titiz A, Tyler A, Holmes GL, Scott RC & Lenck-Santini PP (2013) Speed modulation of hippocampal theta frequency correlates with spatial memory performance. *Hippocampus*. 12:1269-1279.

Rodenas-Ruano A, Chàverz AE, Cossio MJ, Castillo PE & Zukin RS (2012) REST-dependent epigenetic remodeling promotes the developmental switch in synaptic NMDA receptors. *Nature Neuroscience*. 15:1382-1390.

Rovere-Querini P, Capobianco A, Scaffidi P, Valentinis B, Catalanotti F, Giazzon M, Dumitiu IE, Müller S, Iannacone M, Traversari C, Bianchi ME & Manfredi AA (2004) HMGB1 is an endogenous immune adjuvant released by necrotic cells. *EMBO Reports.* 8:825-830.

Roy H, Lippé S, Lussier F, Sauerwin HC, Lortie A, Lacroix J & Lassonde M (2011) Developmental outcome after a single episode of status epilepticus. *Epilepsy Behavior.* 4:430-436.

Santoro B & Baram TZ (2003) The multiple personalities of h-channels. *Trends in Neuroscience.* 10:550-540.

Schlessinger AR & Cowan WM (1975) An autoradiographic study of the time of origin and the pattern of granule cell migration in the dentate gyrus of the rat. *Journal of Comparative Neurology.* 159:149-176.

Schoenherr CJ & Anderson DJ (1995) The neuron-restrictive silencer factor (NRSF): a coordinate repressor of multiple neuron-specific genes. *Science*. 267:

Schwartz M & Kipnis J (2005) Protective autoimmunity and neuroprotection in inflammatory and noninflammatory neurodegenerative diseases. *Journal of the Neurological Sciences.* 233:163-166.

Scantlebury MH, Gibbs SA, Foadjo B, Lema P, Psarropoulou C, Carmant L (2005) Febrile seizures in the predisposed brain: a new model of temporal lobe epilepsy. *Annals of Neurology*. 58:41–49.

Schridde U, Khubchandani M, Motelow JE, Sanganahalli BG, Hyder F, Blumenfeld H (2008) Negative BOLD with Large Increases in Neuronal Activity. *Cerebral Cortex*. 18:1814–1827.

Scott, RC, Gadian, DG, King, MD, Chong, WK, & Cox, TC. (2002). Magnetic resonance imaging findings within 5 days of status epilepticus in childhood. *Brain*. 125:1951-1959.

Seinfeld S, Shinnar S, Sun S, Hesdorffer DC, Deng X, Shinnar RC, O'Hara K, Nordli DR, Frank LM, Gallentine, W, Moshé SL, Pellock JM; FEBSTAT study team (2014) Emergency management of febrile status epilepticus: results of the FEBSTAT study. *Epilepsia*. 55*:*388–395.

Shin M, Brager D, Jaramillo TC, Johnston D & Chetkovich DM (2008) Mislocation of h channel subunits underlies h channellopathy in temporal lobe epilepsy. *Neurobiolgoy of Disease*. 32:26-36.

Singh SP, He X, McNamara JO & Danzer SC (2013) Morphological changes among hippocampal dentate granule cells exposed to early kindling- epileptogenesis. *Hippocampus*. 23:1309-1320.

Shinnar S, Bello JA, Chan S, Hesdorffer DC, Lewis DV, Macfall J, Pellock JM, Nordli DR, Frank LM, Moshé SL, Gomes W, Shinnar RC, Sun S, for the FEBSTAT Study Team (2012) MRI abnormalities following febrile status epilepticus in children: The FEBSTAT study. *Neurology.* 79:871–877.

Shinnar S, Pellock JM, Berg AT, O'Dell C, Driscoll SM, Maytal J, Moshe SL & DeLorenzo RJ (2001) Short-term outcomes of children with febrile status epilepticus. *Epilepsia*. 1:47-53.

Sorrells SF & Sapolsky Rm (2007) An inflammatory review of glucocorticoid actions in the CNS. *Brain, Behavior & Immunity*. 21:259-272.

Sperber EF, Stanton PK, Haas K, Ackermann RF, Moshé SL (1992) Developmental differences in the neurobiology of epileptic brain damage. Epilepsy Res Suppl 9:67–80; discussion 80–81.

Stafstrom CE, Thompson JL, Holmes GL (1992) Kainic acid seizures in the developing brain: status epilepticus and spontaneous recurrent seizures. *Developmental Brain Research*. 65:227–236.

Staley KJ, White AW & Dudek FE (2011) Interictal spikes: harbingers or causes of epilepsy? *Neuroscience letters*. 3:247-250.

Thind KK, Ribak CE & Buckmaster PS (2008) Synaptic input to dentate granule cell basal dendrites in a rat model of temporal lobe epilepsy. *The Journal of Comparative Neurology.* 509:190-202.

Toth Z, Yan XX, Haftoglou, Ribak Ce & Baram TZ (1998) Seizure- induced neuronal injury: Vulnerability to febrile seizures in an immature rat model. *The Journal of Neuroscience.* 18:4285-4294.

Tremblay E, Ben-Ari Y (1984) Usefulness of parenteral kainic acid as a model of temporal lobe epilepsy. Clinical Neurophysiology. 14:241–246.

Tsai ML, Hung KL, Tsan YY & Tung WT (2015) Long-term neurocognitive outcome and auditory event-related potentials after complex febrile seizures in children. *Epilepsy Behavior*. 47:55-60.

van Zijl, P.C.M., Eleff SM, Ulatowski JA, Oja JME, Ulu gcaron AM, Traystman RJ,

Kauppinen RA (1998) Quantitative assessment of blood flow, blood volume and blood oxygenation effects in functional magnetic resonance imaging. *Nature Medicine*. 4:159–167.

VanLandingham, K. E., Heinz, R. E., Cavazos, J. E., & Lewis, D. V. (1998). Magnetic resonance imaging evidence of hippocampal injury after prolonged focal febrile convulsions. *Annals of neurology*, *43*:413–426.

Varghese GI, Purcaro MJ, Motelow JE, Enev M, McNally KA, Levin AR, Hirsch LJ, Tikofsky R, Paige AL, Zubal IG, Spencer SS, Blumenfeld H (2009) Clinical use of ictal SPECT in secondarily generalized tonic-clonic seizures. Brain. 132:2102–2113.

Visser AM, Jaddoe VW, Ghassabian A, Schenk JJ, Verhulst FC, Hofman A, Tiemeier H, Moll HA & Arts WF (2012) Febrile seizures and behavioral and cognitive outcomes in preschool children: the Generation R study. *Developmental Medicine & Child Neurology.* 11:1006-1011.

Vezzani A, Balosso S & Ravizza T (2008) The role of cytokines in the pathophysiology of epilepsy. *Brain.* 22:797-803.

Vezzani A, French J, Bartfai T & Baram TZ (2011) The role of inflammation in epilepsy. *Nature Reviews Neurology*. 7:31-40.

Wasterlain CG, Thompson KW, Suchomelova L, Niquet J (2010) Brain energy metabolism during experimental neonatal seizures. *Neurochemical Research*. 35:2193–2198.

Yang YJ, Baltus AE, Mathew RS, Murphy EA, Evrony GD, Gonzalez DM, Wang EP, Marshall-Walker CA, Barry BJ, Murn J, Tatarakis A, Mahajan MA, Samuels HH, Shi Y, Golden JA, Mahajnah M, Shenhav R & Walsh CA (2012) Microcephaly gene links trithorax and REST/NRSF to control neuronal stem cell proliferation and differentiation. *Cell*. 151:1097-1112.

Young RSK, Cowan B, Briggs RW (1986) Brain metabolism after electroshock seizure in the neonatal dog: A [31p]NMR study. *Brain Research Bulletin*. 18:261–263.